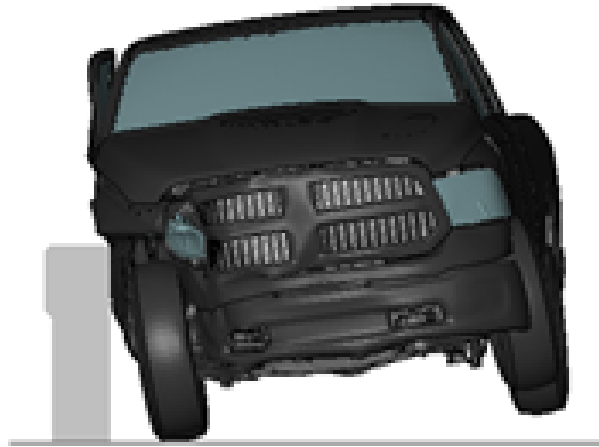




**Report No. 0-7121-R1**



**DETERMINE ADEQUACY OF EXISTING ROADSIDE BARRIERS ON HIGH-SPEED  
ROADWAYS**

**COOPERATIVE RESEARCH PROGRAM**

Texas Department of Transportation  
<https://tti.tamu.edu/documents/0-7121-R1pdf>

**TEXAS A&M TRANSPORTATION INSTITUTE**

Roadside Safety & Physical Security  
Texas A&M University System RELLIS Campus  
Building 7091  
1254 Avenue A  
Bryan, TX 77807



1. Report No. FHWA/TX-23/0-7121-R1		2. Government Accession No.		3. Recipient's Catalog No.	
4. Title and Subtitle DETERMINE ADEQUACY OF EXISTING ROADSIDE BARRIERS ON HIGH-SPEED ROADWAYS				5. Report Date Published: August 2024	
				6. Performing Organization Code	
7. Author(s) Sonal Chamargore, Roger Bligh, Chiara Silvestri-Dobrovolny, Bahar Dadashova, Marcie Perez, Aniruddha Zalani, Sun Hee Park, William Williams, Judong Lee, Maysam Kiani				8. Performing Organization Report No. Report 0-7121-R1	
9. Performing Organization Name and Address Texas A&M Transportation Institute The Texas A&M University System College Station, Texas 77843-3135				10. Work Unit No. (TRAIS)	
				11. Contract or Grant No. Project 0-7121	
12. Sponsoring Agency Name and Address Texas Department of Transportation Research and Technology Implementation Office 125 E. 11th Street Austin, Texas 78701-2483				13. Type of Report and Period Covered Technical Report: September 2021–July 2023	
				14. Sponsoring Agency Code	
15. Supplementary Notes Project sponsored by the Texas Department of Transportation. Project Title: Determine the Adequacy of Installation of Exiting Roadside Barriers on High-Speed Roadways URL: <a href="https://tti.tamu.edu/documents/0-7121-R1.pdf">https://tti.tamu.edu/documents/0-7121-R1.pdf</a>					
16. Abstract <p>Longitudinal barriers (e.g., guardrails, median barriers, and bridge rails) are currently tested and evaluated at a design impact speed of 62 mph. Posted speed limits have increased in recent years. New or modified barrier designs may be needed to withstand high-speed impacts to maintain the desired level of safety for motorists traveling on high-speed sections of highway. The objectives of this project included determining appropriate impact conditions for roadways with posted speed limits of 75 mph and above, and investigating the capability of existing or modified barriers to accommodate these impact conditions. Clinically reconstructed crash data in the National Cooperative Highway Research Program 17-43 database was used to estimate 85th percentile impact conditions for roadways with posted speed limits of 75, 80, and 85 mph.</p> <p>Finite element modeling and simulation were used to assess the impact performance of four concrete barriers at high-speed impact conditions estimated for a posted speed limit of 85 mph. The occupant risk metrics and angular displacements for these barriers were all within MASH thresholds for both the 1100C passenger car and 2270P pickup truck, and it was concluded they are likely to meet MASH evaluation criteria. Two guardrail systems were evaluated through finite element impact simulations for impact conditions estimated for a posted speed limit of 80-mph. Both systems satisfied MASH evaluation criteria for the 1100C passenger car and 2270P pickup truck design vehicles, and it was concluded they have a reasonable probability of complying with MASH for the high-speed impact conditions. Due to a lack of validation of the barrier models for high-speed impact conditions and various limitations associated with predicting some failure modes such as rail rupture, researchers recommend crash testing these systems to verify impact performance.</p>					
17. Key Words Roadside, Roadside Safety, Barrier, Bridge Rail, Median Barrier, Guardrail, High Speed, Finite Element Analysis, Finite Element Modeling			18. Distribution Statement No restrictions. This document is available to the public through NTIS: National Technical Information Service Alexandria, Virginia <a href="https://www.ntis.gov">https://www.ntis.gov</a>		
19. Security Classif. (of this report) Unclassified		20. Security Classif. (of this page) Unclassified		21. No. of Pages 132	
				22. Price	



# **DETERMINE ADEQUACY OF EXISTING ROADSIDE BARRIERS ON HIGH-SPEED ROADWAYS**

by

Sonal Chamargore,  
Student Graduate Worker,

Roger P. Bligh, Ph.D., P.E,  
Senior Research Engineer,

Chiara Silvestri Dobrovolsky, Ph.D.,  
Research Scientist

Bahar Dadashova,  
Associate Research Scientist,

Marcie Perez,  
Associate Research Scientist,

Nathan Schulz, Ph.D., P.E,  
Associate Research Scientist,

James Kovar,  
Assistant Research Scientist,

Nauman Sheikh, P.E.,  
Research Engineer,

William Williams, P.E.,  
Associate Research Engineer,

Aniruddha Zalani,  
Student Graduate Worker,

Sun Hee Park, Ph.D,  
Associate Transportation Researcher,

Judoong Lee,  
Postdoctoral Research Associate,

Maysam Kiani, Ph.D., P.E.,  
Assistant Research Engineer

Report 0-7121-R1

Project 0-7121

Determine Adequacy of Installation of Existing Roadside Barriers on High-Speed Roadways

Sponsored by the  
Texas Department of Transportation  
and the  
Federal Highway Administration

Published: August 2024

Texas A&M Transportation Institute  
College Station, Texas 77843-3135

## **DISCLAIMER**

This research was sponsored by the Texas Department of Transportation (TxDOT) and the Federal Highway Administration (FHWA). The contents of this report reflect the views of the authors, who are responsible for the facts and the accuracy of the data presented herein. The contents do not necessarily reflect the official view or policies of FHWA or TxDOT. This report does not constitute a standard, specification, or regulation.

The United States Government and the State of Texas do not endorse products or manufacturers. Trade or manufacturers' names appear herein solely because they are considered essential to the object of this report.

## **ACKNOWLEDGMENTS**

This project was sponsored by TxDOT and FHWA. The authors thank the project managers, Wade Odell and Darrin Jensen, and the members of the Project Monitoring Committee—Ken Mora, Charles Airiohuodion, Taya Retterer, Tim Wright, Alberto Guevara, and Vincent Shovlin—for their guidance and feedback during the project. The authors also thank Texas A&M High Performance Research Computing for providing computing resources for advance simulation analyses performed under this research.

# TABLE OF CONTENTS

	Page
<b>List of Figures .....</b>	<b>ix</b>
<b>List of Tables .....</b>	<b>vii</b>
<b>Chapter 1. Introduction .....</b>	<b>1</b>
1.1. Roadside Safety Features Crash Testing Guidelines .....	1
1.2. Barrier Systems Used by the Texas Department of Transportation .....	2
<b>Chapter 2. Literature Review .....</b>	<b>3</b>
2.1. TxDOT Project 0-6071 .....	3
2.2. NCHRP Project 17-22 Crash Database .....	4
2.3. NCHRP 17-43 Crash Database.....	4
2.4. NCHRP Project 17-79 .....	5
2.5. Barrier Behavior .....	6
2.5.1. Rigid Concrete Barrier .....	6
2.5.2. Midwest Guardrail System .....	6
2.6. Relationship between Posted Speed Limit and Operating Speed .....	7
<b>Chapter 3. Data Collection and Analysis.....</b>	<b>9</b>
3.1. Data Collection .....	9
3.2. Safety Data Analysis.....	9
3.2.1. Exploratory Data Analysis .....	10
3.2.2. 17-22 Database.....	18
3.2.3. 17-43 Database.....	21
3.3. Conclusion .....	32
<b>Chapter 4. Finite Element Simulation .....</b>	<b>35</b>
4.1. Single Slope Concrete Barrier .....	35
4.2. Single Slope Traffic Rail .....	46
4.3. Vertical Shape Concrete Barrier .....	53
4.4. F-Shape Concrete Barrier .....	64
4.5. Conclusion .....	76
4.5.1. Occupant Risk Comparison .....	76
4.5.2. Angular Displacement Comparison.....	77
<b>Chapter 5. Structural Adequacy .....</b>	<b>79</b>
5.1. Design Impact Loads .....	79
5.2. Yield Line Analysis Procedure .....	80
5.3. Barrier Capacity .....	81
5.4. Conclusion .....	82
<b>Chapter 6. Guardrail.....</b>	<b>83</b>
6.1. Previous Guardrail Testing and Performance Limits .....	83
6.2. Roadside Thrie-Beam Guardrail System .....	85
6.3. Midwest Guardrail System with Shortened Blockouts.....	92
6.4. Conclusions and Recommendations .....	99
<b>Chapter 7. Conclusions and Implementation Recommendations .....</b>	<b>101</b>
<b>References.....</b>	<b>103</b>
<b>Appendix A. SSCB Details .....</b>	<b>105</b>



<b>Appendix B. SSTR Details .....</b>	<b>107</b>
<b>Appendix C. T222 Details .....</b>	<b>109</b>
<b>Appendix D. F-Shape Details .....</b>	<b>111</b>
<b>Appendix E. Value of Research .....</b>	<b>113</b>

## LIST OF FIGURES

Figure 1. Hit Concrete Barrier versus Type of Injuries. ....	13
Figure 2. Hit Median Barrier versus Type of Injuries. ....	13
Figure 3. Hit End of Bridge versus Type of Injuries. ....	14
Figure 4. Hit Guardrail versus Type of Injuries.....	14
Figure 5. Hit Work Zone Barricades, Cones, Signs versus Type of Injuries.....	15
Figure 6. Hit Side of Barrier versus Type of Injuries. ....	15
Figure 7. Number of Fatal Injuries per Year.....	16
Figure 8. Number of Serious Injuries per Year.....	16
Figure 9. Number of Minor Injuries per Year.....	17
Figure 10. Number of Possible Injuries per Year. ....	17
Figure 11. Regression Relationship for Impact Speed by Albuquerque et al. (9). ....	19
Figure 12. Regression Relationship for Impact Angle by Albuquerque et al. (9). ....	19
Figure 13. Linear Regression for 85th Percentile Impact Speed with Updated 17-22 Crash Data Set. ....	20
Figure 14. Linear Regression for 85th Percentile Impact Angle with Updated 17-22 Crash Data Set. ....	21
Figure 15. Case 1: Linear Regression for 85th Percentile Impact Speed with 17-43 Crash Database.....	22
Figure 16. Case 1: Linear Regression for 85th Percentile Impact Angle with 17-43 Crash Database.....	23
Figure 17. Case 2: Linear Regression for 85th Percentile Impact Speed with 17-43 Crash Database.....	24
Figure 18. Case 2: Linear Regression for 85th Percentile Impact Angle with 17-43 Crash Database.....	24
Figure 19. Case 3: Linear Regression for 85th Percentile Impact Speed with 17-43 Crash Database.....	25
Figure 20. Case 3: Linear Regression for 85th Percentile Impact Angle with 17-43 Crash Database.....	26
Figure 21. Case 4: Linear Regression for 85th Percentile Impact Speed with 17-43 Crash Database.....	27
Figure 22. Case 4: Linear Regression for 85th Percentile Impact Angle with 17-43 Crash Database.....	28
Figure 23. Case 5: Linear Regression for 85th Percentile Impact Speed with 17-43 Crash Database.....	29
Figure 24. Case 5: Linear Regression for 85th Percentile Impact Angle with 17-43 Crash Database.....	30
Figure 25. Case 6: Linear Regression for 85th Percentile Impact Speed with 17-43 Crash Database.....	31
Figure 26. Case 6: Linear Regression for 85th Percentile Impact Angle with 17-43 Crash Database.....	32
Figure 27. Roll-Time History for SSCB-Car.....	39
Figure 28. Pitch-Time History for SSCB-Car.....	40
Figure 29. Yaw-Time History for SSCB-Car. ....	40
Figure 30. Roll-Time History for SSCB-Pickup.....	41

Figure 31. Pitch-Time History for SSCB-Pickup. ....	41
Figure 32. Yaw-Time History for SSCB-Pickup. ....	42
Figure 33. Occupant Impact Velocity for SSCB-Car. ....	42
Figure 34. Ridedown Acceleration for SSCB-Car. ....	43
Figure 35. Roll, Pitch, Yaw Comparison for SSCB-Car. ....	43
Figure 36. Occupant Impact Velocity for SSCB-Truck. ....	44
Figure 37. Ridedown Acceleration for SSCB-Truck. ....	45
Figure 38. Roll, Pitch, Yaw Comparison for SSCB-Truck. ....	45
Figure 39. Occupant Impact Velocity for SSTR-Car. ....	49
Figure 40. Ridedown Acceleration for SSTR-Car. ....	50
Figure 41. Roll, Pitch, Yaw for SSTR-Car. ....	50
Figure 42. Occupant Impact Velocity for SSTR-Truck. ....	51
Figure 43. Ridedown Acceleration for SSTR-Truck. ....	52
Figure 44. Roll, Pitch, Yaw for SSTR-Truck. ....	52
Figure 45. Roll-Time History for T222-Car. ....	57
Figure 46. Pitch-Time History for T222-Car. ....	57
Figure 47. Yaw-Time History for T222-Car. ....	58
Figure 48. Roll-Time History for T222-Pickup. ....	58
Figure 49. Pitch-Time History for T222-Pickup. ....	59
Figure 50. Yaw-Time History for T222-Pickup. ....	59
Figure 51. Occupant Impact Velocity for T222-Car. ....	60
Figure 52. Ridedown Acceleration for T222-Car. ....	60
Figure 53. Roll, Pitch, Yaw for T222-Car. ....	61
Figure 54. Occupant Impact Velocity for T222-Truck. ....	62
Figure 55. Ridedown Acceleration for T222-Truck. ....	62
Figure 56. Roll, Pitch, Yaw for T222-Truck. ....	63
Figure 57. Roll-Time History F-Shape-Car. ....	69
Figure 58. Pitch-Time History for F-Shape-Car. ....	70
Figure 59. Yaw-Time History for F-Shape-Car. ....	70
Figure 60. Roll-Time History for F-Shape-Truck. ....	71
Figure 61. Pitch-Time History for F-Shape-Truck. ....	71
Figure 62. Yaw-Time History for F-Shape-Truck. ....	72
Figure 63. Occupant Impact Velocity for F-Shape-Car. ....	72
Figure 64. Ridedown Acceleration for F-Shape-Car. ....	73
Figure 65. Roll, Pitch, Yaw for F-Shape-Car. ....	73
Figure 66. Occupant Impact Velocity for F-Shape-Truck. ....	74
Figure 67. Ridedown Acceleration for F-Shape-Truck. ....	74
Figure 68. Roll, Pitch, Yaw for F-Shape-Truck. ....	75
Figure 69. Yield Line Analysis of Concrete Parapet for Impact within Wall Segment (20). ....	80
Figure 70. Yield Line Analysis of Concrete Parapet for Impact Near End of Segment (20). ....	81
Figure 71. Roadside Thrie-Beam Guardrail System (26). ....	85
Figure 72. Finite Element Model of Roadside Thrie-Beam Guardrail System. ....	86
Figure 73. MASH Test Vehicles: (a) 1100C and (b) 2270P. ....	86
Figure 74. Front Tire of Car Contacts Post in RTGS (T = 0.08 sec). ....	88
Figure 75. Wheel Snagging on Post during Car Interaction with RTGS (T = 0.24 sec). ....	88
Figure 76. Rear of Car Interacts with RTGS (T = 0.335 sec). ....	88

Figure 77. Car Exits RTGS in Stable Manner (T = 0.865 sec).....	89
Figure 78. Effective Plastic Strain in RTGS Rail Segment during Passenger Car Impact at CIP. ....	89
Figure 79. Front Tire of Pickup Truck Contacts Post in RTGS (T = 0.08 sec). ....	91
Figure 80. Pickup Truck Interaction with RTGS (T = 0.22 sec). ....	91
Figure 81. Rear of Pickup Truck Interacts with RTGS (T = 0.29 sec). ....	91
Figure 82. Maximum Roll of Pickup Truck after Exiting System (T = 0.93 sec). ....	92
Figure 83. Effective Plastic Strain in RTGS Rail Segment during Pickup Truck Impact at CIP. ....	92
Figure 84. MGS with Shortened Blockout (23).....	93
Figure 85. Finite Element Model of MGS with Shortened Blockout. ....	94
Figure 86. Front Tire of Car Contacts Post in MGS with Shortened Blockout (T = 0.08 sec). ...	95
Figure 87. Car Interaction with MGS with Shortened Blockout (T = 0.31 sec).....	96
Figure 88. Post Impact Trajectory of Car for MGS with Shortened Blockout (T = 1.1 sec).....	96
Figure 89. Effective Plastic Strain of MGS Rail Segment Impacted by Passenger Car at CIP....	96
Figure 90. Front Tire of Pickup Truck Interacts with Post (T = 0.1 sec). ....	98
Figure 91. Truck Interaction with MGS with Shortened Blockout System (T = 0.25 sec). ....	98
Figure 92. Rear of Pickup Truck Interacts with MGS with Shortened Blockout System (T = 0.38 sec). ....	98
Figure 93. Pickup Truck Exits MGS with Shortened Blockout System in Stable Manner (T = 0.79 sec). ....	99
Figure 94. Effective Plastic Strain of RTGS Rail Segment Impacted by Pickup Truck at CIP. ..	99
Figure 95. Probability Density Function for Impact Speed for Posted Speed Limit of 80 mph. ....	115
Figure 96. Estimated Economic Value of Project.....	116

## LIST OF TABLES

	Pages
Table 1. On-System, One-Motor Vehicle Crashes. ....	11
Table 2. Object Struck Parameter versus Type of Injuries. ....	12
Table 3. Impact Speed and Angle Statistics for Segregated Data by Speed Limit (9). ....	18
Table 4. Descriptive Statistics for Impact Speed for New Updated Data for Speed Limit. ....	20
Table 5. Predicted 85th Percentile Impact Speed through Linear Regression.....	20
Table 6. Descriptive Statistics for Impact Angle for New Updated Data for Speed Limit. ....	20
Table 7. Predicted 85th Percentile Impact Angle through Linear Regression.....	20
Table 8. Case 1: Descriptive Statistics of Impact Speed for 17-43 Database.....	22
Table 9. Case 1: Predicted 85th Percentile Impact Speed through Linear Regression.....	22
Table 10. Case 1: Descriptive Statistics for Impact Angle of 17-43 Database.....	22
Table 11. Case 1: Predicted 85th Percentile Impact Angle through Linear Regression.....	23
Table 12. Case 2: Descriptive Statistics for Impact Speed of 17-43 Database.....	23
Table 13. Case 2: Predicted 85th Percentile Impact Speed through Linear Regression.....	24
Table 14. Case 2: Descriptive Statistics for Impact Angle of 17-43 Database.....	24
Table 15 Case 2: Predicted 85th Percentile Impact Angle through Linear Regression.....	25
Table 16. Case 3: Descriptive Statistics for Impact Speed of 17-43 Database.....	25
Table 17. Case 3: Predicted 85th Percentile Impact Speed through Linear Regression.....	26
Table 18. Case 3: Descriptive Statistics for Impact Angle of 17-43 Database.....	26
Table 19. Case 3: Predicted 85th Percentile Impact Angle through Linear Regression.....	26
Table 20. Case 4: Descriptive Statistics for Impact Speed of 17-43 Database.....	27
Table 21. Case 4: Predicted 85th Percentile Impact Speed through Linear Regression.....	27
Table 22. Case 4: Descriptive Statistics for Impact Angle of 17-43 Database.....	27
Table 23. Case 4: Predicted 85th Percentile Impact Angle through Linear Regression.....	28
Table 24. Case 5: Descriptive Statistics for Impact Speed of 17-43 Database.....	28
Table 25. Case 5: Predicted 85th Percentile Impact Speed through Linear Regression.....	29
Table 26. Case 5: Descriptive Statistics for Impact Angle of 17-43 Database.....	29
Table 27. Case 5: Predicted 85th Percentile Impact Angle through Linear Regression.....	30
Table 28. Case 6: Descriptive Statistics for Impact Speed of 17-43 Database.....	30
Table 29. Case 6: Predicted 85th Percentile Impact Speed through Linear Regression.....	31
Table 30. Case 6: Descriptive Statistics for Impact Angle of 17-43 Database.....	31
Table 31. Case 6: Predicted 85th Percentile Impact Angle through Linear Regression.....	32
Table 32. Summary of 17-43 Data Analysis Cases. ....	33
Table 33. R <sup>2</sup> Value versus Roadway Classification.....	33
Table 34. Proposed Impact Conditions for Very High Speed Roadways.....	34
Table 35. SSCB Impact Conditions for Passenger Car.....	36
Table 36. SSCB Impact Conditions for Pickup Truck.....	36
Table 37. Impact Behavior of Passenger Car with SSCB System.....	37
Table 38. Impact Behavior of Pickup Truck with SSCB System.....	38
Table 39. Occupant Risk Comparison for SSCB-Car.....	44
Table 40. Occupant Risk Comparison for SSCB System-Truck.....	45
Table 41. FEA Validation of SSCB.....	46
Table 42. SSTR Impact Conditions for Passenger Car.....	46
Table 43. SSTR Impact Conditions for Pickup Truck.....	46

Table 44. Impact Behavior of Passenger Car with SSTR System. ....	47
Table 45. Impact Behavior of Pickup Truck with SSTR System. ....	48
Table 46. Occupant Risk Factors for SSTR System-Car. ....	51
Table 47. Occupant Risk Factors for SSTR System-Truck. ....	53
Table 48. T222 Impact Conditions for Passenger Car. ....	53
Table 49. T222 Impact Conditions for Pickup Truck. ....	54
Table 50. Impact Behavior of Passenger Car with T222 System. ....	55
Table 51. Impact Behavior of Pickup Truck with T222 System. ....	56
Table 52. Occupant Risk Factors for T222-Car. ....	61
Table 53. Occupant Risk Factors for T222-Truck. ....	63
Table 54. MASH TL-3 FEA T222 System Validation. ....	64
Table 55. F-Shape Impact Conditions for Passenger Car. ....	64
Table 56. F-Shape Impact Conditions for Pickup Truck. ....	64
Table 57. Post-Impact Trajectory of Passenger Car on F-Shape System—Top View. ....	65
Table 58. Post-Impact Trajectory of Pickup Truck on F-Shape System—Top View. ....	66
Table 59. Post-Impact Trajectory of Passenger Car on F-Shape System—Front View. ....	67
Table 60. Post-Impact Trajectory of Pickup Truck on F-Shape System—Front View. ....	68
Table 61. Occupant Risk Factors for F-Shape-Car. ....	73
Table 62. Occupant Risk Factors for F-Shape-Truck. ....	75
Table 63. MASH TL-3 FEA F-Shape System Validation. ....	76
Table 64. Comparison of Occupant Risk Metrics for Passenger Car Impacting Rigid Concrete Systems. ....	76
Table 65. Comparison of Occupant Risk Metrics for Pickup Truck Impacting Rigid Concrete Systems. ....	77
Table 66. Comparison of Angular Displacements for Passenger Car Impacting Rigid Concrete Systems. ....	78
Table 67. Comparison of Angular Displacements for Pickup Truck Impacting Rigid Concrete Systems. ....	78
Table 68. Total Transverse Barrier Resistance. ....	81
Table 69. Transverse Strength for Recommended End Reinforcement Spacing and Length for 85 mph Posted Speed Limit. ....	82
Table 70. RTGS 1100C Simulation Results with Impact Point at Post. ....	87
Table 71. RTGS 1100C Simulation Results with Impact Point 2 ft Downstream of Post. ....	87
Table 72. RTGS 1100C Simulation Results with Impact Point 2 ft Upstream of Post. ....	87
Table 73. RTGS 2270P Simulation Results with Impact Point at Post. ....	90
Table 74. RTGS 2270P Simulation Results with Impact Point 2 ft Downstream of Post. ....	90
Table 75. RTGS 2270P Simulation Results with Impact Point 2 ft Upstream of Post. ....	90
Table 76. MGS with Shortened Blockout 1100C Simulation Results with Impact at Post. ....	94
Table 77. MGS with Shortened Blockout 1100C Simulation Results with Impact 2 ft Downstream of Post. ....	94
Table 78. MGS with Shortened Blockout 1100C Simulation Results with Impact 2 ft Upstream of Post. ....	95
Table 79. MGS with Shortened Blockouts 2270P Simulation Results with Impact at Post. ....	97
Table 80. MGS 2270P Simulation Results with Impact Point 2ft Downstream of Post. ....	97
Table 81. MGS 2270P Simulation Results with Impact Point 2ft Upstream of Post. ....	97
Table 82 Guardrail Crashes for 80-mph Posted Speed Limit. ....	113

SI* (MODERN METRIC) CONVERSION FACTORS				
APPROXIMATE CONVERSIONS TO SI UNITS				
Symbol	When You Know	Multiply By	To Find	Symbol
<b>LENGTH</b>				
in	inches	25.4	millimeters	mm
ft	feet	0.305	meters	m
yd	yards	0.914	meters	m
mi	miles	1.61	kilometers	km
<b>AREA</b>				
in <sup>2</sup>	square inches	645.2	square millimeters	mm <sup>2</sup>
ft <sup>2</sup>	square feet	0.093	square meters	m <sup>2</sup>
yd <sup>2</sup>	square yards	0.836	square meters	m <sup>2</sup>
ac	acres	0.405	hectares	ha
mi <sup>2</sup>	square miles	2.59	square kilometers	km <sup>2</sup>
<b>VOLUME</b>				
fl oz	fluid ounces	29.57	milliliters	mL
gal	gallons	3.785	liters	L
ft <sup>3</sup>	cubic feet	0.028	cubic meters	m <sup>3</sup>
yd <sup>3</sup>	cubic yards	0.765	cubic meters	m <sup>3</sup>
NOTE: volumes greater than 1000L shall be shown in m <sup>3</sup>				
<b>MASS</b>				
oz	ounces	28.35	grams	g
lb	pounds	0.454	kilograms	kg
T	short tons (2000 lb)	0.907	megagrams (or metric ton")	Mg (or "t")
<b>TEMPERATURE (exact degrees)</b>				
°F	Fahrenheit	5(F-32)/9 or (F-32)/1.8	Celsius	°C
<b>FORCE and PRESSURE or STRESS</b>				
lbf	poundforce	4.45	newtons	N
lbf/in <sup>2</sup>	poundforce per square inch	6.89	kilopascals	kPa
APPROXIMATE CONVERSIONS FROM SI UNITS				
Symbol	When You Know	Multiply By	To Find	Symbol
<b>LENGTH</b>				
mm	millimeters	0.039	inches	in
m	meters	3.28	feet	ft
m	meters	1.09	yards	yd
km	kilometers	0.621	miles	mi
<b>AREA</b>				
mm <sup>2</sup>	square millimeters	0.0016	square inches	in <sup>2</sup>
m <sup>2</sup>	square meters	10.764	square feet	ft <sup>2</sup>
m <sup>2</sup>	square meters	1.195	square yards	yd <sup>2</sup>
ha	hectares	2.47	acres	ac
km <sup>2</sup>	Square kilometers	0.386	square miles	mi <sup>2</sup>
<b>VOLUME</b>				
mL	milliliters	0.034	fluid ounces	oz
L	liters	0.264	gallons	gal
m <sup>3</sup>	cubic meters	35.314	cubic feet	ft <sup>3</sup>
m <sup>3</sup>	cubic meters	1.307	cubic yards	yd <sup>3</sup>
<b>MASS</b>				
g	grams	0.035	ounces	oz
kg	kilograms	2.202	pounds	lb
Mg (or "t")	megagrams (or "metric ton")	1.103	short tons (2000lb)	T
<b>TEMPERATURE (exact degrees)</b>				
°C	Celsius	1.8C+32	Fahrenheit	°F
<b>FORCE and PRESSURE or STRESS</b>				
N	newtons	0.225	poundforce	lbf
kPa	kilopascals	0.145	poundforce per square inch	lb/in <sup>2</sup>

\*SI is the symbol for the International System of Units





## CHAPTER 1. INTRODUCTION

The 82nd Texas Legislature amended Section 545.353 of the Transportation Code by adding Subsection (h-2), which permits speed limits up to 85 miles per hour on parts of the state highway system. An 85-mph speed limit can be posted if an engineering and traffic investigation determines that the speed limit is reasonable and safe for that part of the highway system.

Longitudinal barriers (e.g., guardrails, median barriers, bridge rails) are currently tested and evaluated at a design impact speed of 62 mph. For economic reasons, many existing barrier systems are optimized for the current design impact conditions and have little or no factor of safety for accommodating more severe impacts. New or modified barrier designs may be needed to withstand high-speed impacts to maintain the desired level of safety for motorists traveling on high-speed sections of highway.

The objectives of this project include determining appropriate impact conditions for roadways with posted speed limits of 75 mph and above and exploring the capability of existing or modified barriers to accommodate these impact conditions. The following sections first review applicable roadside hardware testing standards and past speed-related safety studies associated with roadside hardware treatments.

### 1.1. ROADSIDE SAFETY FEATURES CRASH TESTING GUIDELINES

The first step in designing new roadside hardware for high-speed roadways is to define the design impact requirements. The design requirements for roadside hardware are typically performance based and described by a crash test matrix with a prescribed set of impact conditions defined in terms of vehicle type, vehicle mass, impact speed, and impact angle.

The earliest guidelines for testing roadside appurtenances date back to the 1960s. Periodically, these standards have been updated to reflect changes in the vehicle fleet, impact conditions, etc.

The American Association of State Highway and Transportation Officials (AASHTO) *Manual for Assessing Safety Hardware* (MASH) is the latest in a series of documents that provides guidance on testing and evaluation of roadside safety features (1). This document was published in 2009 and represented a comprehensive update to crash test and evaluation procedures to reflect changes in the vehicle fleet, operating conditions, and roadside safety knowledge and technology. It superseded National Cooperative Highway Research Program (NCHRP) Report 350, Recommended Procedures for the Safety Performance Evaluation of Highway Features (2). AASHTO published an updated edition of the MASH document, MASH 2<sup>nd</sup> Edition, in 2016 (3). Along with this, the Federal Highway Administration (FHWA) and AASHTO adopted a joint implementation agreement that established dates for implementing MASH compliant safety hardware for new installations and full replacements on the National Highway System (NHS).

MASH was developed to incorporate changes to procedures for safety-performance evaluation of roadside safety features, and updated to reflect the changing character of the highway network and the vehicles using it (3). For example, MASH increased the weight of the pickup truck design test vehicle from 4409 lb to 5000 lb, changed the body style from a ¾-ton, standard cab to a ½-ton 4-door, and imposed a minimum height for the vertical center of gravity

of 28 inches. The increase in vehicle mass represents an increase in impact severity of approximately 13 percent for pickup truck design test vehicles with respect to the impact conditions of NCHRP Report 350 (2). The impact conditions for the passenger car test also changed. The weight of the passenger car design test vehicle increased from 1800 lb to 2420 lb, and impact angle increased from 20 degrees to 25 degrees. These changes represent an increase in impact severity of 206 percent for Test 3-10 with the small passenger car design test vehicle, with respect to the impact conditions of NCHRP Report 350.

MASH defines six test levels for longitudinal barriers. Each test level places an increasing level of demand on the structural capacity of a barrier system. The basic test level is Test Level 3 (TL-3). The structural adequacy test for this test level consists of a 5000-lb pickup truck (denoted 2270P) impacting a barrier at 62 mph and 25 degrees. The severity test consists of a 2420-lb passenger car (denoted 1100C) impacting the barrier at 62 mph and 25 degrees. Barriers on high-speed roadways on the NHS are required, at a minimum, to meet TL-3 requirements. The passenger vehicle impact speed recommended in MASH (i.e., 62 mph) was derived from analyses of reconstructed crash data collected on roads with design speeds up to 70 mph.

## **1.2. BARRIER SYSTEMS USED BY THE TEXAS DEPARTMENT OF TRANSPORTATION**

The Texas Department of Transportation (TxDOT) standards include various guardrail, median barrier, and bridge rail systems. Barrier types investigated under this project were selected by the TxDOT project panel. These included W-beam guardrail, single slope (SSCB) and F-Shape (CSB) concrete median barrier, and single slope (SSTR) and vertical (T222) concrete bridge rails.

## **CHAPTER 2. LITERATURE REVIEW**

Determination of impact conditions for single vehicle run-off-road crashes requires in-depth investigation and reconstruction of detailed crash data. Police-level crash data do not provide sufficient detail for this purpose. Due to the high cost associated with detailed data collection and in-depth crash investigation and reconstruction, only a few studies of this type have been performed. There have also been some limited prior investigations of barriers at higher impact speeds that were reviewed for use under this project.

### **2.1. TXDOT PROJECT 0-6071**

TxDOT funded Project 0-6071 as part of a proactive consideration of roadside safety on high-speed facilities (5,6). The first step in evaluating the performance of hardware for high-speed roadways is to define the design impact requirements. Impact conditions are generally defined by vehicle type, vehicle mass, impact speed, and impact angle.

The 0-6071 project aimed to use high design speeds (above 80 mph) on some roads for faster and more efficient travel. However, the current roadside safety hardware is tested at a speed of 62 mph, and its ability to handle higher impacts is uncertain. The objective of this research was to develop roadside safety hardware suitable for very high-speed highways. They use finite element simulations to evaluate the impact performance of various roadside safety devices and recommend design modifications for further consideration. The design vehicles chosen were those specified in MASH and included a 5000-lb pickup truck and a 2420-lb passenger car.

In the first part of the project (6071-1) (5), the researchers utilized computer simulation techniques to obtain better understanding about vehicle impact performance at high speeds. Engineering analyses and finite element simulations were used to evaluate the impact performance of selected roadside safety devices. For safety considerations, the project prioritizes the development of guardrails, bridge rails, breakaway hardware, and median barriers. They evaluated the impact performance of modified three-beam guardrails, box beam guardrails, single-slope concrete barriers, and slip-base sign supports. The results of the high-speed impact simulations into the single-slope barrier indicate marginal to unacceptable performance. While it is predicted that the single slope barrier will contain and redirect the design pickup truck in a stable manner, the occupant risk numbers and occupant compartment deformation are expected to be close to the allowable limits of the MASH criteria.

In 2015, researchers performed a crash data analysis of high-speed roads in Texas with posted speed limits of 70, 75, 80, and 85 mph (6,7). The purpose was to investigate whether MASH test guidelines were applicable for roadside safety appurtenances placed on roads with posted speed limits greater than 75 mph. A representative sample of real-world, single-vehicle, run-off-road crashes involving longitudinal barriers as the first harmful event was extracted from TxDOT's Crash Records Information System (CRIS). Specific data were compiled with respect to vehicle information including injury severity.

The relevance of current longitudinal roadside safety barriers designed for 62 mph oblique impacts was examined by determining whether injury severity has increased for real-world vehicle crashes that occurred on higher speed roads, among other factors. At the 5 percent significance level, the fatal and incapacitating injury severity percentage was not statistically

different between roadways with a 70-mph posted speed limit and those with a speed limit  $\geq$  80 mph for years 2010–2013. However, the combined crash data for all four years did show a statistically significant increase at the 5 percent level. This suggests that the 85th percentile impact speed for real-world crashes occurring on roads with posted speed limit  $\geq$  80 mph could be higher. Key study results were:

- Plots of crashes showed that fatal and incapacitating injury crashes are not concentrated in one area, but some highways consistently experienced more severe injuries for consecutive years.
- The K+A injury severity percentages increased as the posted speed limit increased from 70 mph to  $\geq$  80 mph.
- The K+A percentages between roadways with posted speed limits of 70 mph and  $\geq$  80 mph were not statistically different at the 5 percent significance level. This was consistent for every year and was attributed to the small sample size.
- The K+A percentages for the combined 2010–2013 data showed significance at the 5 percent level between 70 mph and  $\geq$  80 mph posted speed limit roads.
- Since the combined data showed a statistically significant difference, it was concluded that there is a possibility that the severity of injuries increases as the posted speed limit increases.

## **2.2. NCHRP PROJECT 17-22 CRASH DATABASE**

Under NCHRP Project 17-22, Identification of Vehicular Impact Conditions Associated with Serious Run-Off-Road Crashes, a database of reconstructed, single-vehicle, run-off-road crashes was developed. While prior analyses of impact data were based primarily on roadway functional classification, Albuquerque et al. used the 17-22 database (8) to develop impact speed and angle distributions for different posted speed values in addition to functional class and type of access control (9). In their study, they found that impact speed and impact angle were well-defined by normal distributions and that impact speed and impact angle are not well-correlated. A surprising observation is that “highways with 60 to 65 mph speed limits had higher impact speeds than roadways with 70 to 75 mph speed limits” (9). The 85th percentile values of the impact speed were 61.5 and 60 mph for highways with speed limits of 60–65 mph and 70–75 mph, respectively. Similarly, the 85th percentile impact angle values showed the same behavior with values of 31 and 27 degrees for highways with speed limits of 60–65 mph and 70–75 mph, respectively.

## **2.3. NCHRP 17-43 CRASH DATABASE**

The National Automotive Sampling System (NASS) provides the National Highway Traffic Safety Administration (NHTSA) a resource with which to conduct data collection representing a broad spectrum of American society. NASS is composed of two systems—the Crashworthiness Data System (CDS) and the General Estimates System. The NASS CDS data have detailed data on a representative, random sample of thousands of minor, serious, and fatal passenger vehicle crashes. Field research teams located at Primary Sampling Units (PSUs) across the country study crashes involving passenger cars, light trucks, vans, and utility vehicles. These

data are used to investigate injury mechanisms to identify potential improvements in vehicle design.

In 2010, NCHRP Project 17-43, Long-Term Roadside Crash Data Collection Program, was funded with the objective to develop a crash database that included roadside encroachment, impact, trajectory, and terrain data. The NCHRP 17-43 database was developed as a relational database interfacing with the NASS CDS database (10). All crashes included in the 17-43 database were clinically reconstructed to estimate impact speed and impact angle among other data elements.

The NCHRP 17-43 database consists of nine related tables. The highest-level table is the Road Table. The Roadside and Trajectory tables are children of the Road Table. The tables regarding roadside objects and rollovers are children of the Trajectory Table.

Roadside and Trajectory tables are linked to the Road Table through the case year, PSU, case number, and vehicle number. The Trajectory Table has one record for each event recorded in NASS-CDS containing the details of the vehicle leading up to and during that event.

## **2.4. NCHRP PROJECT 17-79**

Under NCHRP Project 17-79, Safety Effects of Raising Speed Limits to 75 mph and Higher, researchers investigated crash testing parameters (specifically impact speed and angle) for high-speed roadways with the NCHRP 17-43 database and associated NASS-CDS crash data (11). They obtained a beta version (20190624) of the NCHRP 17-43 database for the analysis. This version of the NCHRP 17-43 database contained 1,582 crashes between 2011–2015.

The crashes were grouped in posted speed categories of 50–55 mph, 60–65 mph, and 70–75 mph. An inclusive 50–75 mph posted speed category was also considered. Crashes that involved a rollover event were excluded from the analysis.

Weighted cumulative distribution functions were developed based on the weighted number of cases calculated through use of the ratio inflation factor to adjust for differences between actual and estimated totals. The 85th percentile impact speed and impact angle were determined for each posted-speed limit roadway category.

The Texas A&M Transportation Institute (TTI) researchers utilized linear regression of the 85th percentile impact speed and angle values to extrapolate the impact speed and angle for roadways with an 85-mph posted speed limit. The analysis suggested an impact speed of 69 mph and an impact angle of 33.5 degrees for designing roadside hardware for roadways with a posted speed limit of 85 mph.

The analysis suggested that a higher impact speed and impact angle may be appropriate for roadways with posted speed limits in the 70–75 mph category. The weighted 85th percentile impact speed and angle for this speed category were 67.7 mph and 33 degrees, respectively. These values are different from the impact conditions of the 62-mph speed and 25-degree angle utilized in MASH for evaluating roadside hardware for high-speed applications. The number of crashes in the posted speed category was limited, and further investigation was recommended to confirm these results.

## **2.5. BARRIER BEHAVIOR**

For economic reasons, many roadside safety features are optimized for the currently prescribed design MASH impact conditions and may have little or no factor of safety for accommodating more severe impacts. The potential increases in test impact speed and angle recommended for evaluating roadside safety devices for higher speed roadways will place more structural demand on barrier systems, may aggravate stability problems associated with some existing barriers, and will may necessitate the redesign of some roadside appurtenances.

### **2.5.1. Rigid Concrete Barrier**

Concrete barriers are frequently used as bridge rails or in narrow medians along high-speed, high-volume roadways due to their negligible deflection, low life-cycle cost, and maintenance-free characteristics. The rigid nature of these concrete barriers results in essentially no dynamic deflection. Thus, vehicle deceleration rates and probability of injury are greater for concrete barriers than for more flexible systems. Although the installation cost is relatively high, concrete barriers require little maintenance or repair after an impact. This reduces the risk of maintenance personnel and congestion due to lane closures.

Concrete median barriers in TxDOT standards include the 32-inch F-Shape and 42-inch SSCB. Concrete bridge rails in TxDOT standards include the 36-inch SSTR and 36-inch vertical parapet (T222) among others. The F-Shape and single slope profiles promote some vehicles' climb compared to the vertical parapet. A vertical wall of proper height reduces vehicle climb but will impart slightly higher decelerations and cause more vehicle damage.

### **2.5.2. Midwest Guardrail System**

As stated in the AASHTO (2002) Roadside Design Guide, "A roadside barrier is a longitudinal barrier used to shield motorists from natural or man-made obstacles located along either side of a traveled way" (12). A barrier is typically warranted when the consequences of a vehicle leaving the traveled way and striking a fixed object or traversing a terrain feature are judged to be more severe than striking the barrier.

The most common configuration of guardrail is the strong-post W-beam guardrail commonly referred to as the Midwest Guardrail System (MGS). TxDOT includes a variation of this system with 8-inch-deep offset blocks in its standards. The mounting height of the W-beam rail is 31 inches and moves the rail splice locations to be located midspan between the support posts, which may be wood or steel.

Various applications of the MGS W-beam guardrail system have been successfully crash tested in accordance with MASH TL-3 impact conditions. However, when tested on a 7:1 flare rate at an effective impact angle of 33 degrees and a nominal speed of 62 mph under MASH Test 3-10 impact conditions, the W-beam rail ruptured, resulting in failure to contain the 1100C passenger car (13). The MGS guardrail system was subsequently tested per MASH Test 3-11 impact conditions installed on an 11:1 flare at a reduced effective impact angle of 30.2 degrees. During the impact, the upstream terminal anchor failed, permitting the pickup truck to penetrate behind the guardrail system (13). Based on the results of these full-scale crash tests,

it is unknown whether the current strong-post MGS system can accommodate increased test impact severity associated with higher impact speeds.

## **2.6. RELATIONSHIP BETWEEN POSTED SPEED LIMIT AND OPERATING SPEED**

Speed is used both as a design criterion to promote consistency and as a performance measure to evaluate highway and street designs. Geometric design practitioners and researchers are, however, increasingly recognizing that the current design process does not ensure consistent roadway alignment or driver behavior along these alignments. Strong relationships between design speed, operating speed, and posted speed limit would be desirable, and these relationships could be used to design and build roads that would produce the speed desired for a facility.

Design speed is a selected speed used to determine the various geometric features of the roadway. It is the safe speed that can be maintained over a specified section of highway when conditions are so favorable that the design features of the highway govern. The selected design speed is with respect to the anticipated operating speed, topography, the adjacent land use, and the functional classification of the highway.

The operating speed is the speed at which drivers are observed operating their vehicles. The 85th percentile of a sample of observed speeds is the most frequently used descriptive statistic for the operating speed associated with a particular location or geometric feature. Posted speed refers to the maximum speed limit posted on a section of highway using the regulatory sign.





## CHAPTER 3. DATA COLLECTION AND ANALYSIS

### 3.1. DATA COLLECTION

The applicability of currently available data for the assessment of commonly used generic longitudinal barrier systems installed on Texas roadways with different posted speed limits was assessed. Databases considered for use in the analyses are:

- **National Automotive Sampling System—Crashworthiness Data System and Crash Investigation Sampling System (CISS)** collect data on approximately 5,000 and 3,000 cases annually, respectively. The database is maintained by NHTSA. The NASS CDS/CISS database has detailed data on a representative, random sample of thousands of minor, serious, and fatal passenger vehicle crashes. Field research teams located at PSUs across the country study crashes involving passenger cars, light trucks, vans, and utility vehicles. These data are used to investigate injury mechanisms to identify potential improvements in vehicle design.
- **Event Data Recorder Data** are collected from vehicles involved in crashes and include data on vehicle kinematics during the crash event such as time series data for vehicle speed, delta-v, pedal application, and steering wheel application. These data have been combined in a database with NASS CDS/CISS data by researchers at Virginia Tech.
- **NCHRP Project 17-22 Database** includes reconstructed run-off-the-road crashes. The data are segregated by posted speed limits. The database was developed using data from 1998–2001; therefore, the Performing Agency suggests using newer datasets that better reflect current operating conditions, posted speed limits, and vehicle fleet characteristics.
- **NCHRP 17-43 Database** includes reconstructed run-off-the-road crashes and was developed using more recent crash data. The current database contains a total of 1,582 crash cases from 2011–2015 and includes data related to crashes that occurred on highways having posted speed limits up to 75 mph. This version also includes an “Object Angle” variable that records the impact angle of the vehicle with respect to the impacted object.
- **Crash Records Information Systems** contains Texas crash data collected from Texas Peace Officer Crash Reports (form CR-3). CRIS contains data from the year 2011 to current date. The data include crashes that occur on public roadways and result in a death, injury, and/or \$1,000 in damage.
- **Roadway Highway Inventory Network Offload (RHiNO) database** includes a variety of roadway characteristics. The location data in CRIS can be linked to RHiNO data to gain further information about the roadway inventory data.
- **TxDOT Speed Limits Data** are an extract from the Geospatial Roadway Inventory Database (GRID) that is used for managing roadway assets in Texas. Extracts from GRID are made on a regular basis and reflect the state of the data at that moment. It is available from the TxDOT Open Data Portal.

### 3.2. SAFETY DATA ANALYSIS

Texas has some unique characteristics in that most rural interstates and significant miles on rural highways have a posted speed limit of 75 mph and above. However, most of the crash

investigation databases listed above do not have many crashes where the posted speed limit was 75 mph and above. Therefore, identifying the impact conditions for 75-mph roadways using these databases is challenging. Safety data analysis was performed to identify the underperforming barrier systems on high-speed roadways, where a high-speed roadway is defined as a roadway segment having a speed limit of 75 mph and above. The researchers conducted exploratory data analysis (EDA) and cross-sectional data analysis using the most relevant barrier impact data to determine how commonly used generic longitudinal barrier systems are performing on Texas roadways with high posted speeds relative to barriers installed on roadways with posted speeds of 70 mph and below.

### **3.2.1. Exploratory Data Analysis**

Using CRIS data, extracted on November 16, 2021, for the years 2016 to 2021, and TxDOT's speed limit data, available through the TxDOT Open Data Portal, crashes were linked with the roadway speed limit data using ArcMap. The speed limit data are a subset of the larger GRID. The CRIS data only included crashes that were identified as "TxDOT reportable," which means they occurred on a public roadway and resulted in a fatality or injury or in \$1000 or more of damage.

The linked data were filtered to developed two data sets: crashes on roadways with speed limits of greater than 70 mph and crashes on roadways with speed limits between 50 and 70 mph. The resulting data sets were used to develop a Power Bi report that allows for the interactive exploration of the data. While analyzing the CRIS database, six different object-struck parameters were considered: hit concrete traffic barrier, hit end of bridge (abutment or rail end), hit guard post and guardrail, hit median barrier, hit side of barrier (bridge rail), hit work zone barricades, codes, signs, or material.

Table 1 shows the number of crashes and types of injuries for on-system, one-motor vehicle crashes extracted from the Power Bi Database. Table 2 lists the number of crashes based on object struck parameters and injury types from 2016 to September 2021, which helps determine which object is more crucial for which sort of injury.

Figure 1 to Figure 6 provide percentage values in a bar chart of injury type versus object struck. These figures help with visualization of the injury data.

The data were also analyzed for all six object struck categories to examine injury frequency for the combined high posted speed categories. The Power Bi report was filtered for different injury types for speed limits of 75, 80, and 85 mph, as shown in Figure 7 to Figure 10.

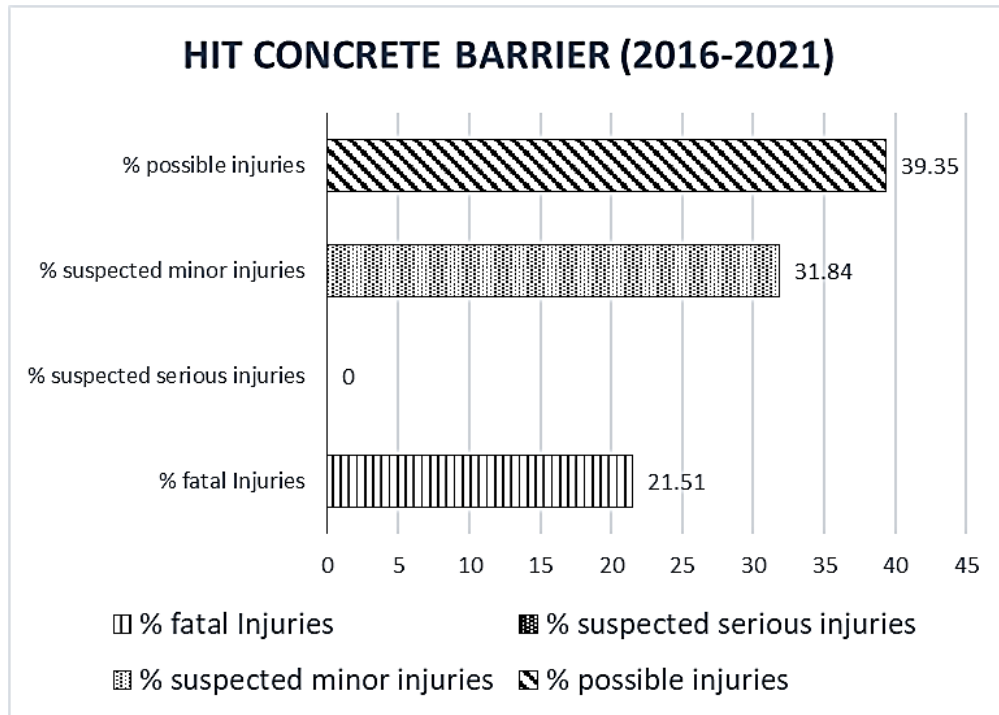
**Table 1. On-System, One-Motor Vehicle Crashes.**

Crash Year	Fatal Injuries			Serious Injuries			Minor Injuries			Possible Injuries		
Speed (mph)	75	80	85	75	80	85	75	80	85	75	80	85
2016	27	3	—	82	3	—	341	13	3	382	12	4
2017	30	1	—	97	7	1	331	14	—	357	8	1
2018	32	1	—	95	3	—	339	24	—	393	15	—
2019	25	4	—	65	5	1	282	20	—	386	16	—
2020	37	1	—	83	8	—	304	11	—	342	17	1
2021 (Till September)	30	4	1	100	7	—	286	24	—	321	15	—
Individual Total	181	14	1	522	33	2	1883	106	3	2181	83	6
Total	196			557			1992			2270		
% Total no. of Injuries	3.80	5.93	8.33	10.95	13.98	16.67	39.50	44.92	25.00	45.75	35.17	50.00

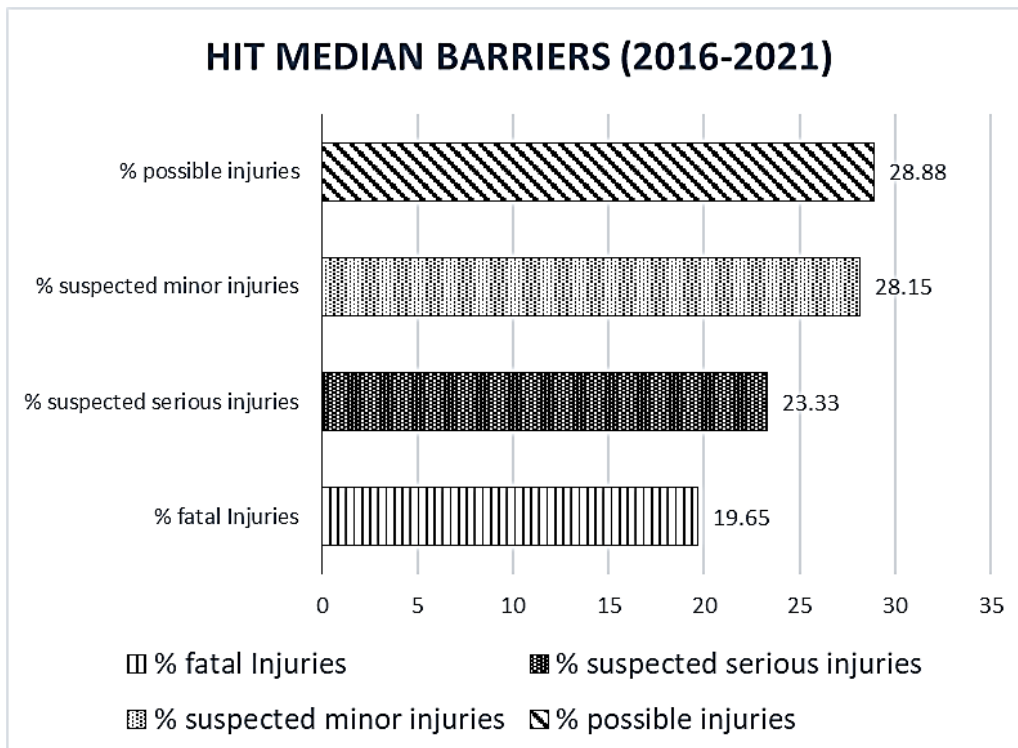
Note: — = not applicable.

**Table 2. Object Struck Parameter versus Type of Injuries.**

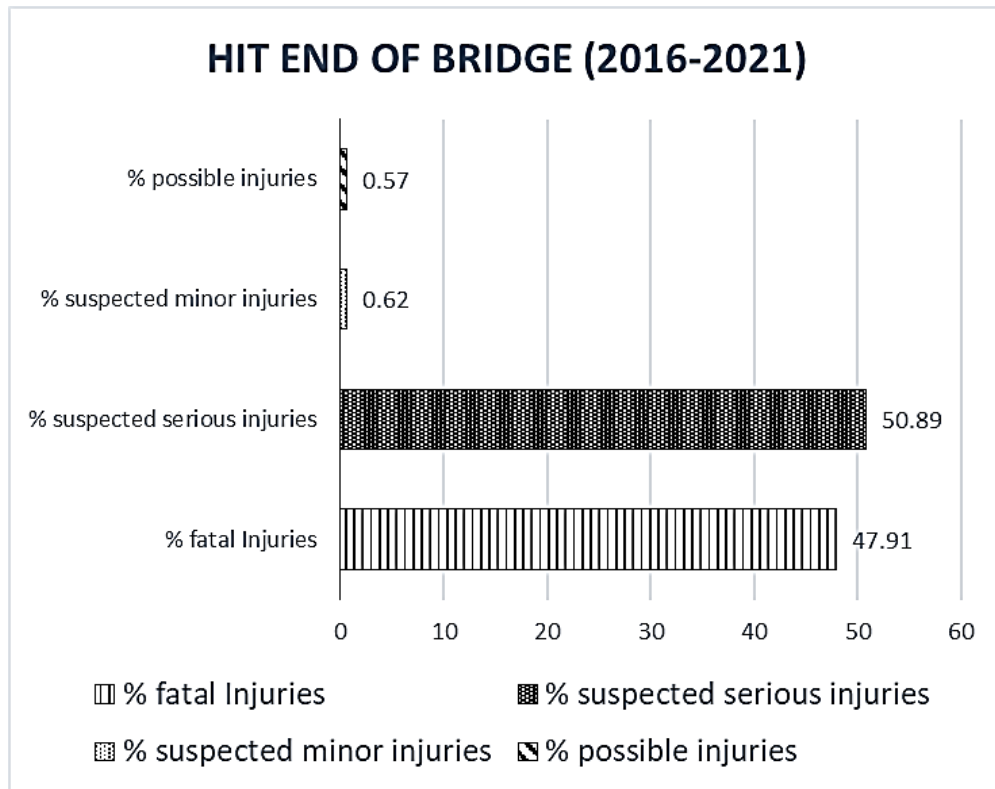
<b>Object Struck Properties</b>	<b>Speed (mph)</b>	<b>Type of Injuries</b>							
		Fatal Injuries	% Fatal Injuries	Serious Injuries	% Serious Injuries	Minor Injuries	% Minor Injuries	Possible Injuries	% Possible Injuries
Hit Concrete Traffic Barrier	75	15	8.29	0	0	197	10.46	232	10.63
	80	2	2.13	0	0	9	8.49	7	8.43
	85	0	0	0	0	0	0	0	0
Hit Guard Post	75	1	0.55	0	0	0	0	0	0
	80	0	0	0	0	0	0	0	0
	85	0	0	0	0	0	0	0	0
Hit Guardrail	75	82	45.31	212	40.62	595	31.6	571	26.18
	80	5	5.32	18	54.54	58	54.71	49	59.04
	85	0	0	2	100	3	100	3	50
Hit Median Barrier	75	121	66.85	387	74.14	1459	77.48	1702	78.03
	80	11	11.7	29	87.88	83	78.3	70	84.38
	85	1	100	1	50	3	100	6	100
Hit Work Zone Barricade	75	12	6.63	33	6.32	61	3.24	76	3.48
	80	0	0	0	0	7	6.61	1	1.21
	85	0	0	0	0	0	0	0	0
Hit End of Bridge	75	7	3.86	2	1.1	1	0.05	1	0.046
	80	0	0	1	3	0	0	0	0
	85	0	0	0	0	0	0	0	0
Hit Side of Barrier	75	26	14.36	51	9.77	133	7.06	142	6.51
	80	0	0	0	0	9	8.49	3	3.61
	85	0	0	0	0	0	0	0	0



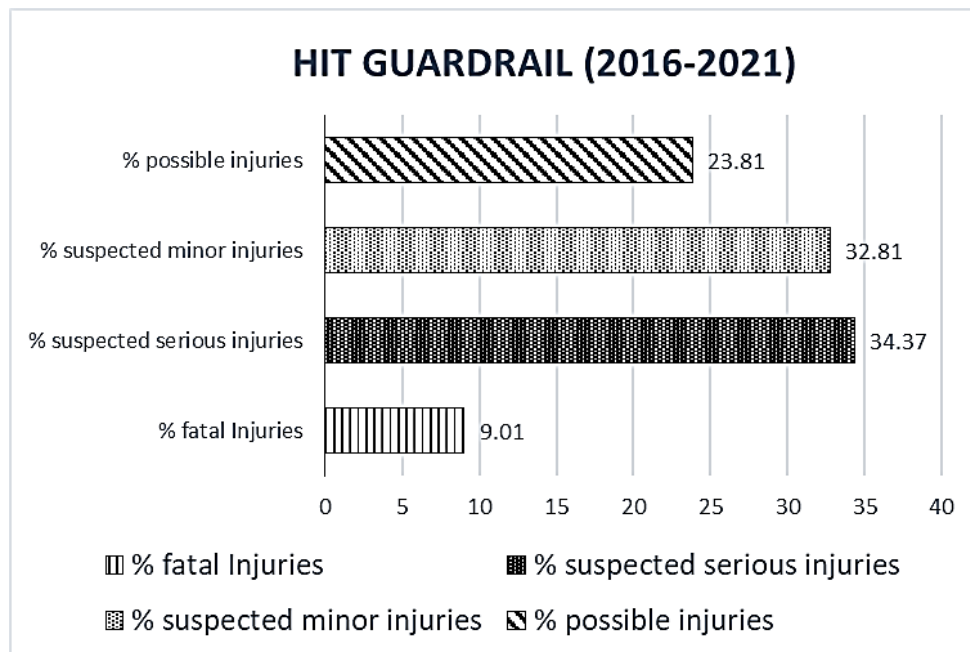
**Figure 1. Hit Concrete Barrier versus Type of Injuries.**



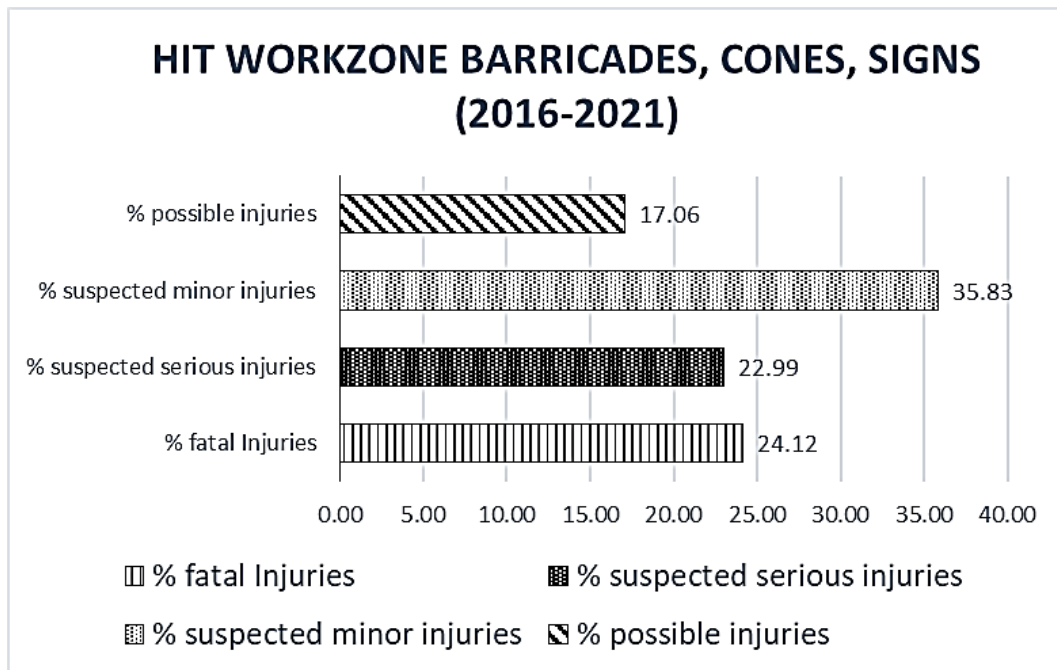
**Figure 2. Hit Median Barrier versus Type of Injuries.**



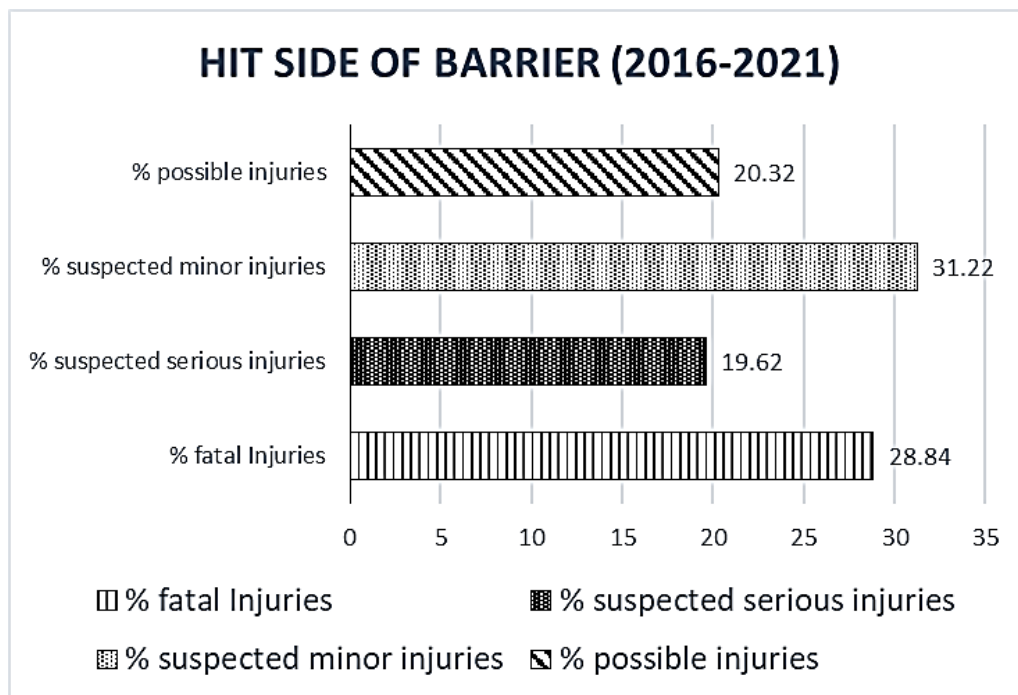
**Figure 3. Hit End of Bridge versus Type of Injuries.**



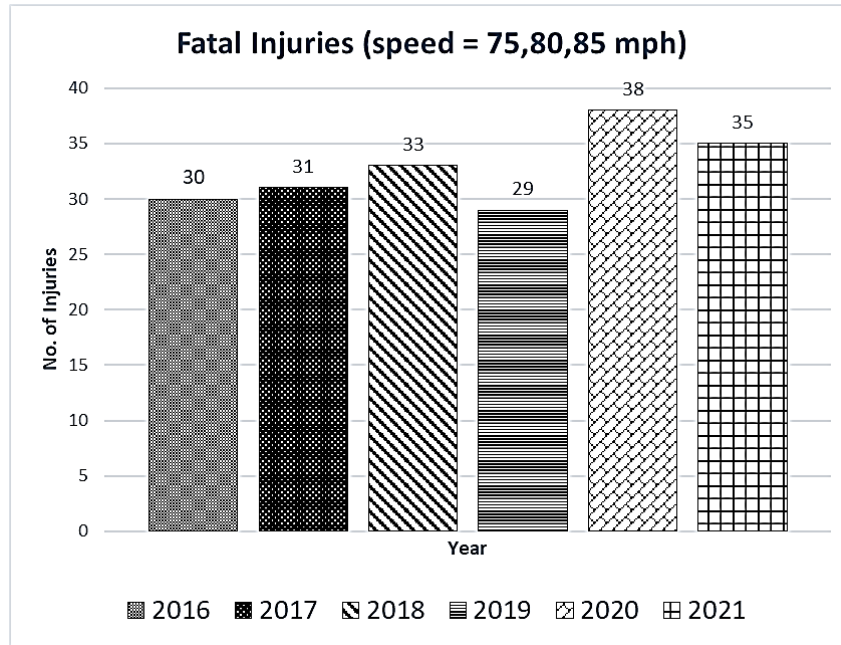
**Figure 4. Hit Guardrail versus Type of Injuries.**



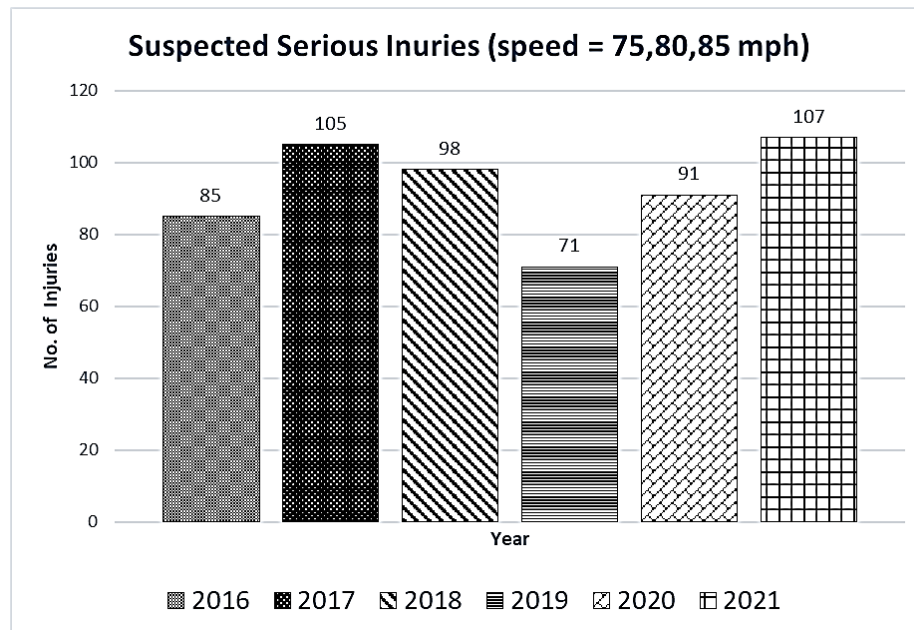
**Figure 5. Hit Work Zone Barricades, Cones, Signs versus Type of Injuries.**



**Figure 6. Hit Side of Barrier versus Type of Injuries.**

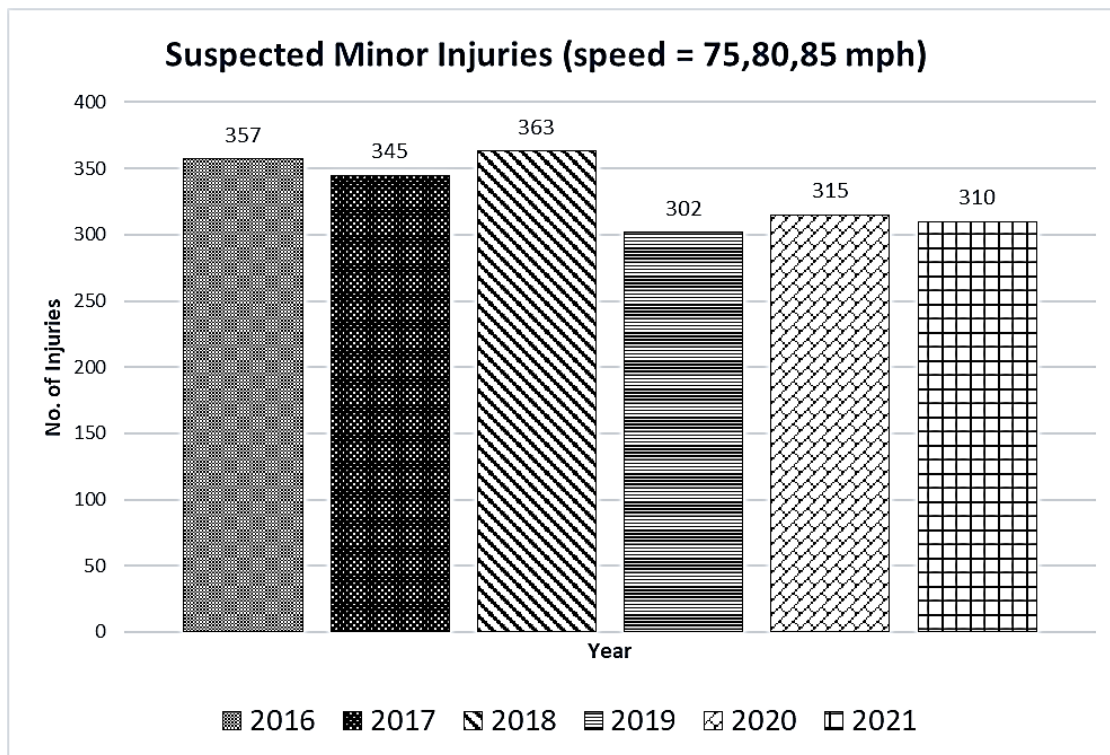


**Figure 7. Number of Fatal Injuries per Year.**

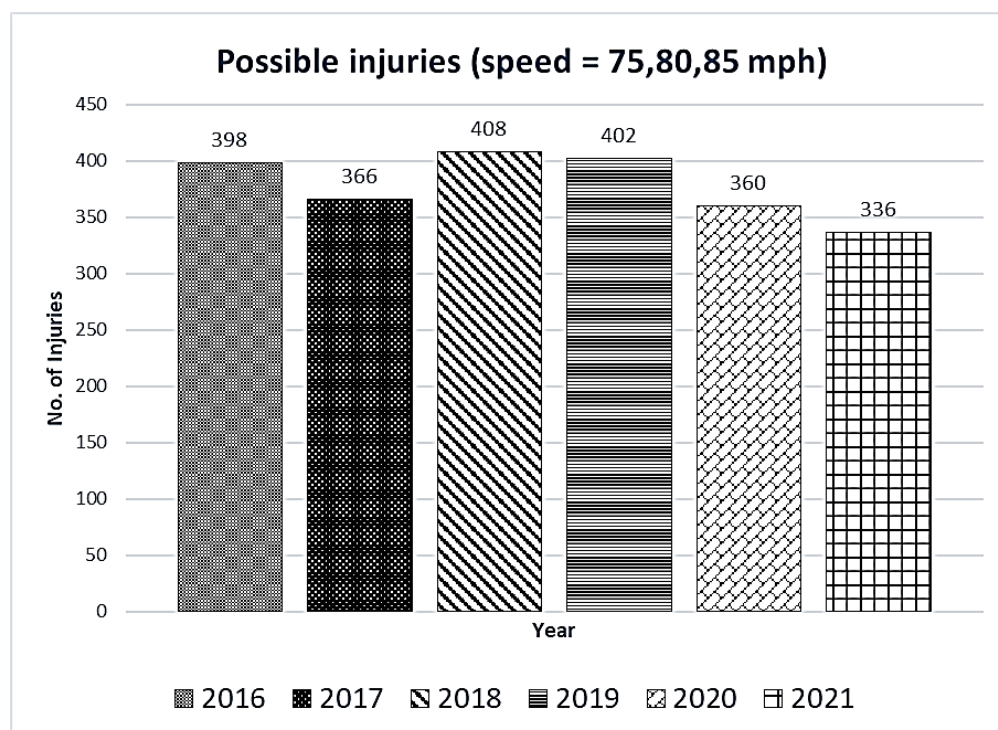


**Figure 8. Number of Serious Injuries per Year.**





**Figure 9. Number of Minor Injuries per Year.**



**Figure 10. Number of Possible Injuries per Year.**

### 3.2.2. 17-22 Database

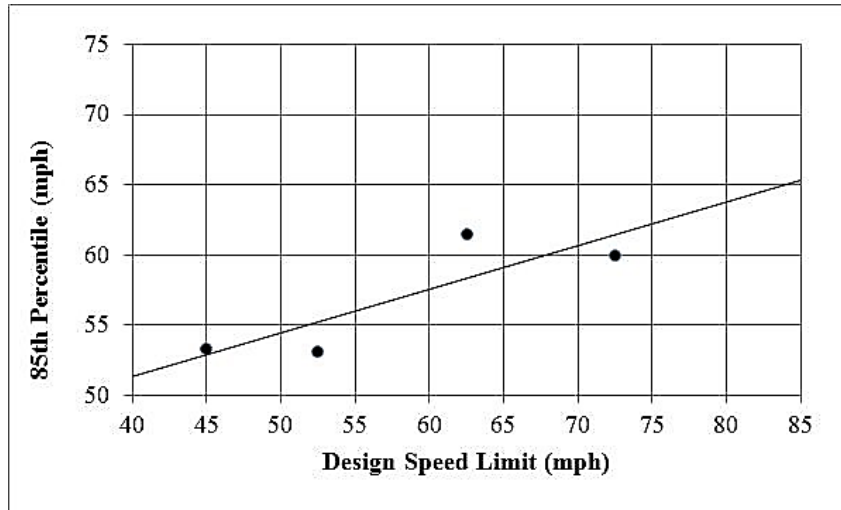
Determination of impact conditions for single-vehicle run-off-road crashes requires in-depth investigation and reconstruction of detailed crash data. Police-level crash data do not provide sufficient detail for this purpose. Due to the high cost associated with detailed data collection and in-depth crash investigation and reconstruction, few studies of this type have been performed. Under NCHRP Project 17-22, a database of reconstructed run-off-road crashes was developed (8).

Historically, the 85th percentile impact speed has been selected as a design impact speed for the testing and evaluation of roadside safety hardware. Using the 17-22 database, Albuquerque et al. found that the 85th percentile impact speed for controlled access freeways, interstate highways, and highways with a 70-mph to 75-mph design speed to be 59.7 mph, 60.1 mph, and 60.0, respectively (9). The researchers used linear regression of the 85th percentile impact speed and angle values to estimate the relationship with posted speed and extrapolate the impact speed and angle for a road segment with an 85-mph posted speed limit. Table 3 shows descriptive statistics for impact speed and angle for the 17-22 data segregated by speed limit (9). A surprising observation is that “highways with 60 to 65-mph speed limits had higher impact speeds than roadways with 70 to 75-mph speed limits” (9).

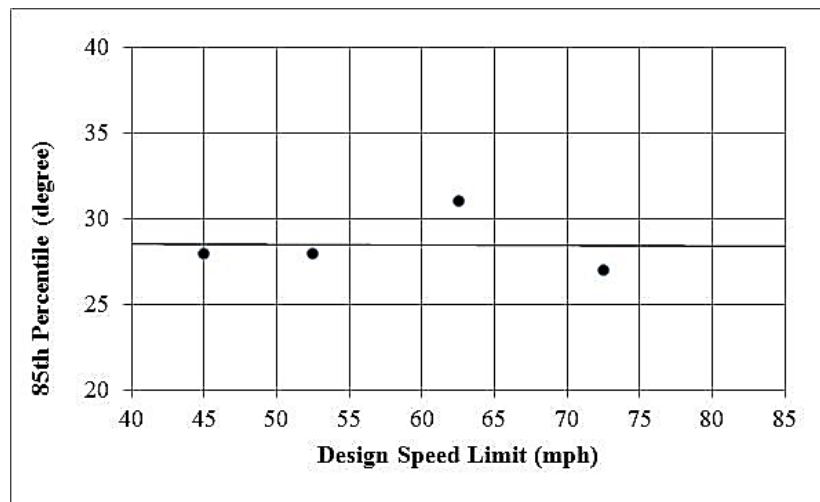
**Table 3. Impact Speed and Angle Statistics for Segregated Data by Speed Limit (9).**

<b>Posted Speed (mph)</b>	<b>N</b>	<b>Mean</b>	<b>Median</b>	<b>SD</b>	<b>Maximum 85th Percentile</b>
<b>Impact Speed (mph)</b>					
50–55	375	37.3	36.3	15.9	<b>53.1</b>
60–65	72	46.1	48	16.7	<b>61.5</b>
70–75	161	43.9	45	16.8	<b>60.0</b>
<b>Impact Angle (degrees)</b>					
50–55	422	16.9	14.0	12.4	<b>28.0</b>
60–65	73	18.7	19.0	11.0	<b>31.0</b>
70–75	166	17.7	17.0	11.3	<b>27.0</b>

Figure 11 and Figure 12 present the linear regression results for the evaluation of the 85th percentile impact speed and impact angle based on descriptive statistics from Albuquerque et al. (9).



**Figure 11. Regression Relationship for Impact Speed by Albuquerque et al. (9).**



**Figure 12. Regression Relationship for Impact Angle by Albuquerque et al. (9).**

The impact speeds suggested by Albuquerque et al. seem low. TTI researchers obtained a later version of the 17-22 database and reanalyzed the impact speed distributions associated with run-off-road crashes. To achieve sufficient sample sizing, the following posted speed categories were considered: 45 mph, 50–55 mph, 60–65 mph, and 70–75 mph. Normal distributions were fit to the data, and the 85th percentile impact speed was determined for each category of posted speed limit.

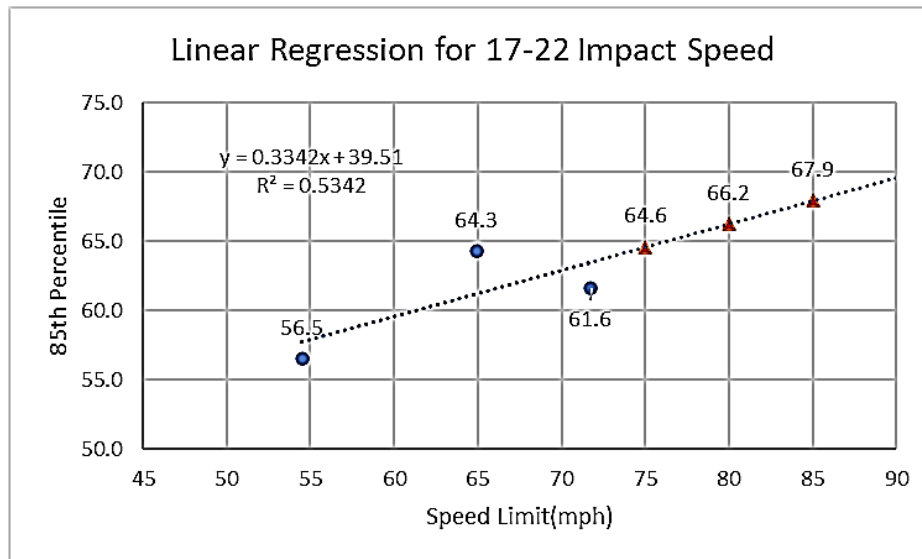
While performing the linear regression and forecasting impact data for roadways with 75, 80, and 85-mph posted speed limits, the R-squared value was examined as a measure of goodness-of-fit. This statistic indicates the percentage of the variance in the dependent variable that the independent variables collectively explain. The results of the updated data and associated linear regression relationships are presented in Table 4, Table 5, and Figure 13 for impact speed and Table 6, Table 7, and Figure 14 for impact angle. The results showed slightly higher values of impact speed compared to the previous analysis by Albuquerque et al.

**Table 4. Descriptive Statistics for Impact Speed for New Updated Data for Speed Limit.**

Speed	N	Weighted Mean	85th Percentile
50-55	418	53.58	56.5
60-65	75	63.15	64.3
70-75	169	71.07	61.6

**Table 5. Predicted 85th Percentile Impact Speed through Linear Regression.**

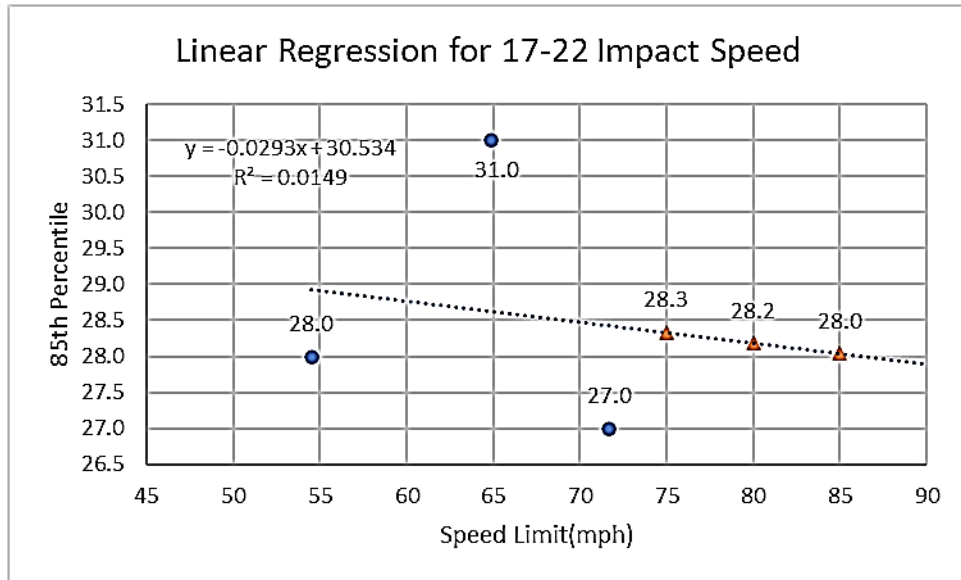
Posted Speed Limit	85th Percentile
75	<b>64.6</b>
80	<b>66.2</b>
85	<b>67.9</b>

**Figure 13. Linear Regression for 85th Percentile Impact Speed with Updated 17-22 Crash Data Set.****Table 6. Descriptive Statistics for Impact Angle for New Updated Data for Speed Limit.**

Speed	N	Weighted Mean	85th Percentile
50-55	256	53.58	26
60-65	97	63.15	17.98
70-75	58	71.07	33

**Table 7. Predicted 85th Percentile Impact Angle through Linear Regression.**

Posted Speed Limit	85th Percentile
75	<b>28.3</b>
80	<b>28.2</b>
85	<b>28.0</b>



**Figure 14. Linear Regression for 85th Percentile Impact Angle with Updated 17-22 Crash Data Set.**

### 3.2.3. 17-43 Database

NCHRP 17-43 Roadside Database was developed as a relational database interfacing with the NASS-CDS database, incorporating additional information about run-off-road crashes. It has a total of 1582 reconstructed cases from 2011–2015 that includes impact speed and angle along with other data about the event as well as roadside and the associated NASS-CDS data.

Linear regression analysis was performed for both impact speed and impact angle to obtain an estimate for high-speed roadways with posted speed limits of 75, 80, and 85 mph. The impact conditions provided in the results are based on weighted data considering the Ratwgt for each crash event included in the NASS-CDS. Ratwgt is used to obtain a national estimate from the sampled crashes.

The R-squared parameter was determined as a goodness-of-fit measure for the linear regression models. The higher the R-squared, the better the model fits the data. R-squared ( $R^2$ ) is a statistical measure that represents the percentage of the variance of a dependent variable that is explained by an independent variable or variables in a regression model. Whereas correlation explains the strength of the relationship between an independent and dependent variable,  $R^2$  explains to what extent the variance of one variable explains the variance of the second variable. So, if the  $R^2$  of a model is 0.50, then approximately half of the observed variation can be explained by the model's input.

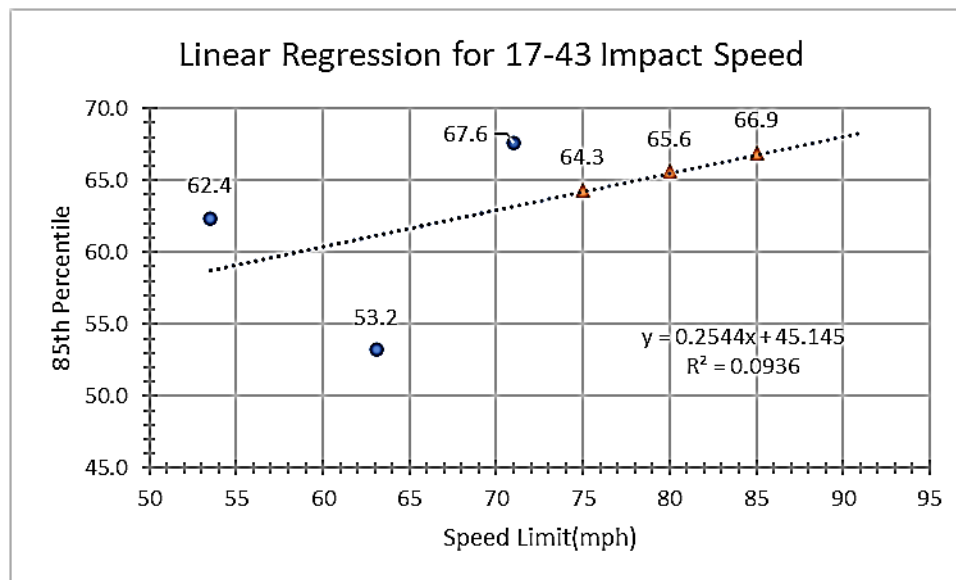
The posted speed categories were grouped due to the small sample size for some posted speed values. The regression analysis was performed for different groupings of posted speed categories to obtain the best fit of the data.

### 3.2.3.1. Case 1: Speed Categorization as 50–55 mph, 60–65 mph, 70–75 mph

Statistical linear regression analysis was performed on Case 1 of the 17-43 data, where the posted speed limit was categorized as 50–55 mph, 60–65 mph, and 70–75 mph. The descriptive statistics for this grouping of posted speeds is presented in Table 8. The linear regression results for impact speed are shown in Figure 15. The estimates of 85th percentile impact speed for posted speed limits of 75, 80, and 85 mph are summarized in Table 9. Similar data for impact angle are presented in Table 10, Figure 16, and Table 11.

**Table 8. Case 1: Descriptive Statistics of Impact Speed for 17-43 Database.**

Speed	N	Weighted Mean	85th Percentile
50–55	109	53.6	<b>62.37</b>
60–65	35	63.1	<b>53.2</b>
70–75	28	71.1	<b>67.6</b>



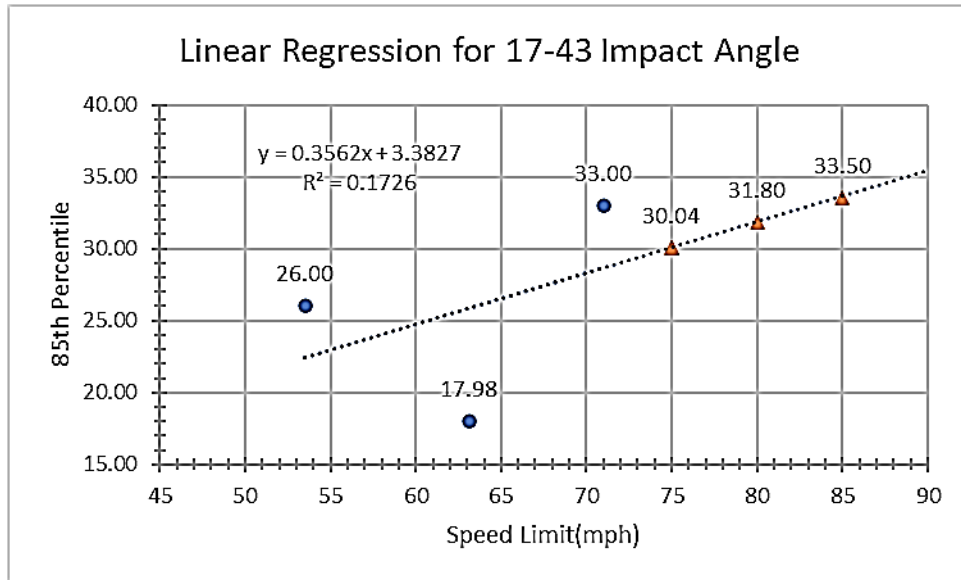
**Figure 15. Case 1: Linear Regression for 85th Percentile Impact Speed with 17-43 Crash Database.**

**Table 9. Case 1: Predicted 85th Percentile Impact Speed through Linear Regression.**

Posted Speed Limit	85th Percentile
75	<b>64.3</b>
80	<b>65.6</b>
85	<b>66.9</b>

**Table 10. Case 1: Descriptive Statistics for Impact Angle of 17-43 Database.**

Speed	N	Weighted Mean	85th Percentile
50–55	256	53.6	<b>26</b>
60–65	97	63.1	<b>17.98</b>
70–75	58	71.1	<b>33</b>



**Figure 16. Case 1: Linear Regression for 85th Percentile Impact Angle with 17-43 Crash Database.**

**Table 11. Case 1: Predicted 85th Percentile Impact Angle through Linear Regression.**

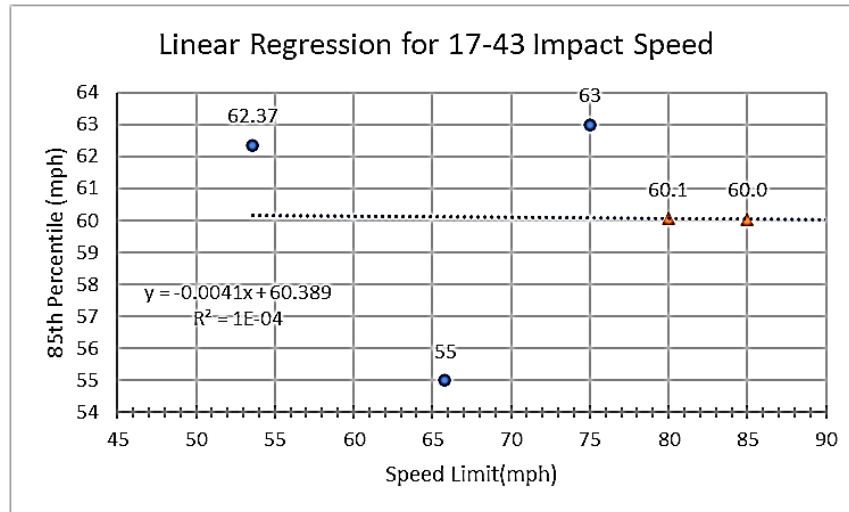
Posted Speed Limit	85th Percentile
75	<b>30.04</b>
80	<b>31.8</b>
85	<b>33.50</b>

### 3.2.3.2. Case 2: Speed Categorization as 50–55 mph, 60-65-70 mph, 75 mph

Statistical linear regression analysis was performed on Case 2 of the 17-43 data, where the posted speed limit was categorized as 50–55 mph, 60-65-70 mph, and 75 mph. The descriptive statistics for this grouping of posted speeds is presented in Table 12. The linear regression results for impact speed are shown in Figure 17. The estimates of 85th percentile impact speed for posted speed limits of 75, 80, and 85 mph are summarized in Table 13. Similar data for impact angle are presented in Table 14, Figure 18, and Table 15.

**Table 12. Case 2: Descriptive Statistics for Impact Speed of 17-43 Database.**

Speed	N	Weighted Mean	85th Percentile
50–55	109	53.6	<b>62.37</b>
60-65-70	57	65.8	<b>55</b>
75	6	75	<b>63</b>



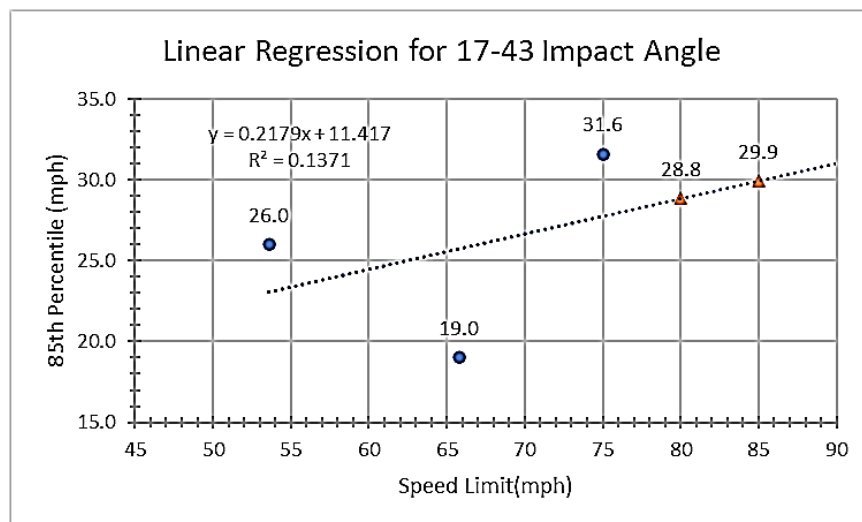
**Figure 17. Case 2: Linear Regression for 85th Percentile Impact Speed with 17-43 Crash Database.**

**Table 13. Case 2: Predicted 85th Percentile Impact Speed through Linear Regression.**

Posted Speed Limit	85th Percentile
75	<b>63</b>
80	<b>60.1</b>
85	<b>60.0</b>

**Table 14. Case 2: Descriptive Statistics for Impact Angle of 17-43 Database.**

Speed	N	Weighted Mean	85th Percentile
50-55	256	53.6	<b>26</b>
60-65-70	142	65.8	<b>19</b>
75	18	75	<b>31.61</b>



**Figure 18. Case 2: Linear Regression for 85th Percentile Impact Angle with 17-43 Crash Database.**



**Table 15 Case 2: Predicted 85th Percentile Impact Angle through Linear Regression**

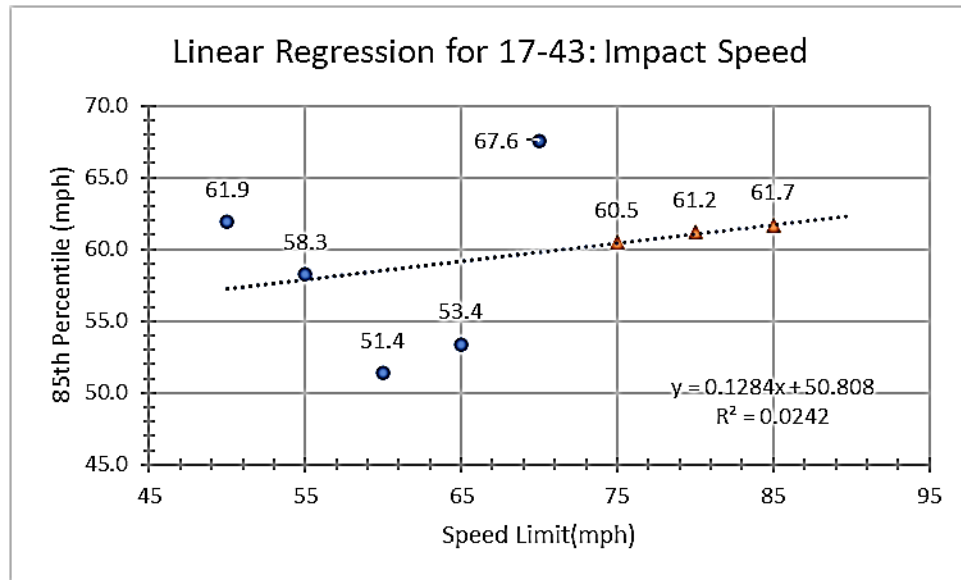
Posted Speed Limit	85th Percentile
75	<b>31.6</b>
80	<b>28.8</b>
85	<b>29.9</b>

**3.2.3.3. Case 3: Individual Speed Categorization as 50, 55, 60, 65, 70 mph**

Statistical linear regression analysis was performed on Case 3 of the 17-43 data, where the posted speed limit was categorized as 50, 55, 60, 65, and 70 mph. The descriptive statistics for this grouping of posted speeds is presented in Table 16. The linear regression results for impact speed are shown in Figure 19. The estimates of 85th percentile impact speed for posted speed limits of 75, 80, and 85 mph are summarized in Table 17. Similar data for impact angle are presented in Table 18, Figure 20, and Table 19.

**Table 16. Case 3: Descriptive Statistics for Impact Speed of 17-43 Database.**

Speed	N	Weighted Mean	85th Percentile
50	31	50	<b>61.9</b>
55	77	55	<b>58.3</b>
60	13	60	<b>51.4</b>
65	22	65	<b>53.4</b>
70	22	70	<b>67.6</b>

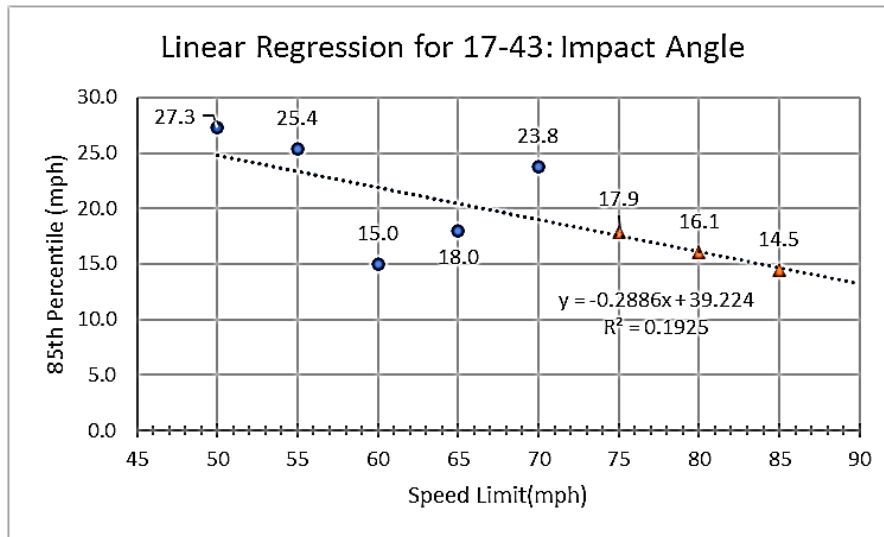
**Figure 19. Case 3: Linear Regression for 85th Percentile Impact Speed with 17-43 Crash Database.**

**Table 17. Case 3: Predicted 85th Percentile Impact Speed through Linear Regression.**

Posted Speed Limit	85th Percentile
75	<b>60.5</b>
80	<b>61.2</b>
85	<b>61.7</b>

**Table 18. Case 3: Descriptive Statistics for Impact Angle of 17-43 Database.**

Speed	N	Weighted Mean	85th Percentile
50	63	50	<b>27.3</b>
55	193	55	<b>25.4</b>
60	34	60	<b>15.0</b>
65	63	65	<b>18.0</b>
70	45	70	<b>23.8</b>

**Figure 20. Case 3: Linear Regression for 85th Percentile Impact Angle with 17-43 Crash Database.****Table 19. Case 3: Predicted 85th Percentile Impact Angle through Linear Regression.**

Posted Speed Limit	85th Percentile
75	<b>17.9</b>
80	<b>16.1</b>
85	<b>14.5</b>

To further analyze the impact conditions from the 17-43 database, a few additional cases were analyzed based on roadway classifications.

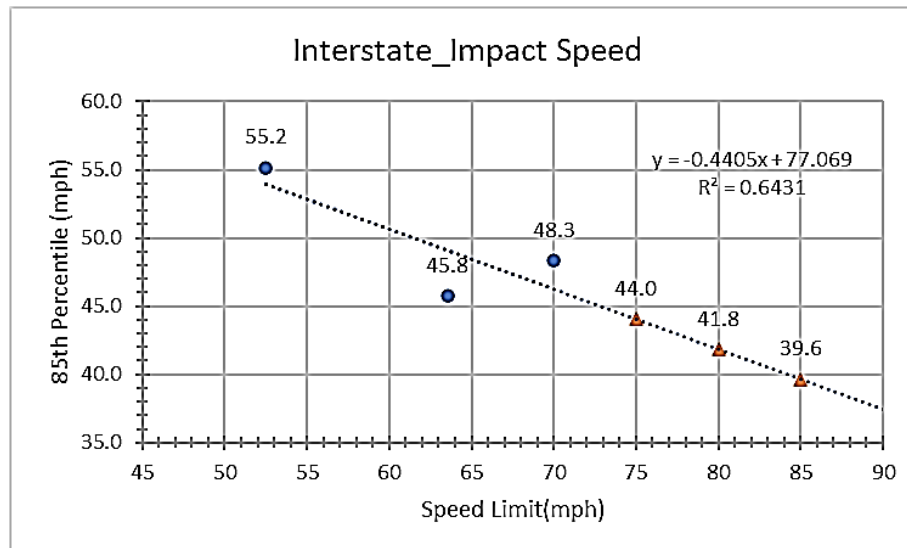
#### 3.2.3.4. Case 4: Interstate Roadways Classification for 50–55 mph, 60–65 mph, 70–75 mph Speed Categories

Statistical linear regression analysis was performed on Case 4 of the 17-43 data for interstates with posted speed limit categories of 50–55 mph, 60–65 mph, and 70–75 mph. The descriptive statistics for interstate roadways for this grouping of posted speeds is presented in

Table 20. The linear regression results for impact speed are shown in Figure 21. The estimates of 85th percentile impact speed for posted speed limits of 75, 80, and 85 mph are summarized in Table 21. Similar data for impact angle are presented in Table 22, Figure 22, and Table 23.

**Table 20. Case 4: Descriptive Statistics for Impact Speed of 17-43 Database.**

Speed	N	Weighted Mean	85th Percentile
50–55	8	52.5	<b>55.2</b>
60–65	7	63.6	<b>45.8</b>
70–75	7	70	<b>48.3</b>



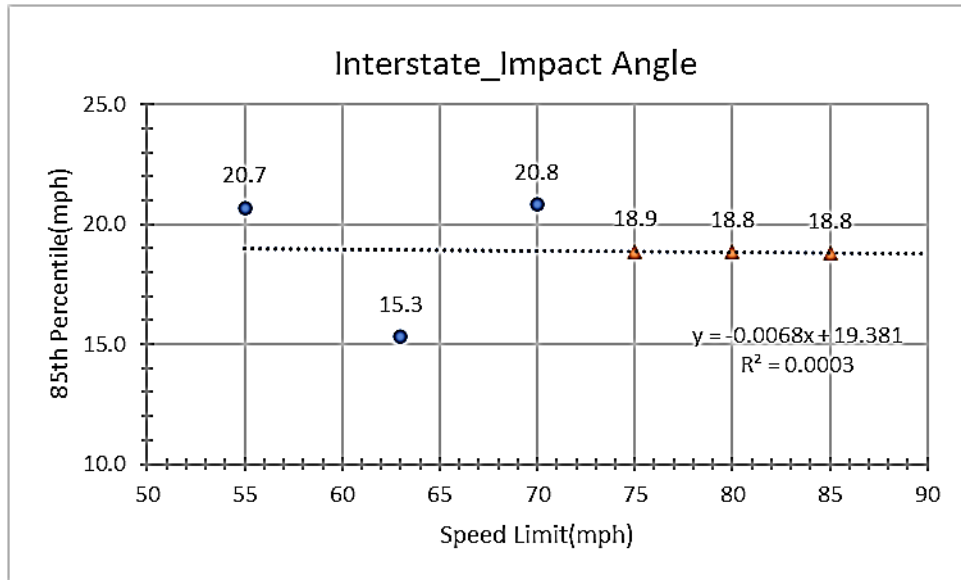
**Figure 21. Case 4: Linear Regression for 85th Percentile Impact Speed with 17-43 Crash Database.**

**Table 21. Case 4: Predicted 85th Percentile Impact Speed through Linear Regression.**

Posted Speed Limit	85th Percentile
75	<b>44.0</b>
80	<b>41.8</b>
85	<b>39.6</b>

**Table 22. Case 4: Descriptive Statistics for Impact Angle of 17-43 Database.**

Speed	N	Weighted Mean	85th Percentile
50–55	17	55	<b>20.7</b>
60–65	25	63	<b>15.3</b>
70–75	12	70	<b>20.8</b>



**Figure 22. Case 4: Linear Regression for 85th Percentile Impact Angle with 17-43 Crash Database.**

**Table 23. Case 4: Predicted 85th Percentile Impact Angle through Linear Regression.**

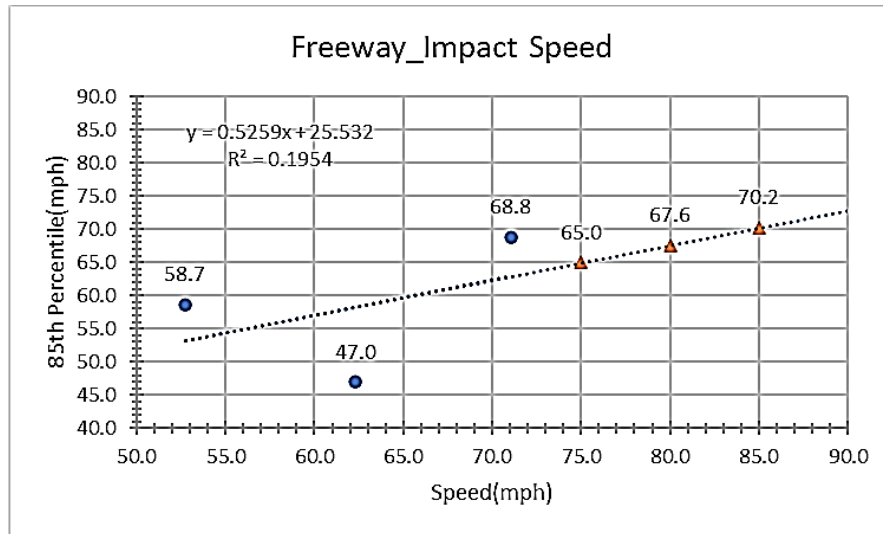
Posted Speed Limit	85th Percentile
75	<b>18.9</b>
80	<b>18.8</b>
85	<b>18.8</b>

### 3.2.3.5. Case 5: Freeway Roadways Classification for 50–55 mph, 60–65 mph, 70–75 mph Speed Categories

Statistical linear regression analysis was performed on Case 4 of the 17-43 data for freeways with posted speed limit categories of 50–55 mph, 60–65 mph, and 70–75 mph. The descriptive statistics for interstate roadways for this grouping of posted speeds is presented in Table 24. The linear regression results for impact speed are shown in Figure 23. The estimates of 85th percentile impact speed for posted speed limits of 75, 80, and 85 mph are summarized in Table 25. Similar data for impact angle are presented in Table 26, Figure 24, and Table 27.

**Table 24. Case 5: Descriptive Statistics for Impact Speed of 17-43 Database.**

Speed	N	Weighted Mean	85th Percentile
50–55	11	52.7	<b>58.66</b>
60–65	13	62.3	<b>47.00</b>
70–75	14	71.1	<b>68.81</b>



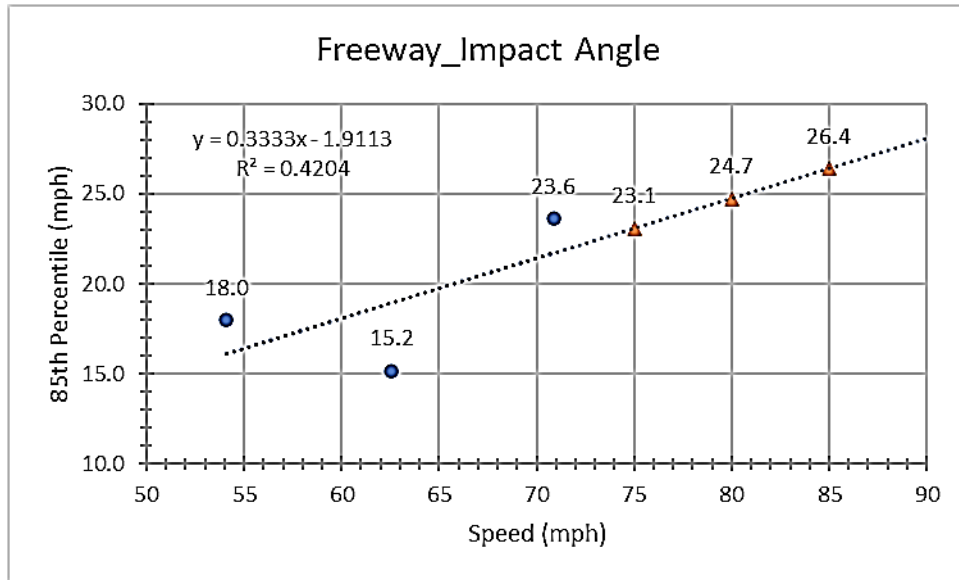
**Figure 23. Case 5: Linear Regression for 85th Percentile Impact Speed with 17-43 Crash Database.**

**Table 25. Case 5: Predicted 85th Percentile Impact Speed through Linear Regression.**

Posted Speed Limit	85th Percentile
75	<b>65.0</b>
80	<b>67.6</b>
85	<b>70.2</b>

**Table 26. Case 5: Descriptive Statistics for Impact Angle of 17-43 Database.**

Speed	N	Weighted Mean	85th Percentile
50–55	38	54.1	<b>18.00</b>
60–65	37	62.6	<b>15.15</b>
70–75	28	70.9	<b>23.63</b>



**Figure 24. Case 5: Linear Regression for 85th Percentile Impact Angle with 17-43 Crash Database.**

**Table 27. Case 5: Predicted 85th Percentile Impact Angle through Linear Regression.**

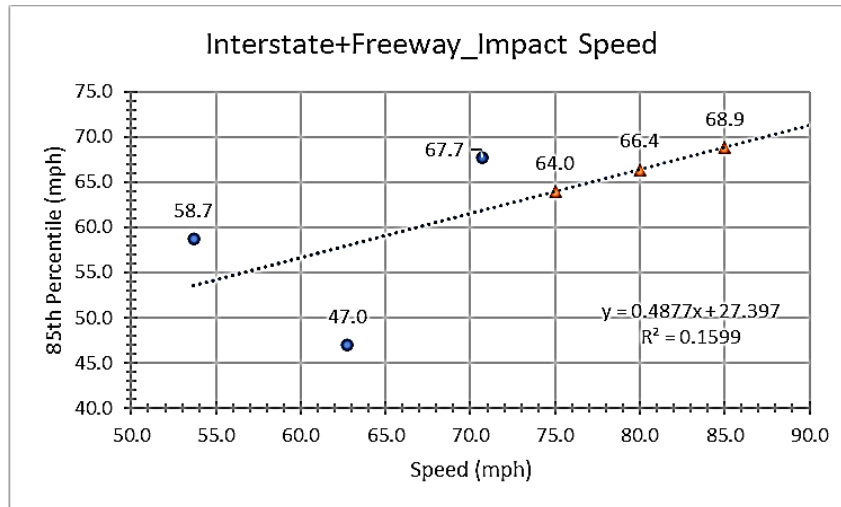
Posted Speed Limit	85th Percentile
75	<b>23.1</b>
80	<b>24.7</b>
85	<b>26.4</b>

### 3.2.3.6. Case 6: Interstate and Freeway Roadways Classification for 50–55 mph, 60–65 mph, 70–75 mph Speed Categories

Statistical linear regression analysis was performed on Case 6 of the 17-43 data for combined interstate and freeway classifications with posted speed limit categories of 50–55 mph, 60–65 mph, and 70–75 mph. The descriptive statistics for interstate roadways for this grouping of posted speeds is presented in Table 28. The linear regression results for impact speed are shown in Figure 25. The estimates of 85th percentile impact speed for posted speed limits of 75, 80, and 85 mph are summarized in Table 29. Similar data for impact angle are presented in Table 30, Figure 26, and Table 31.

**Table 28. Case 6: Descriptive Statistics for Impact Speed of 17-43 Database.**

Speed	N	Weighted Mean	85th Percentile
50–55	19	53.7	<b>58.7</b>
60–65	20	62.8	<b>47.0</b>
70–75	21	70.7	<b>67.7</b>



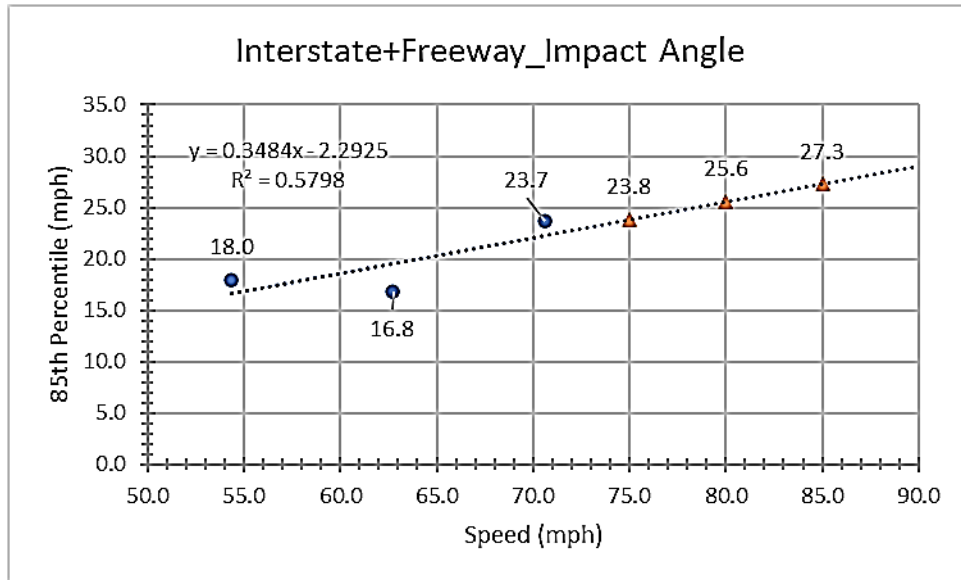
**Figure 25. Case 6: Linear Regression for 85th Percentile Impact Speed with 17-43 Crash Database.**

**Table 29. Case 6: Predicted 85th Percentile Impact Speed through Linear Regression.**

Posted Speed Limit	85th Percentile
75	<b>64.0</b>
80	<b>66.4</b>
85	<b>68.9</b>

**Table 30. Case 6: Descriptive Statistics for Impact Angle of 17-43 Database.**

Speed	N	Weighted Mean	85th Percentile
50–55	55	54.4	<b>18</b>
60–65	61	62.7	<b>16.8</b>
70–75	40	70.6	<b>23.7</b>



**Figure 26. Case 6: Linear Regression for 85th Percentile Impact Angle with 17-43 Crash Database.**

**Table 31. Case 6: Predicted 85th Percentile Impact Angle through Linear Regression.**

Posted Speed Limit	85th Percentile
75	<b>23.8</b>
80	<b>25.6</b>
85	<b>27.3</b>

### 3.3. CONCLUSION

The applicability of currently available data for the assessment of commonly used generic longitudinal barrier system crashworthiness on Texas roadways with different posted speed limits were identified and assessed. Linear regression analyses were performed on the 17-43 data to estimate impact conditions for roadways with posted speeds of 75, 80, and 85 mph. Different groupings of data by posted speed and highway classification were performed. The predicted 85th percentile impact speed and angle for these cases is summarized in Table 32. One of the important parameters in the interpretation of the linear regression analyses results is the  $R^2$  value. The  $R^2$  value is associated with how well the regression model explains the observed data. The  $R^2$  values associated with the regression relationships obtained from the 17-43 data for the different roadway classifications are shown in Table 33.



**Table 32. Summary of 17-43 Data Analysis Cases.**

Category	Speed Categorization	Impact Speed	Impact Angle
All Roadways	50–55	62.4	26.0
	60–65	53.2	17.9
	70–75	67.6	33.0
	75	64.3	30.0
	80	65.6	31.8
	85	66.9	33.5
Interstate Roadways	50–55	55.2	20.7
	60–65	45.8	15.3
	70–75	48.3	20.8
	75	44.0	18.9
	80	41.8	18.8
	85	39.6	18.8
Freeway Roadways	50–55	58.7	18.0
	60–65	47.0	15.2
	70–75	68.8	23.6
	75	65.0	23.1
	80	67.6	24.7
	85	70.2	26.4
Interstate and Freeway Roadways	50–55	58.7	18.0
	60–65	47.0	16.8
	70–75	67.7	23.7
	75	64.0	23.8
	80	66.4	25.6
	85	68.9	27.3

**Table 33. R<sup>2</sup> Value versus Roadway Classification.**

Category	R <sup>2</sup> Value for Impact Speed	R <sup>2</sup> Value for Impact Angle
All Roadways	0.7036	0.4895
Interstate Roadways	0.6431	0.0003
Freeway Roadways	0.1954	0.4201
Interstate and Freeway Roadways	0.1599	0.5798

After review and comparison of the different data groupings, it was recommended to use Case 6: Interstate and Freeway Roadway Classifications with 50–55 mph, 60–65 mph, 70–75 mph speed categories to forecast impact conditions for high-speed roadways with posted speed limits of 75 mph, 80 mph, and 85 mph, as shown in Table 31. This case was recommended because it is considered to best represent the character of highspeed roadways in Texas, which consist of both state highways and rural interstates. Based on the regression analysis for Case 6, estimated impact conditions for testing and evaluation of roadside safety barriers on roadways with high posted speed limits are shown in Table 34.

**Table 34. Proposed Impact Conditions for Very High Speed Roadways.**

Posted Speed Limit (mph)	Impact Speed (mph)	Impact Angle (degree)	Impact Severity (kip-ft) (m = 5000 lb)
75	64.0	23.8	111.4
80	66.4	25.6	127.7
Average 80 and 85	$67.7 = (66.4 + 68.9) \div 2$	$26.5 = (25.6 + 27.3) \div 2$	152.5
85	68.9	27.3	166.8

It was noted that the impact speed of 64 mph for a posted speed limit of 75 mph is within the current MASH tolerance for impact speed for TL-3, which is  $62 \text{ mph} \pm 2.5 \text{ mph}$ . The impact angle for a posted speed limit of 75 mph is slightly lower than the nominal impact angle for TL-3 but within the allowable tolerance ( $25 \text{ degrees} \pm 1.5 \text{ degrees}$ ). The resulting impact severity (IS) associated with the 75-mph posted speed limit impact conditions is lower than the IS for the nominal TL-3 impact conditions, which is 114.7 kip-ft. Consequently, the research team concluded that current MASH impact conditions are adequate for evaluating roadside barriers for roadways having a posted speed limit of 75 mph.

Engineering analyses and finite element computer simulations were used to assess the impact performance of current concrete barrier and guardrail systems for the impact conditions associated with roadways having posted speed limits of 80 mph and 85 mph. These analyses are described in the following chapters.

## **CHAPTER 4. FINITE ELEMENT SIMULATION**

This chapter documents the finite element analyses (FEA) performed on rigid concrete median barriers and bridge rails using the proposed high-speed impact conditions for higher posted speed limits. The simulations were performed with a RAM pickup truck model that is representative of the MASH 2270P design vehicle and a Toyota Yaris passenger car that is representative of the MASH 1100C design vehicle.

The impact conditions associated with an 85-mph posted speed limit were selected for use in evaluating the concrete barrier systems. These conditions involve an impact speed of 68.9 mph and impact angle of 27.3 degrees. If a system demonstrates acceptable impact performance for these impact conditions, the system would be considered acceptable for any lower posted speed limit categories.

The following concrete barrier systems were selected for evaluation in consultation with the project panel:

- SSCB (42-inch-tall single slope median barrier).
- SSTR (36-inch-tall single slope bridge rail).
- T222 (36-inch-tall vertical profile bridge rail).
- CSB (32-inch-tall safety shape median barrier).

The researchers used available MASH crash tests to validate the concrete barrier models. The validation between test and simulation consisted of comparison of vehicle behavior, MASH occupant risk indices such as occupant impact velocity (OIV) and ridedown acceleration (RA), and roll, pitch, and yaw angles. Angular velocities and linear acceleration time histories were extracted from the simulations and processed using the Test Risk Assessment Program (TRAP).

Concrete barriers anchored or keyed into a bridge deck or roadway pavement behave rigidly with little or no movement. Therefore, the concrete barrier systems were modeled using a rigid material definition having the correct geometry and profile.

### **4.1. SINGLE SLOPE CONCRETE BARRIER**

Details of the 42-inch-tall SSCB are found in TxDOT standard SSCB(1)-16, which is presented in Appendix A. The FEA simulations were performed with both the 1100C passenger car and 2270P pickup truck. The impact conditions for the crash test, validation simulation, and high-speed simulation (representative of an 85-mph posted speed limit) are shown in Table 35 and Table 36 for the passenger car and pickup truck, respectively.

A comparison of vehicle behavior for the crash test, validation simulation performed at the same impact conditions as the crash test, and the high-speed simulation for 85-mph posted speed limit is shown in Table 37 for the passenger car and Table 38 for the pickup truck.








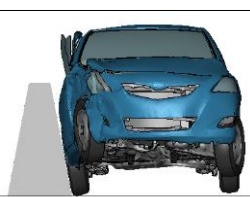
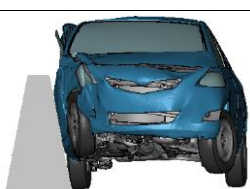


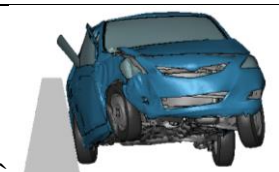

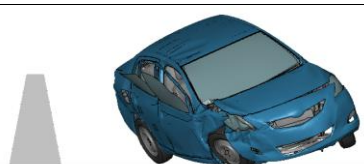

**Table 35. SSCB Impact Conditions for Passenger Car.**

Description	Impact Speed (mph)	Impact Angle (degrees)
Test 611901-03-1 (15)	62.7	27.5
Baseline Simulation	62.7	27.5
High-Speed Simulation	68.9	27.3
















**Table 36. SSCB Impact Conditions for Pickup Truck.**

Description	Impact Speed (mph)	Impact Angle (degrees)
Test 611901-04-1 (15)	63.2	24.9
Baseline Simulation	63.2	24.9
High-Speed Simulation	68.9	27.3

**Table 37. Impact Behavior of Passenger Car with SSCB System.**

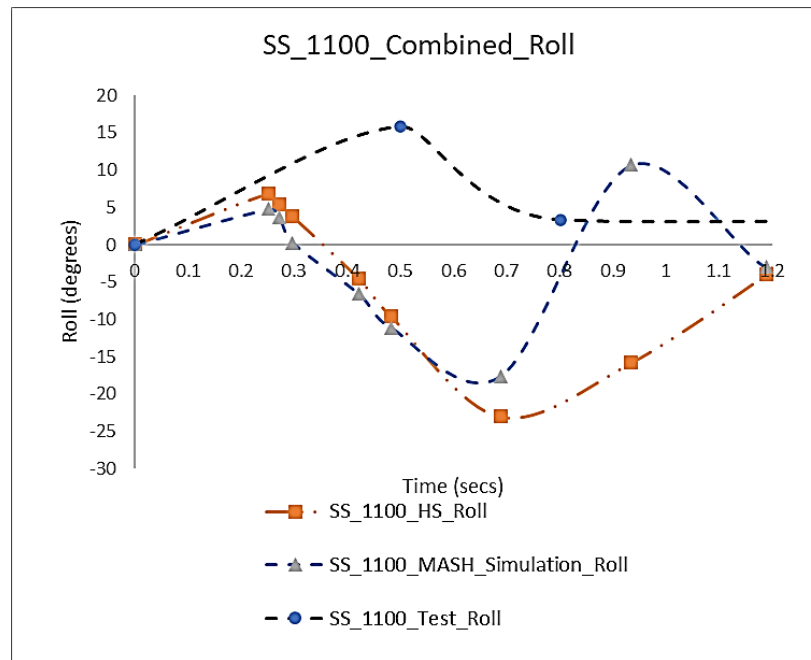
DESCRIPTION	SS_1100C_Test (15)	SS_1100_MASH_Simulation	SS_1100_High-Speed_Simulation
The front tire of vehicle contacts barrier.			
Vehicle begins to climb as it interacts with sloped barrier face.			
Rear tire of vehicle contacts barrier.			
Rear tire loses contact with barrier.			
Vehicle after exiting system.			

**Table 38. Impact Behavior of Pickup Truck with SSCB System.**

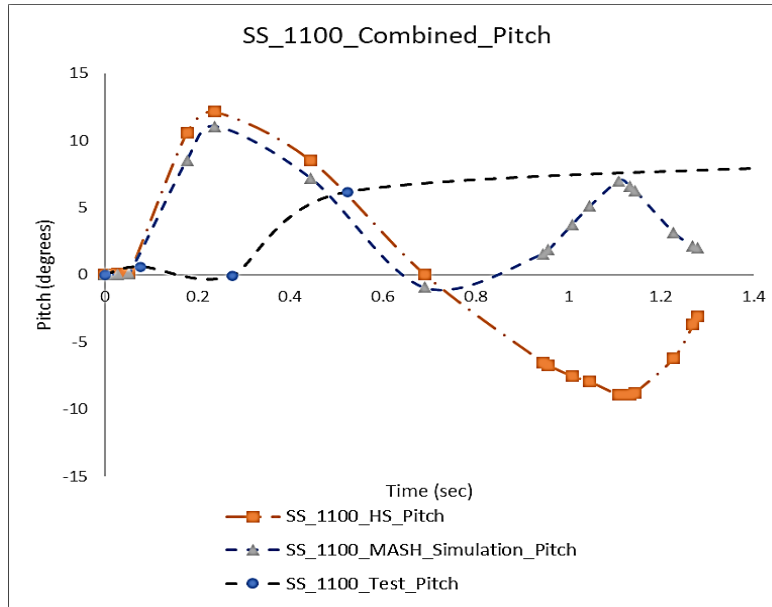
DESCRIPTION	SS_2270P_Test (15)	SS_2270_MASH_Simulation	SS_2270_High-Speed Simulation
Front tire of vehicle contacts barrier.			
Vehicle parallel to system.			
Rear tire of vehicle contacts barrier.			
Vehicle at exit from system.			
Vehicle recontacts ground.			

The angular roll, pitch and yaw displacement comparison is shown in Figure 27, Figure 28, and Figure 29, respectively, for the passenger car and Figure 30, Figure 31, and Figure 32, respectively, for the pickup truck impacting the SSCB.

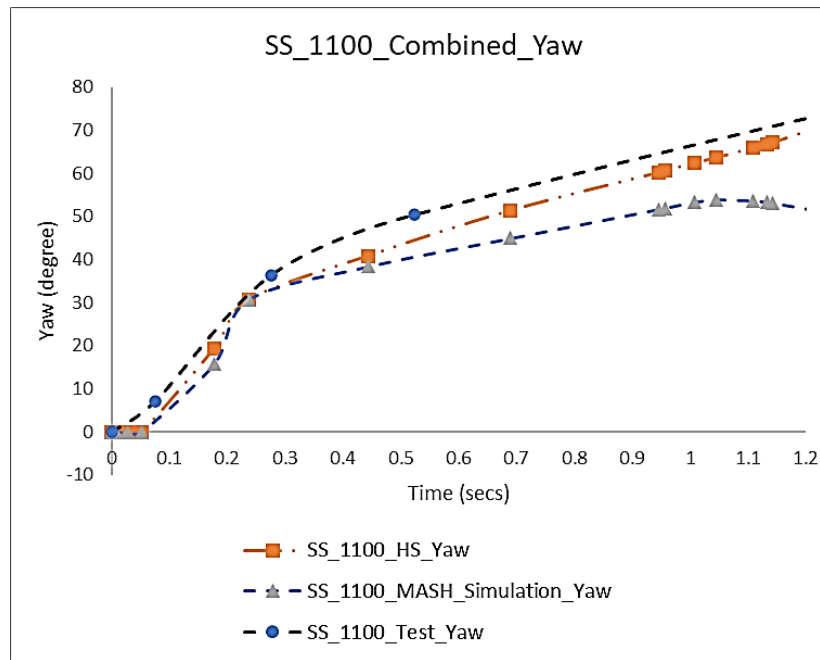
The TRAP was used to calculate the OIV, RA, and maximum roll, pitch, and yaw angles. A comparison of OIV, RA, and maximum roll, pitch, and yaw angles for the passenger car are shown in Figure 33 to Figure 35, respectively. These values are summarized and compared against MASH criteria in Table 39. A similar comparison for the pickup truck impacts with the SSCB are shown in Figure 36 to Figure 38, respectively. A summary against MASH criteria is provided in Table 40.



**Figure 27. Roll-Time History for SSCB-Car.**

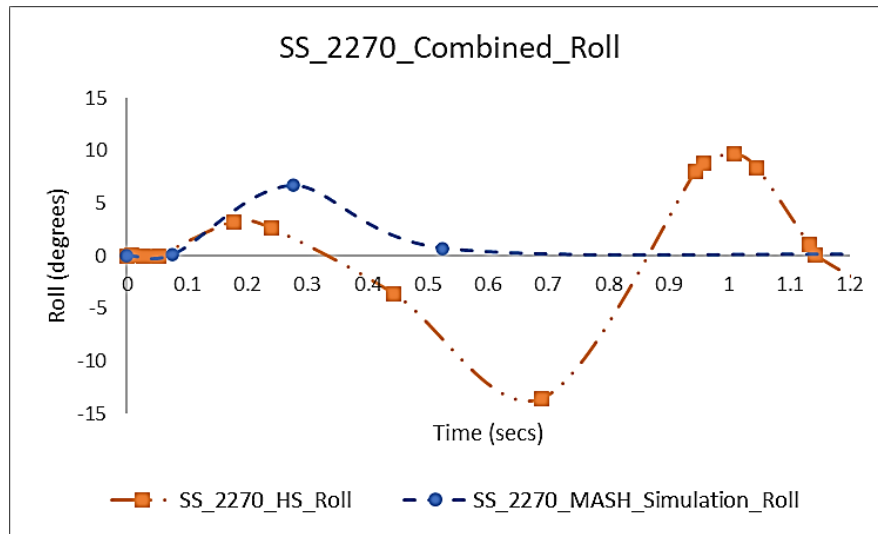


**Figure 28. Pitch-Time History for SSCB-Car.**

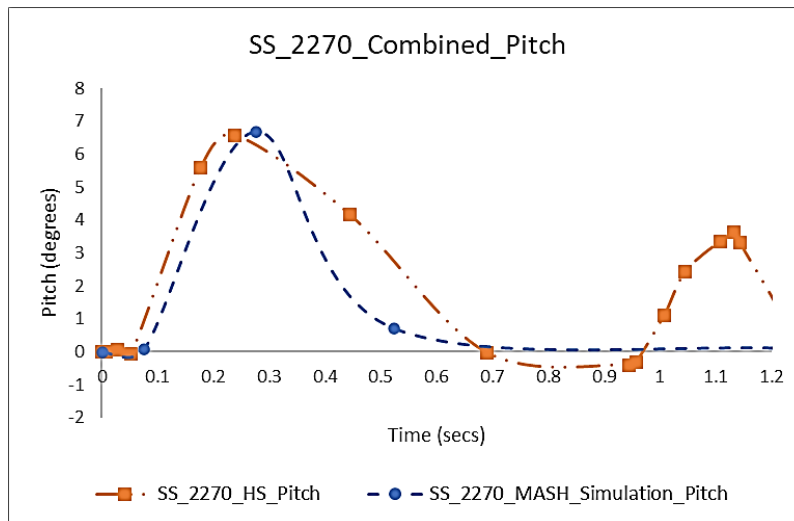


**Figure 29. Yaw-Time History for SSCB-Car.**

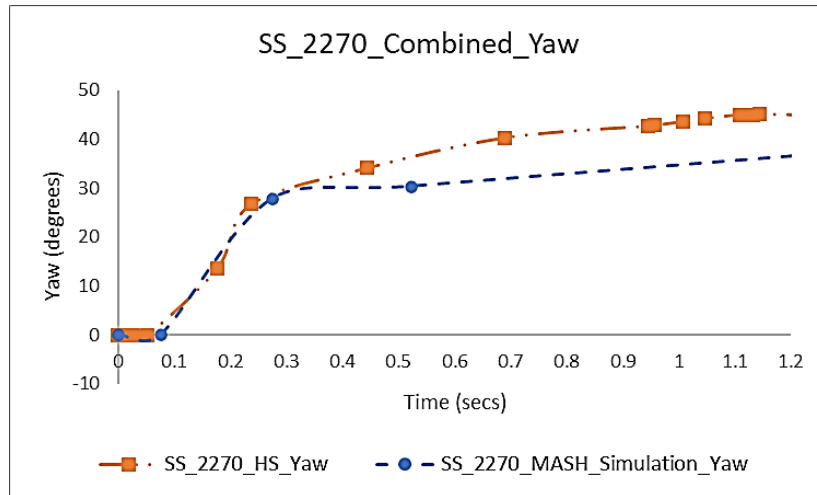




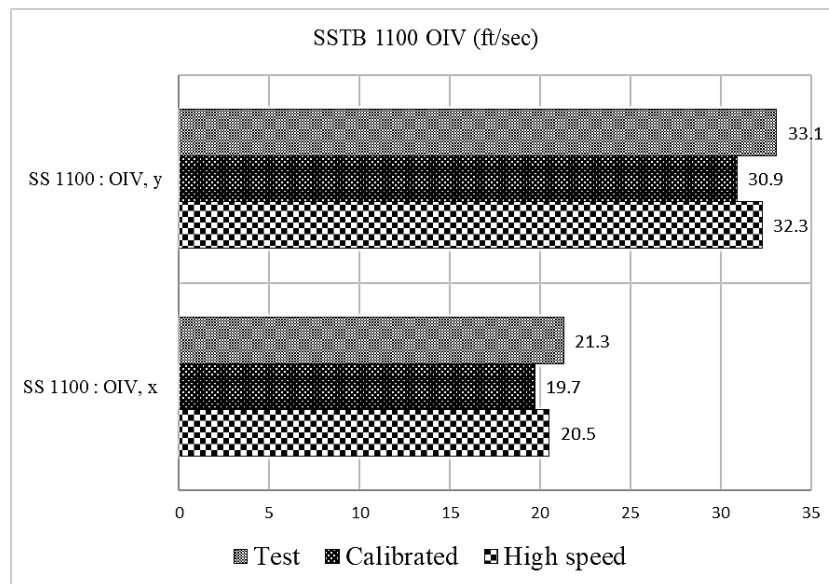
**Figure 30. Roll-Time History for SSCB-Pickup.**



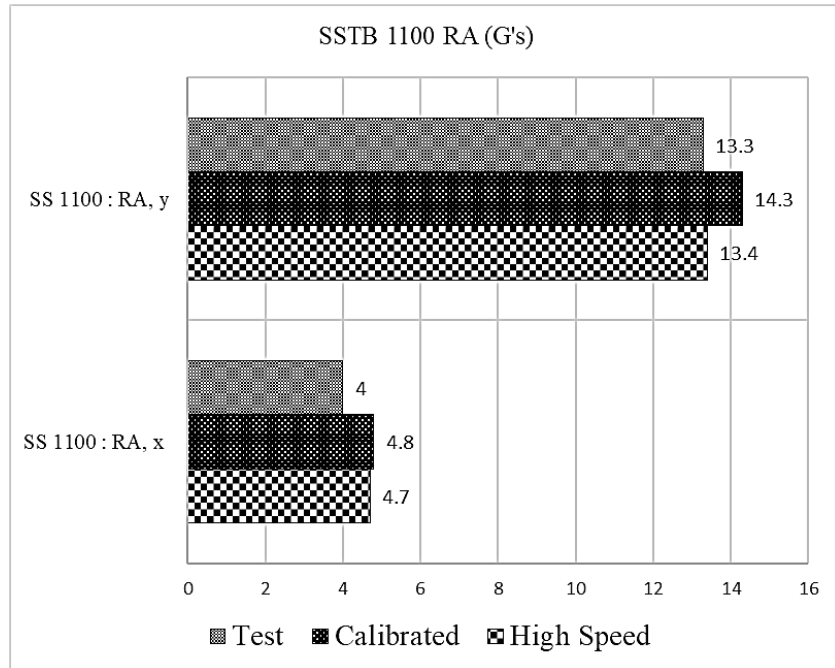
**Figure 31. Pitch-Time History for SSCB-Pickup.**



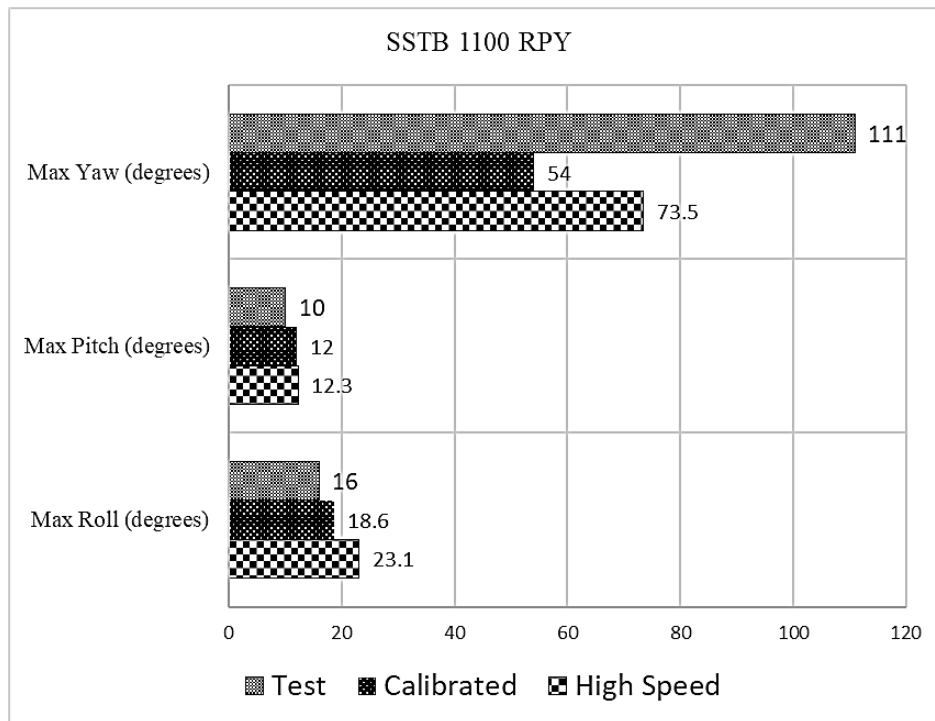
**Figure 32. Yaw-Time History for SSCB-Pickup.**



**Figure 33. Occupant Impact Velocity for SSCB-Car.**



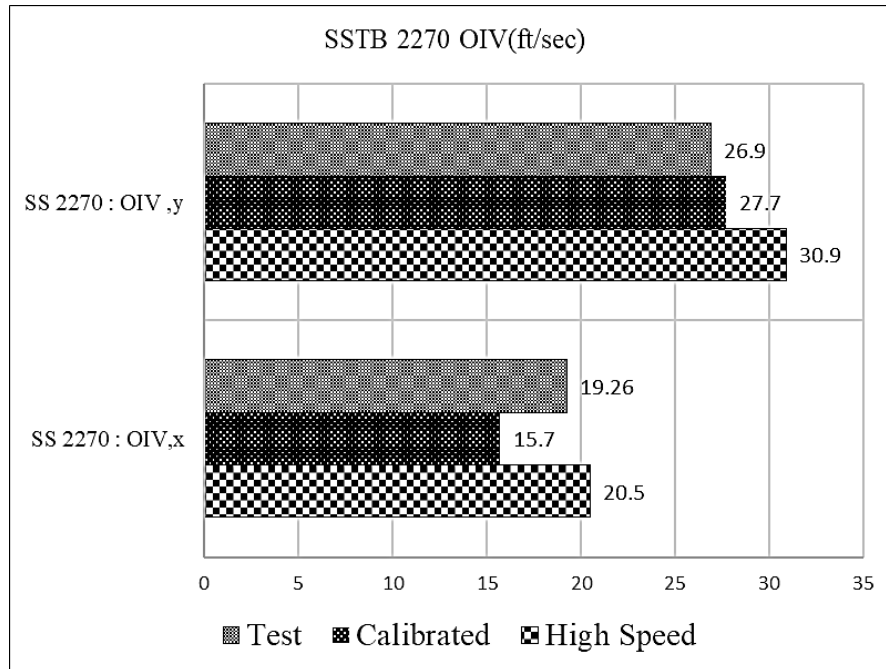
**Figure 34. Ridedown Acceleration for SSCB-Car.**



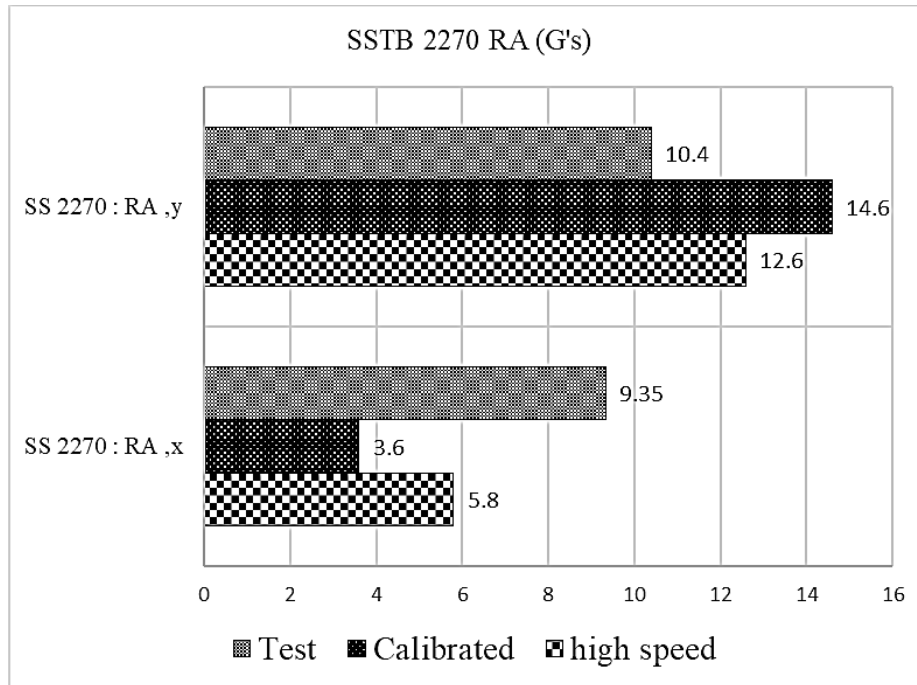
**Figure 35. Roll, Pitch, Yaw Comparison for SSCB-Car.**

**Table 39. Occupant Risk Comparison for SSCB-Car.**

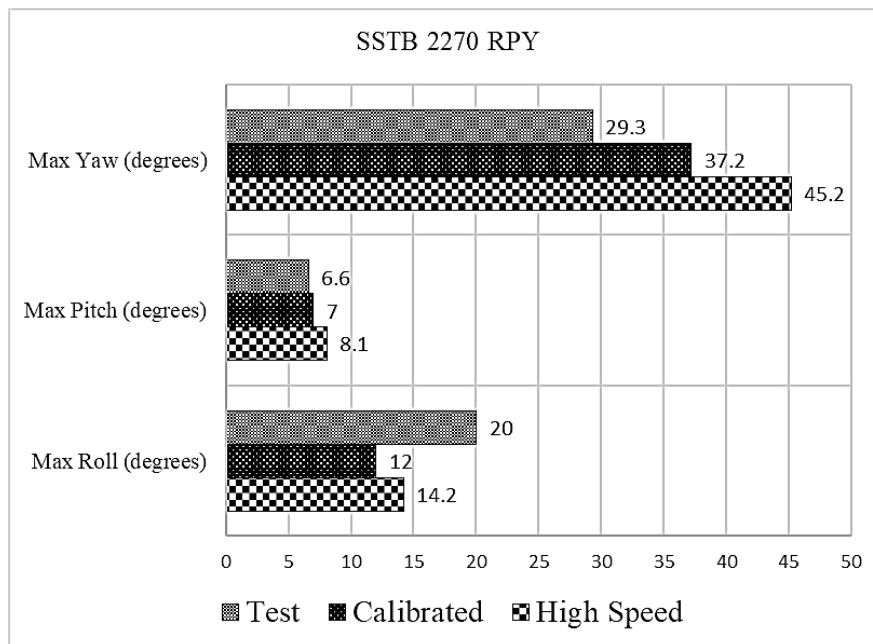
Test Parameter	MASH Criteria	Crash Test (15)	Baseline Simulation	High Speed Simulation
OIV, Longitudinal (ft/s)	$\leq 40.0$	21.3	19.7	20.5
OIV, Lateral (ft/s)	$\leq 40.0$	33.1	30.9	32.3
RA, Longitudinal (g)	$\leq 20.49$	4.0	4.8	4.7
RA, Lateral (g)	$\leq 20.49$	13.3	14.3	13.4
Max. Roll (deg.)	$\leq 75$	16	18.6	23.1
Max. Pitch (deg.)	$\leq 75$	10	12	12.3
Max. Yaw (deg.)	N/A	111	54	73.5



**Figure 36. Occupant Impact Velocity for SSCB-Truck.**



**Figure 37. Ridedown Acceleration for SSCB-Truck.**



**Figure 38. Roll, Pitch, Yaw Comparison for SSCB-Truck.**

**Table 40. Occupant Risk Comparison for SSCB System-Truck.**

Test Parameter	MASH	Crash Test (15)	Baseline Simulation	High Speed Simulation
OIV, Longitudinal (ft/s)	≤ 40.0	18.7	15.7	20.5
OIV, Lateral (ft/s)	≤ 40.0	28.9	27.7	30.9
RA, Longitudinal (g)	≤ 20.49	3.3	3.6	5.8

RA, Lateral (g)	$\leq 20.49$	10.8	14.6	12.6
Roll (deg.)	$\leq 75$	22	12	14.2
Pitch (deg.)	$\leq 75$	6	7	8.1
Yaw (deg.)	N/A	41	37.2	45.2

Table 41 provides a comparison between the test and baseline validation simulation for the SSCB for both passenger car and pickup truck. The comparison includes the maximum absolute values of OIV and RA, as well as the absolute percentage variation between the test and simulation. The comparison was less than 10 percent for the passenger car and the pickup truck OIV. The pickup truck RA had a larger difference, but the simulation was conservative with a prediction of a higher value.

**Table 41. FEA Validation of SSCB.**

Vehicle	Parameter	Crash Test (15)	Baseline Simulation	$ \% \text{ Variation}  = \frac{100 * (\text{MASH Simulation} - \text{Test})}{\text{Test}}$
Passenger Car	OIV (ft/s)	33.1	30.9	6.65
Passenger Car	RA (g)	13.1	14.3	7.52
Pickup Truck	OIV (ft/s)	28.9	27.7	4.15
Pickup Truck	RA (g)	10.8	14.6	40.38

## 4.2. SINGLE SLOPE TRAFFIC RAIL

Details of the 36-inch-tall single slope traffic rail are found in TxDOT bridge rail standard Type SSSTR, which is presented in Appendix B. The FEA simulations were performed with both the 1100C passenger car and 2270P pickup truck. The impact conditions for the crash test, validation simulation, and high-speed simulation (representative of an 85-mph posted speed limit) are shown in Table 42 and Table 43 for the passenger car and pickup truck, respectively.

A comparison of vehicle behavior for the crash test, validation simulation performed at the same impact conditions as the crash test, and the high-speed simulation for 85-mph posted speed limit is shown in Table 44 for the passenger car and Table 45 for the pickup truck.


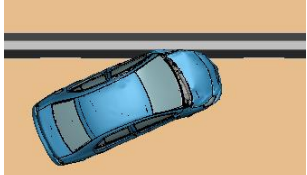
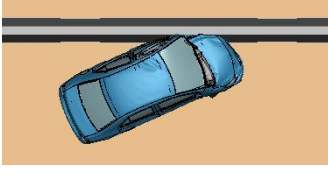

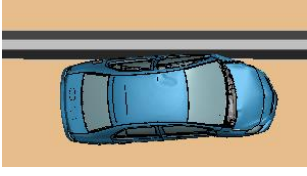
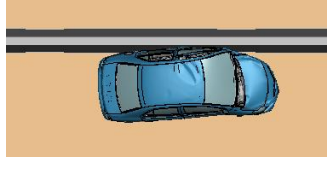

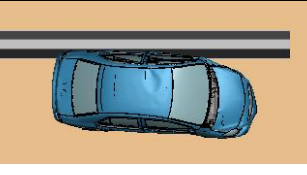
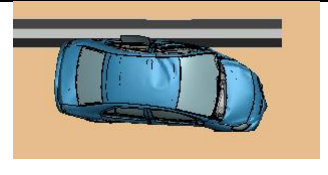

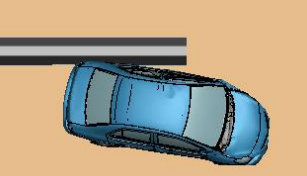
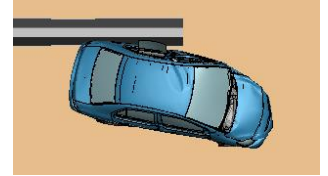

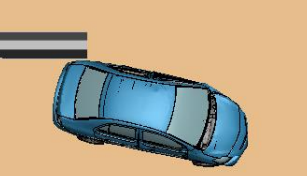
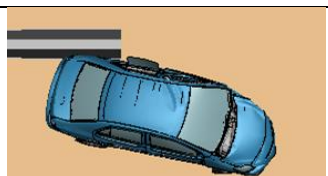
**Table 42. SSSTR Impact Conditions for Passenger Car.**

Description	Impact Speed (mph)	Impact Angle (degrees)
Test 140MASH3C16-04 (16)	61.2	25.7
Baseline Simulation	61.2	25.7
High-Speed Simulation	68.9	27.3












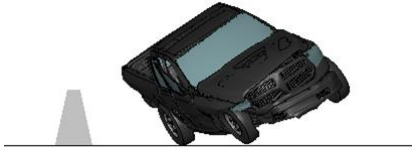
**Table 43. SSSTR Impact Conditions for Pickup Truck.**

Description	Impact Speed (mph)	Impact Angle (degrees)
Test 420020-3 (17)	63.8	24.8
Baseline Simulation	63.8	24.8
High-Speed Simulation	68.9	27.3

**Table 44. Impact Behavior of Passenger Car with SSTR System.**

DESCRIPITON	SSTR_1100_Test (16)	SSTR_1100_MASH_Simulation	SSTR_1100_High_Speed_Simulation
Front tire contact with barrier.			
Vehicle parallel to system.			
Rear tire contact with barrier.			
Rear tire loss of contact from the barrier.			
Vehicle exit from system.			

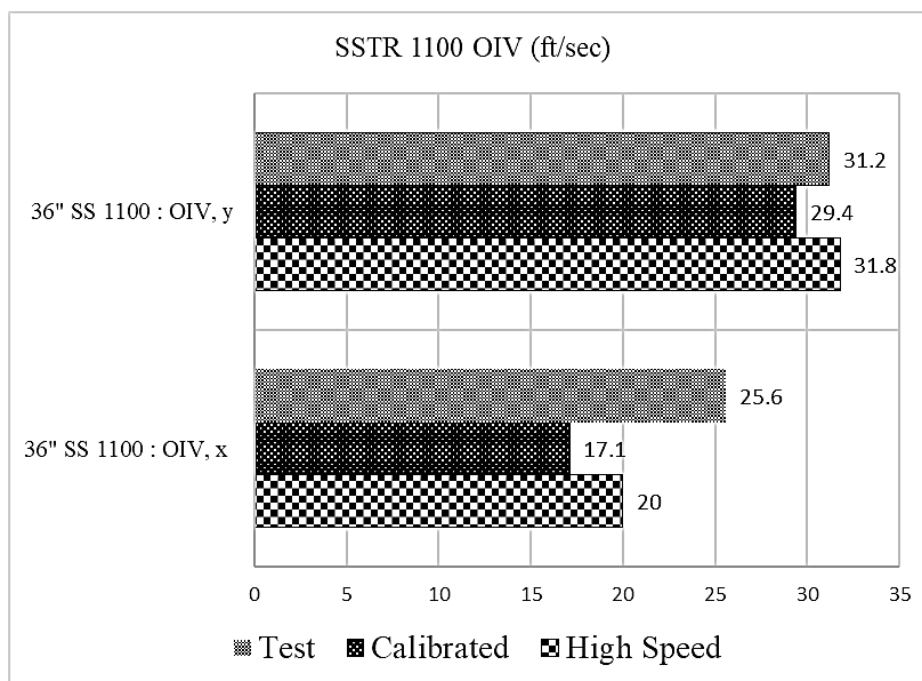
**Table 45. Impact Behavior of Pickup Truck with SSTR System.**

DESCRIPTION	SS_2270_Test (17)	SS_2270_MASH_Simulation	SS_2270_High Speed_Simulation
Front tire contact with barrier.			
Vehicle begins to climb as it interacts with sloped barrier face.			
Rear tire contact with barrier.			
Rear after exiting system.			

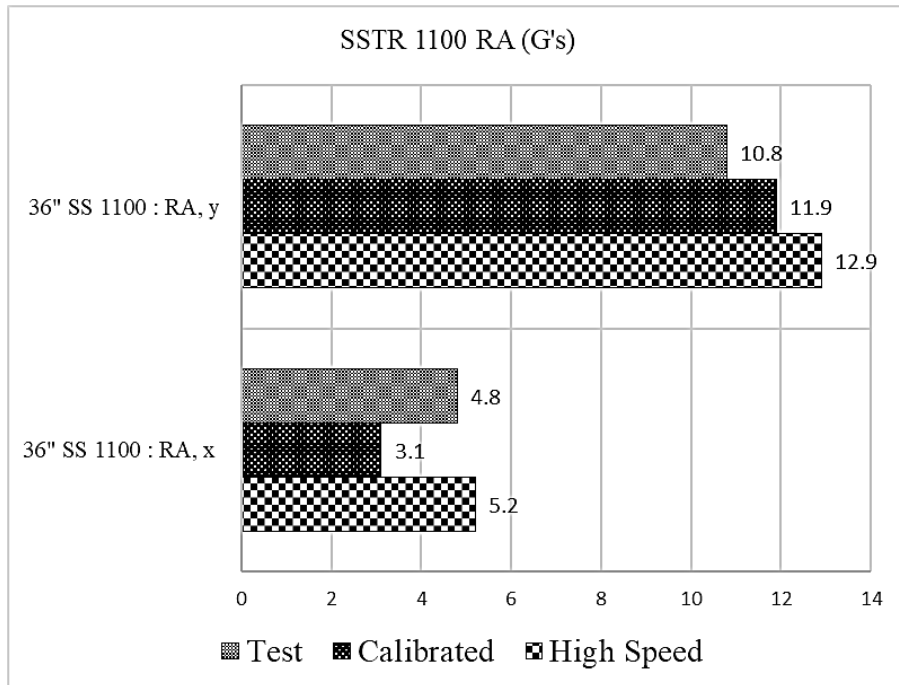


Note that the single slope barrier model used in the simulations corresponded to a single slope concrete median barrier (CMB). The single slope CMB was modeled as rigid and has the same slope profile as the single-sided SSTR. The simulation results are applicable to both a single-sided and symmetrical rigid, single slope concrete barrier.

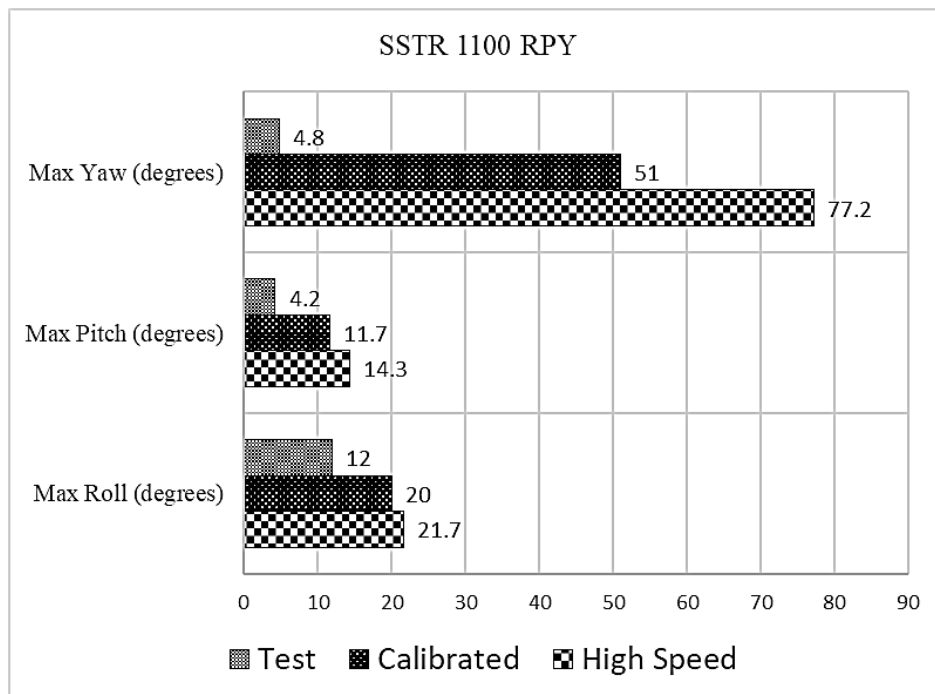
The TRAP was used to calculate the OIV, RA, and maximum roll, pitch, and yaw angles. A comparison of OIV, RA, and maximum roll, pitch, and yaw angles for the passenger car are shown in Figure 39 to Figure 41, respectively. These values are summarized and compared against MASH criteria in Table 46. A similar comparison for the pickup truck impacts with the SSCB are shown in Figure 42 to Figure 44, respectively. A summary against MASH criteria is provided in Table 47.



**Figure 39. Occupant Impact Velocity for SSTR-Car.**



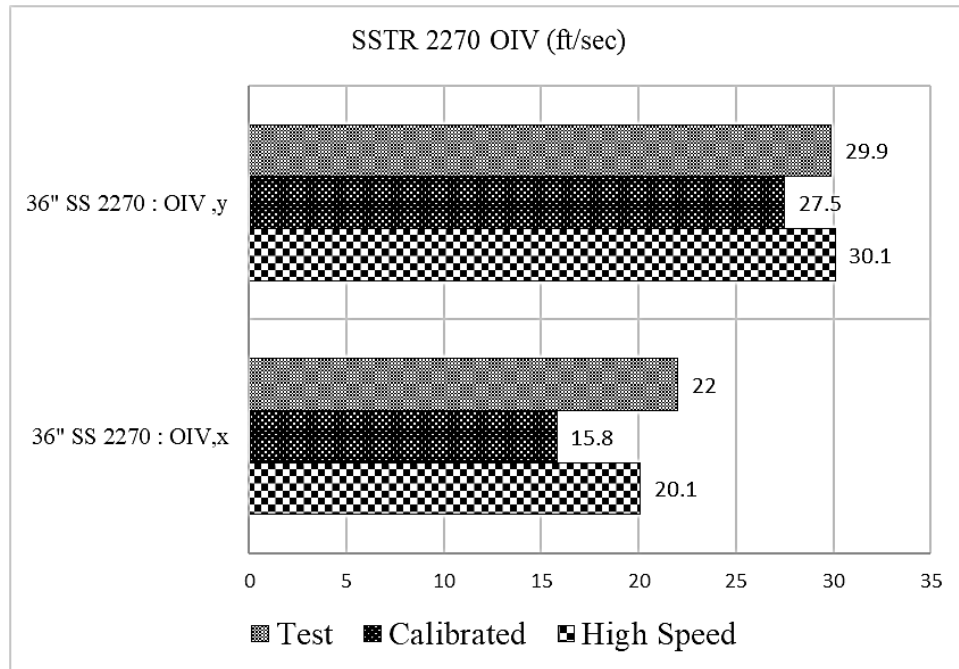
**Figure 40. Ridedown Acceleration for SSTR-Car.**



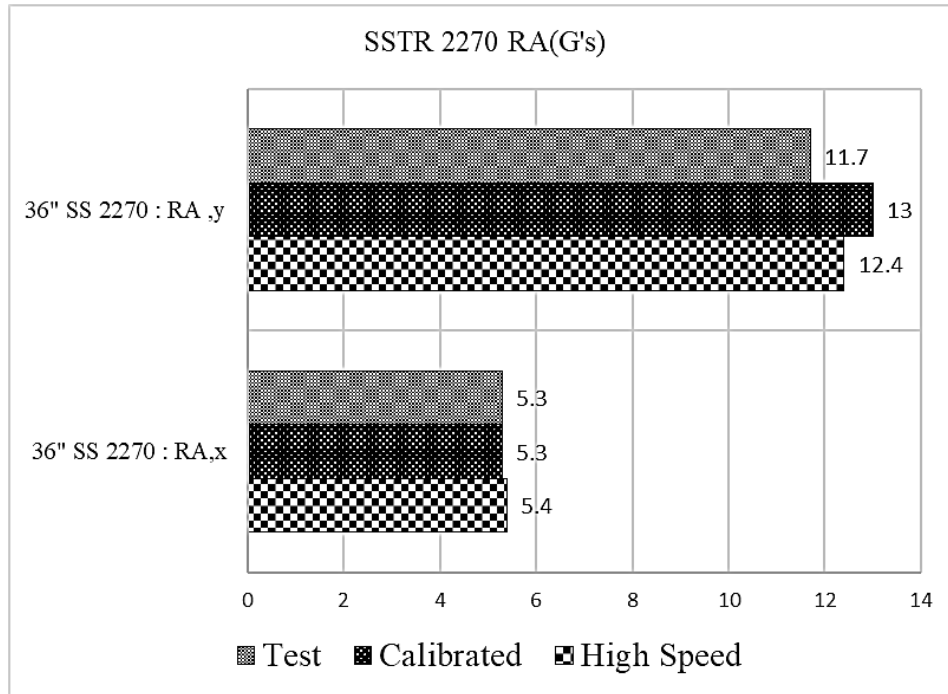
**Figure 41. Roll, Pitch, Yaw for SSTR-Car.**

**Table 46. Occupant Risk Factors for SSTR System-Car.**

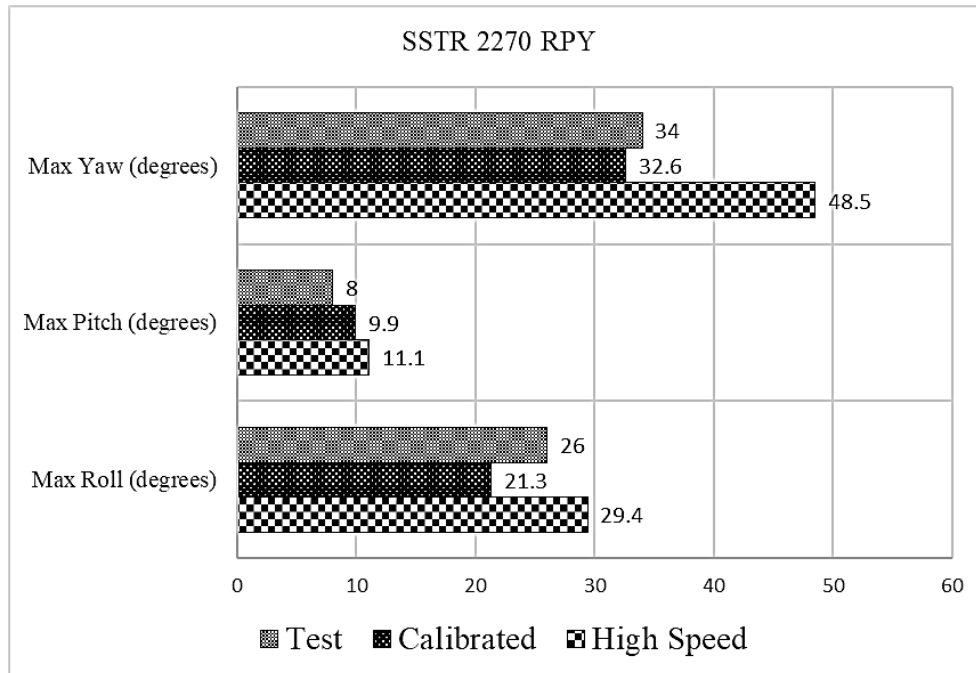
Test Parameter	MASH	Crash Test (16)	Baseline Simulation	High Speed Simulation
OIV, Longitudinal (ft/s)	$\leq 40.0$	25.6	17.1	20.0
OIV, Lateral (ft/s)	$\leq 40.0$	31.2	29.4	31.8
RA, Longitudinal (g)	$\leq 20.49$	4.8	3.1	5.2
RA, Lateral (g)	$\leq 20.49$	10.8	11.9	12.9
Roll (deg.)	$\leq 75$	12	20.0	21.7
Pitch (deg.)	$\leq 75$	4.2	11.7	14.3
Yaw (deg.)	N/A	4.8	51.0	77.2



**Figure 42. Occupant Impact Velocity for SSTR-Truck.**



**Figure 43. Ridedown Acceleration for SSTR-Truck.**



**Figure 44. Roll, Pitch, Yaw for SSTR-Truck.**

**Table 47. Occupant Risk Factors for SSTR System-Truck.**

Test Parameter	MASH	Crash Test (17)	Baseline Simulation	High Speed Simulation
OIV, Longitudinal (ft/s)	$\leq 40.0$	22	15.8	20.1
OIV, Lateral (ft/s)	$\leq 40.0$	29.9	27.5	30.1
RA, Longitudinal (g)	$\leq 20.49$	5.3	5.3	5.4
RA, Lateral (g)	$\leq 20.49$	11.7	13.0	12.4
Roll (deg.)	$\leq 75$	26	21.3	29.4
Pitch (deg.)	$\leq 75$	8	9.9	11.1
Yaw (deg.)	N/A	34	32.6	48.5

Comparison of the SSCB and SSTR high-speed simulation results indicates that the height of the single slope barrier system (42 inches for SSCB versus 36 inches for SSTR) does not result in a significant difference in vehicle occupant risk (OIV, RA) or stability (maximum yaw, pitch, roll angles). The occupant risk metrics tended to increase for both single slope barrier systems for the high-speed impact conditions compared to the MASH impact conditions, but the values were well within MASH thresholds.

The maximum roll angle was underpredicted for the pickup truck impact in the validation simulations compared to the measured crash test values. The maximum roll angle comparison between validation simulation and crash test was reasonable for the passenger car. In the high-speed simulations, the roll angle increased, but the vehicles remained relatively stable.

Based on the simulation results, the SSCB and SSTR are likely to meet MASH evaluation criteria for the high-speed impact conditions associated with a posted speed limit of 85 mph.

#### 4.3. VERTICAL SHAPE CONCRETE BARRIER

Details of the 36-inch-tall T222 vertical concrete bridge rail are found in TxDOT bridge rail standard Type T222, which is presented in Appendix C. The FEA simulations were performed with both the 1100C passenger car and 2270P pickup truck. The impact conditions for the crash test, validation simulation, and high-speed simulation (representative of an 85-mph posted speed limit) are shown in Table 48 and Table 49 for the passenger car and pickup truck, respectively.

**Table 48. T222 Impact Conditions for Passenger Car.**

Description	Impact Speed (mph)	Impact Angle (degrees)
MASH Test 3-10	62.2	25
Baseline Simulation	62.2	25
High-Speed Simulation	68.9	27.3

**Table 49. T222 Impact Conditions for Pickup Truck.**


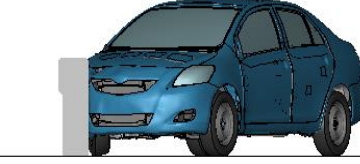
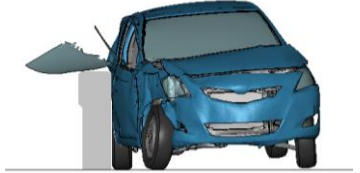
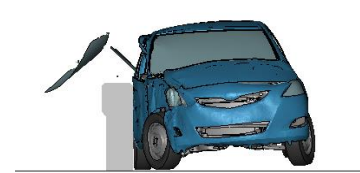
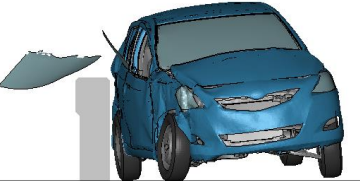
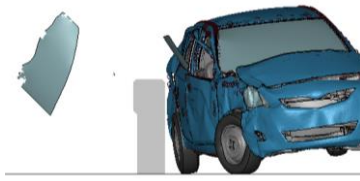


Description	Impact Speed (mph)	Impact Angle (degrees)
Test 490024-2-1 (18)	64.4	25.5
Baseline Simulation	64.4	25.5
High-Speed Simulation	68.9	27.3

A comparison of vehicle behavior for the crash test, validation simulation performed at the same impact conditions as the crash test, and the high-speed simulation for 85-mph posted speed limit is shown in Table 50 for the passenger car and for the pickup truck.














A comparison of roll, pitch, and yaw angle time histories for the MASH and high-speed impact conditions for the passenger car with the T222 are shown in Figure 45, Figure 46, and Figure 47, respectively. A similar comparison for the pickup truck impacts with the T222 are shown in Figure 48, Figure 49, and Figure 50, respectively.

The TRAP was used to calculate the OIV, RA, and maximum roll, pitch, and yaw angles. A comparison of OIV, RA, and maximum roll, pitch, and yaw angles for the passenger car are shown in Figure 51 to Figure 53, respectively. These values are summarized and compared against MASH criteria in Table 52. A similar comparison for the pickup truck impacts with the SSCB are shown in Figure 54 to Figure 56, respectively. A summary against MASH criteria is provided in Table 53.

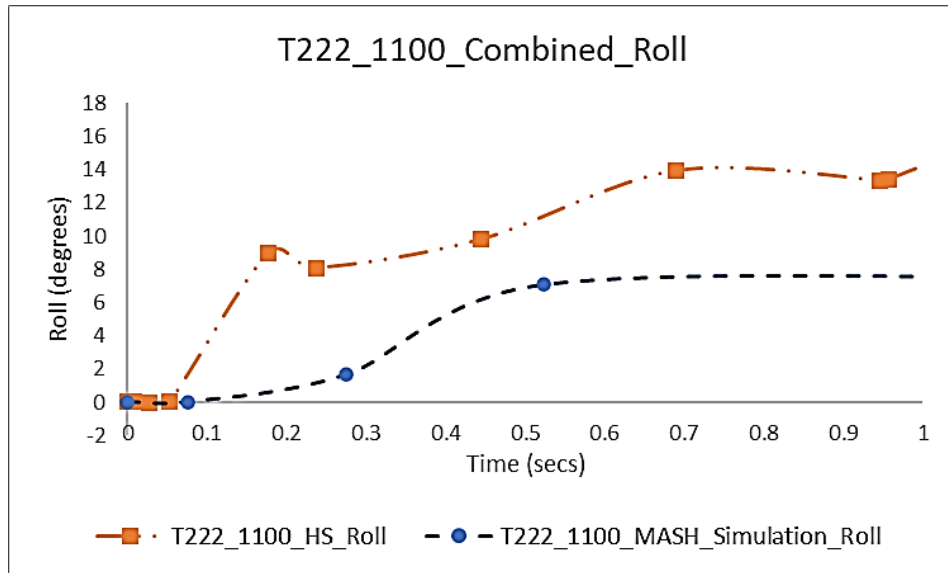
**Table 50. Impact Behavior of Passenger Car with T222 System.**

DESCRIPTION	T222_1100_MASH_Simulation	T222_1100_High_Speed_Simulation
Front tire contact with barrier.		
Rear tire contact with barrier.		
Vehicle exit from system.		
Vehicle stable after exit from system.		

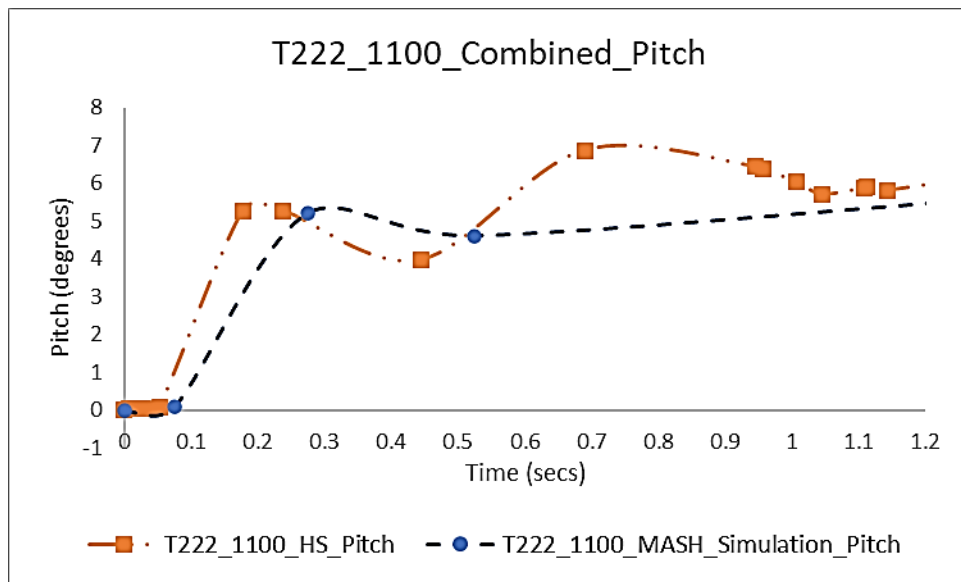
**Table 51. Impact Behavior of Pickup Truck with T222 System.**

DESCRIPTION	T222_1100_Test (18)	T222_1100_MASH_Simulation	T222_1100_High_Speed_Simulation
Front tire contact with barrier.			
Vehicle engaged with system.			
Rear tire contact with barrier.			
Rear tire loss of contact with barrier.			
Vehicle exit from system.			

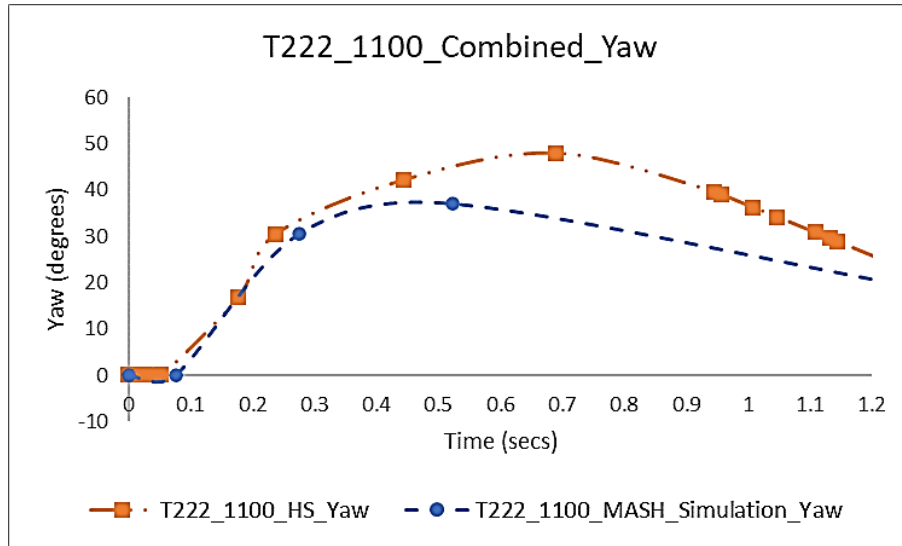




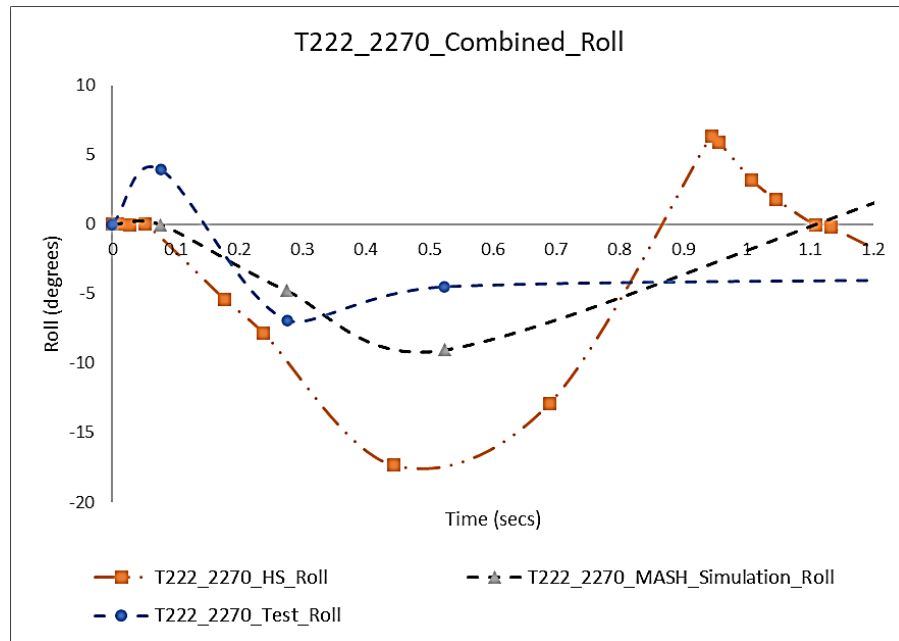
**Figure 45. Roll-Time History for T222-Car.**



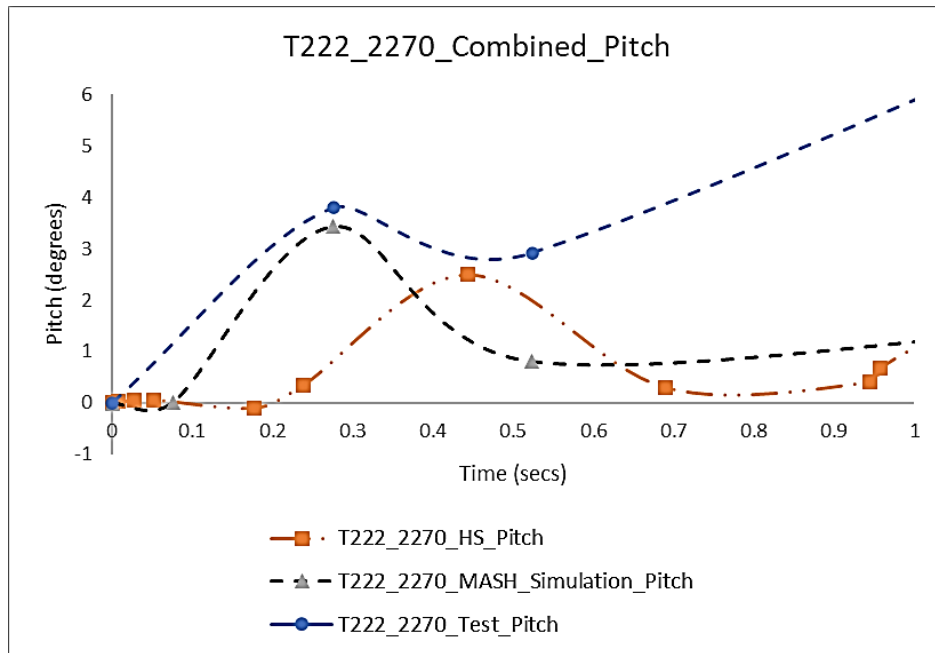
**Figure 46. Pitch-Time History for T222-Car.**



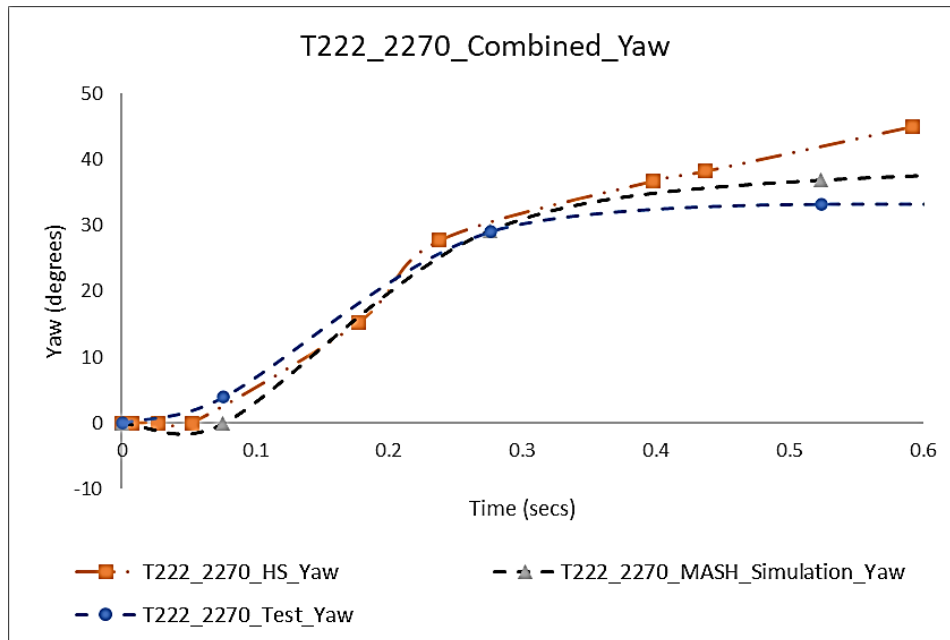
**Figure 47. Yaw-Time History for T222-Car.**



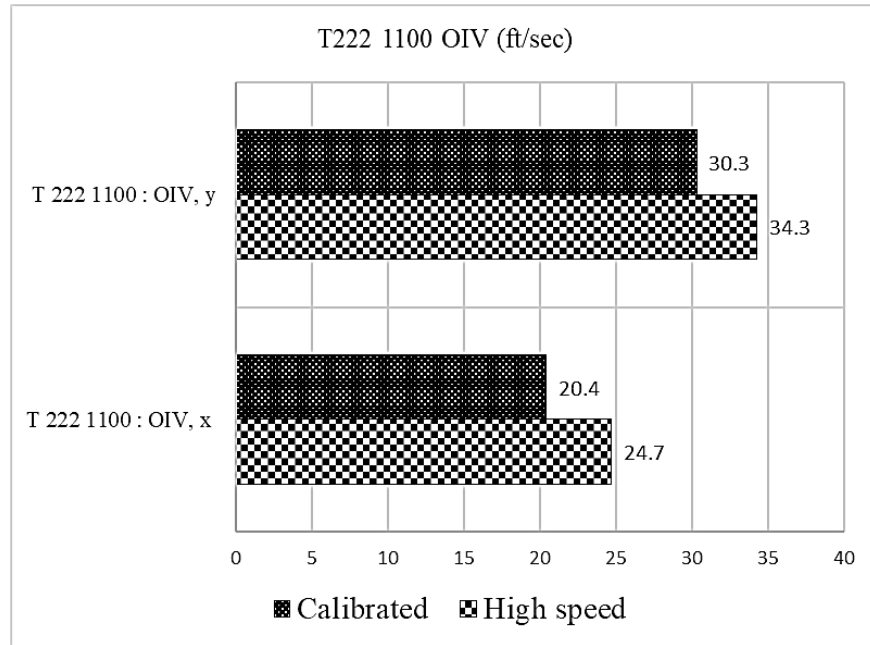
**Figure 48. Roll-Time History for T222-Pickup.**



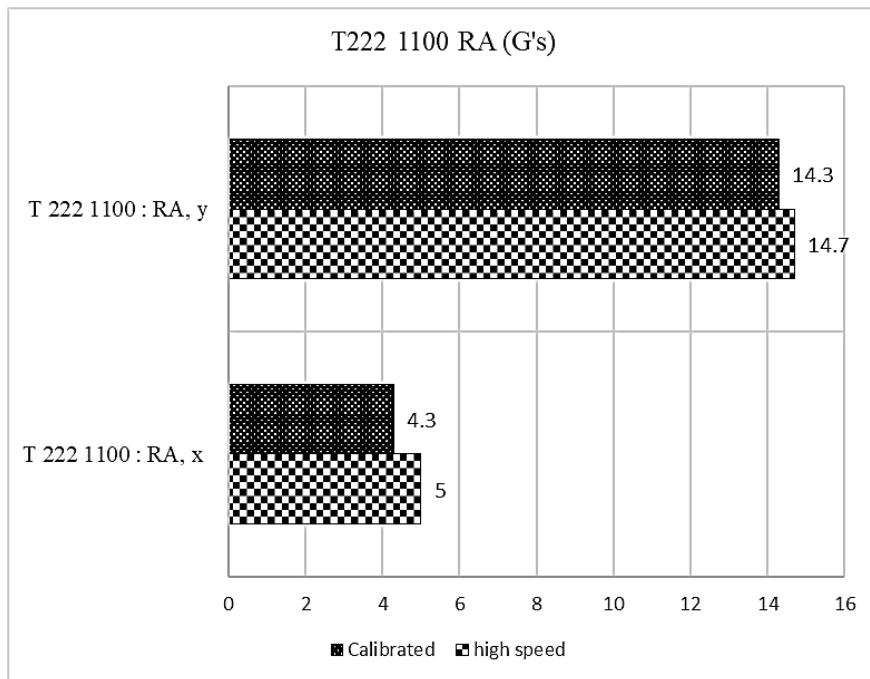
**Figure 49. Pitch-Time History for T222-Pickup.**



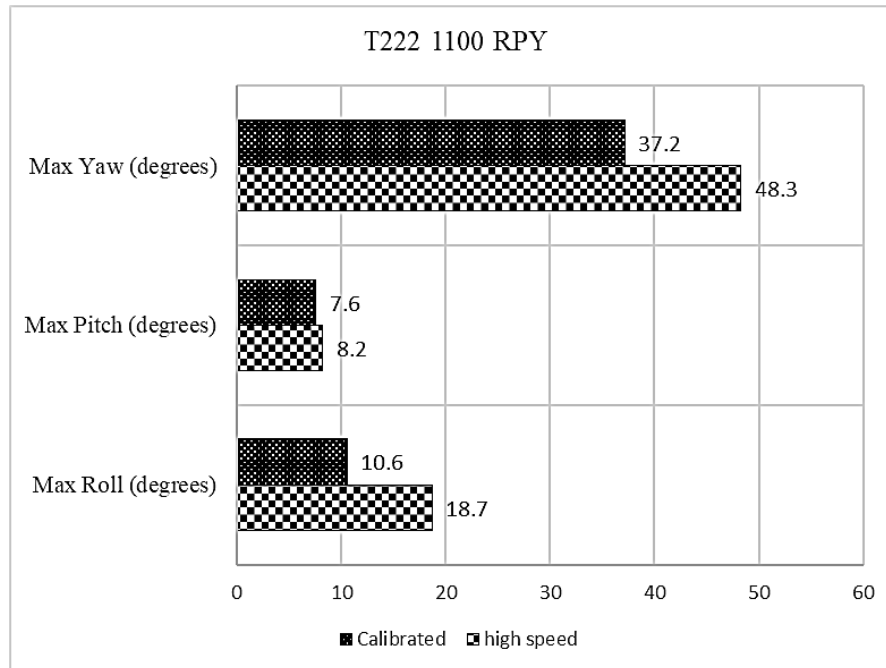
**Figure 50. Yaw-Time History for T222-Pickup.**



**Figure 51. Occupant Impact Velocity for T222-Car.**



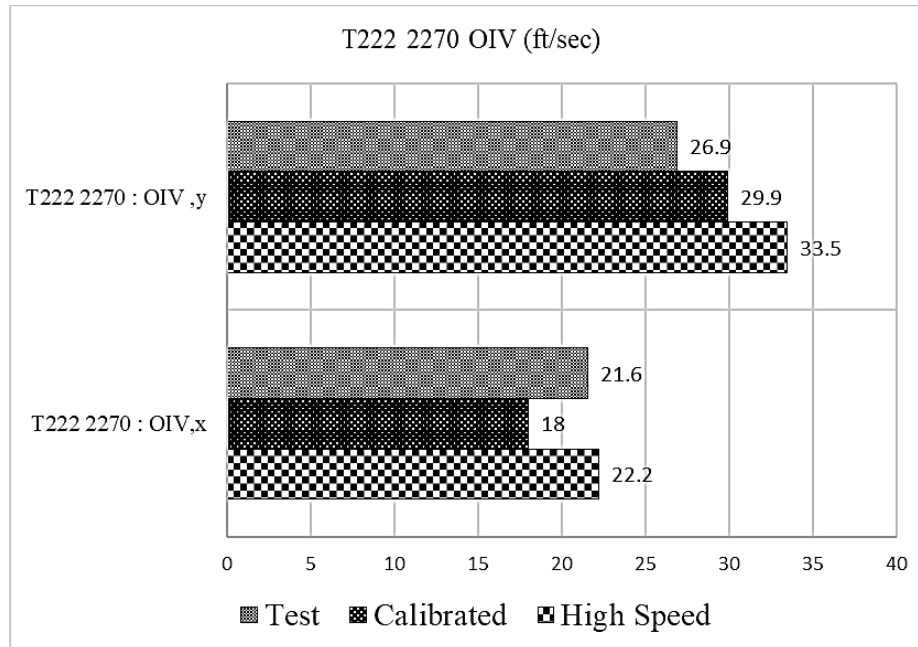
**Figure 52. Ridedown Acceleration for T222-Car.**



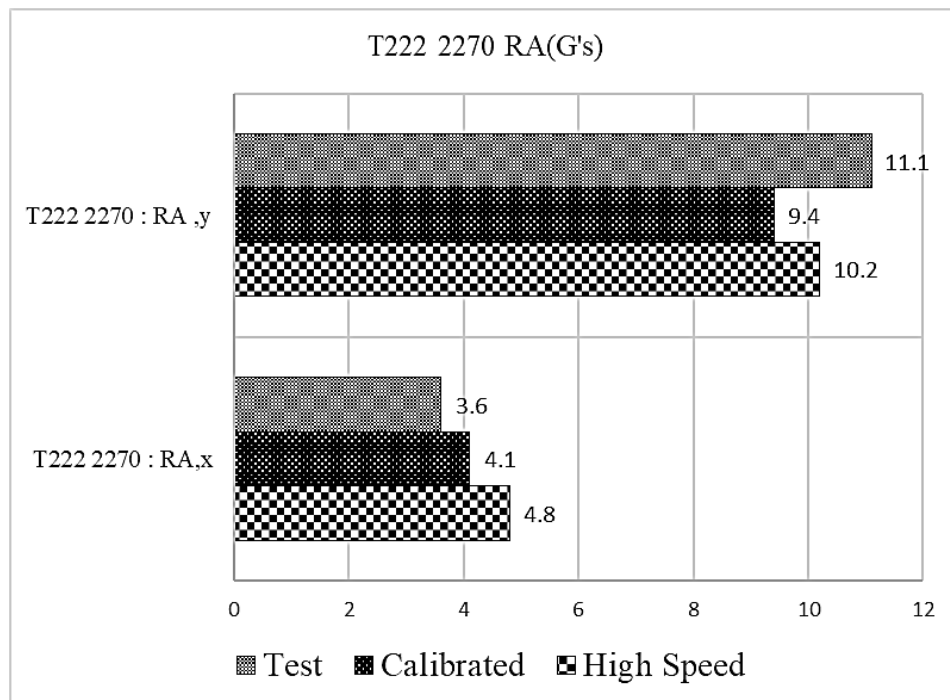
**Figure 53. Roll, Pitch, Yaw for T222-Car.**

**Table 52. Occupant Risk Factors for T222-Car.**

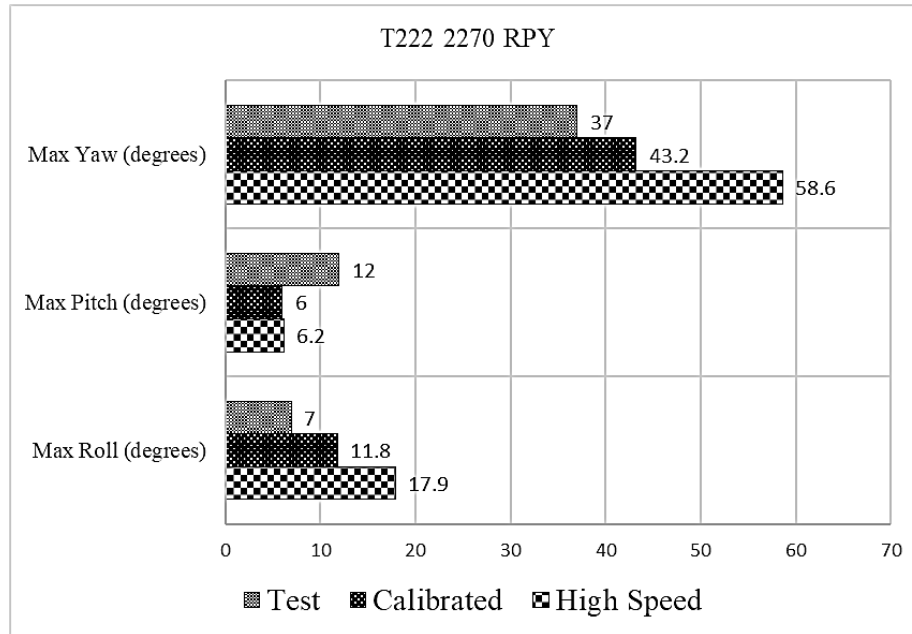
Test Parameter	MASH	Baseline Simulation	High Speed Simulation
OIV, Longitudinal (ft/s)	$\leq 40.0$	20.4	24.7
OIV, Lateral (ft/s)	$\leq 40.0$	30.3	34.3
RA, Longitudinal (g)	$\leq 20.49$	4.3	5.0
RA, Lateral (g)	$\leq 20.49$	14.3	14.7
Roll (deg.)	$\leq 75$	10.6	18.7
Pitch (deg.)	$\leq 75$	7.6	8.2
Yaw (deg.)	N/A	37.2	48.3



**Figure 54. Occupant Impact Velocity for T222-Truck.**



**Figure 55. Ridedown Acceleration for T222-Truck.**



**Figure 56. Roll, Pitch, Yaw for T222-Truck.**

**Table 53. Occupant Risk Factors for T222-Truck.**

Test Parameter	MASH	Crash Test (18)	Baseline Simulation	High Speed Simulation
OIV, Longitudinal (ft/s)	$\leq 40.0$	21.6	18.1	22.3
OIV, Lateral (ft/s)	$\leq 40.0$	26.9	29.2	33.4
RA, Longitudinal (g)	$\leq 20.49$	3.6	4.1	4.8
RA, Lateral (g)	$\leq 20.49$	11.1	9.4	10.2
Roll (deg.)	$\leq 75$	7	11.7	17.8
Pitch (deg.)	$\leq 75$	12	6.2	6.3
Yaw (deg.)	N/A	37	43.2	58.6

Table 54 provides a comparison between the test and baseline validation simulation for the T222 vertical concrete bridge rail for both passenger car and pickup truck. No passenger car test was available, so only the MASH simulation results are shown. The comparison for the pickup truck impact includes the maximum absolute values of OIV and RA, as well as the absolute percentage variation between the test and simulation. The comparison is reasonable, with a difference of approximately 11 percent for the OIV and 15 percent for RA.

**Table 54. MASH TL-3 FEA T222 System Validation.**

Vehicle	Parameter	Crash Test (18)	Baseline Simulation	$ \% \text{ Variation}  = 100 * (\text{MASH Simulation} - \text{Test}) / \text{Test}$
Passenger Car	OIV (ft/sec)	N/A	30.3	N/A
Passenger Car	RA (g)	N/A	14.3	N/A
Pickup Truck	OIV (ft/s)	26.9	29.9	11.15
Pickup Truck	RA (g)	11.1	9.4	15.31

The occupant risk metrics and angular displacements associated with the high-speed impact conditions increased for both vehicles for the T222 compared to the MASH impact conditions. However, the values were well within MASH thresholds. Based on the simulation results, the T222 vertical concrete bridge rail is likely to meet MASH evaluation criteria for the high-speed impact conditions associated with a posted speed limit of 85 mph.

#### 4.4. F-SHAPE CONCRETE BARRIER

Details of the 32-inch-tall F-Shape concrete safety barrier are found in TxDOT bridge rail standard Type T551, which is presented in Appendix D. The FEA simulations were performed with both the 1100C passenger car and 2270P pickup truck. The impact conditions for the crash test, validation simulation, and high-speed simulation (representative of an 85-mph posted speed limit) are shown in Table 55 and Table 56 for the passenger car and pickup truck, respectively.

**Table 55. F-Shape Impact Conditions for Passenger Car.**

Description	Impact Speed (mph)	Impact Angle (degrees)
Test 603111-1 (19)	62.3	25.8
Baseline Simulation	62.3	25.8
High-Speed Simulation	68.9	27.3


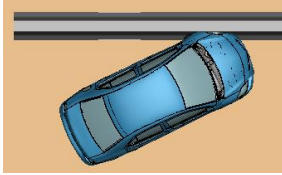


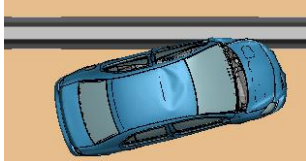


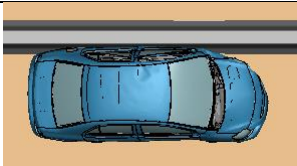
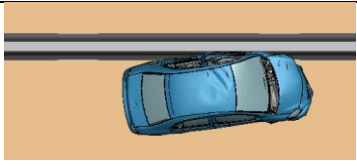

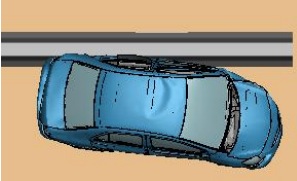
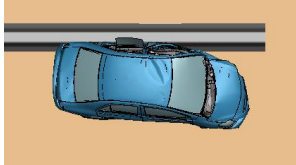

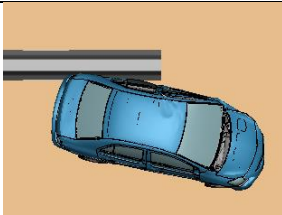
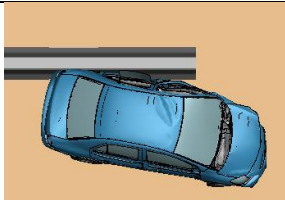
**Table 56. F-Shape Impact Conditions for Pickup Truck.**

Description	Impact Speed (mph)	Impact Angle (degrees)
Test 603111-12 (19)	62.8	25.2
Baseline Simulation	62.8	25.2
High-Speed Simulation	68.9	27.3


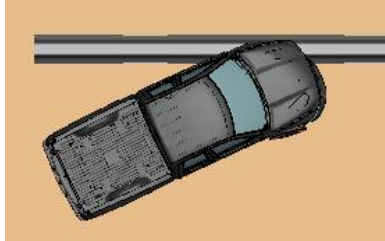
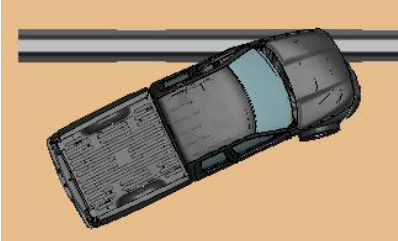

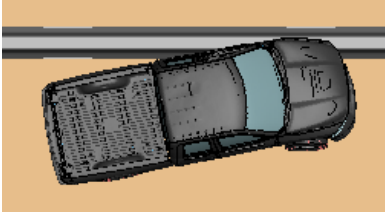
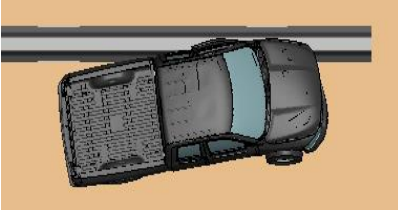

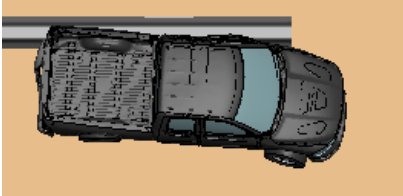
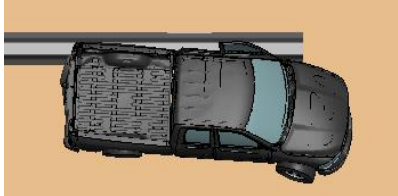

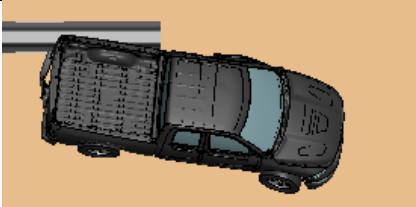

A comparison of vehicle behavior for the crash test, validation simulation performed at the same impact conditions as the crash test, and the high-speed simulation for 85-mph posted speed limit is shown in Table 57 for the passenger car and Table 58 for the pickup truck from an overhead perspective. Additional comparisons of vehicle behavior from a frontal view between the MASH simulation and high-speed simulation are shown in Table 59 and Table 60 for the passenger car and pickup truck, respectively.



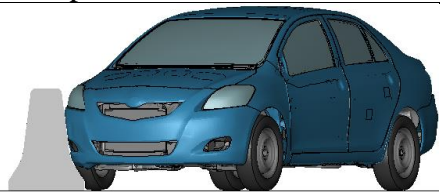
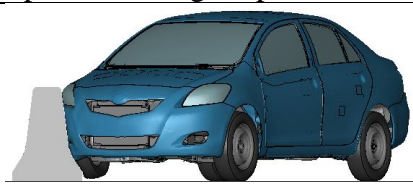
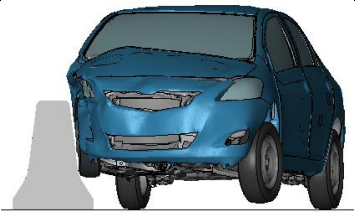
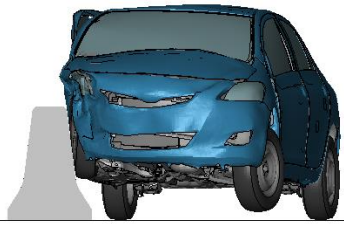
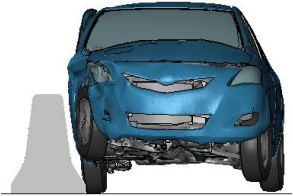
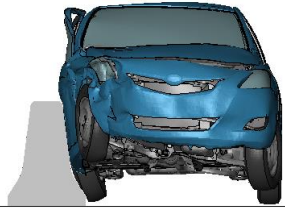
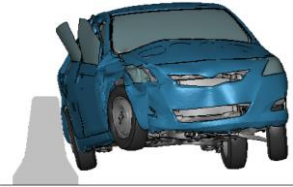

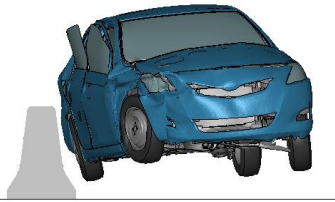
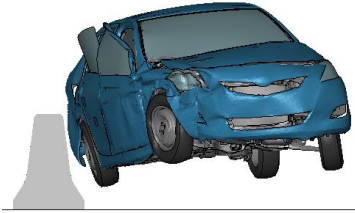
**Table 57. Post-Impact Trajectory of Passenger Car on F-Shape System—Top View.**

DESCRIPTION	F-Shape_1100_Test (19)	F-Shape_1100_MASH_Simulation	F-Shape_1100_High_Speed_Simulation
The front tire of the vehicle contacted the barrier.			
Vehicle ramps up after impacting the system.			
Rear tire of the vehicle contacted the barrier.			
Rear tire lost contact from the barrier			
Vehicle starting to exit the system.			




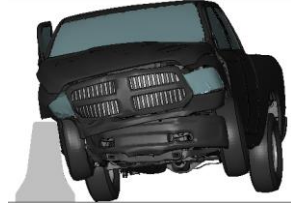
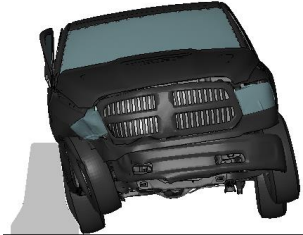



**Table 58. Post-Impact Trajectory of Pickup Truck on F-Shape System—Top View.**

DESCRIPTION	F-Shape_2270_Test (19)	F-Shape_2270_MASH_Simulation	F-Shape_2270_High_Speed_Simulation
The front tire of the vehicle contacted the barrier.			
Vehicle ramps up after impacting the system.			
Rear tire of the vehicle contacted the barrier.			
Rear tire lost contact with the system.			

**Table 59. Post-Impact Trajectory of Passenger Car on F-Shape System—Front View.**

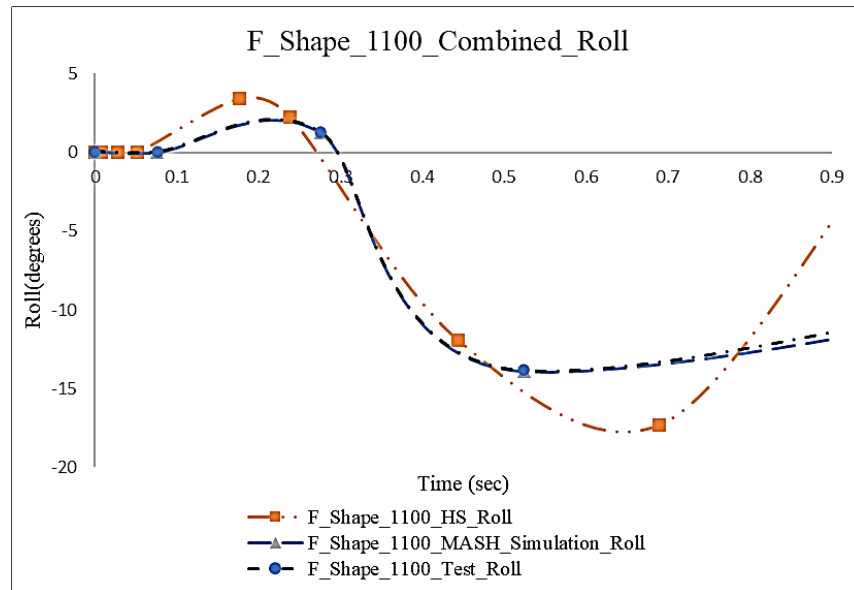
DESCRIPTION	F-Shape_1100_MASH_Simulation	F-Shape_1100_High_Speed_Simulation
The front tire of the vehicle contacted the barrier.		
Vehicle ramps up after impacting the system.		
Rear tire of the vehicle contacted the barrier.		
Rear tire lost contact from the barrier.		
Vehicle starting to exit the system.		

**Table 60. Post-Impact Trajectory of Pickup Truck on F-Shape System—Front View.**

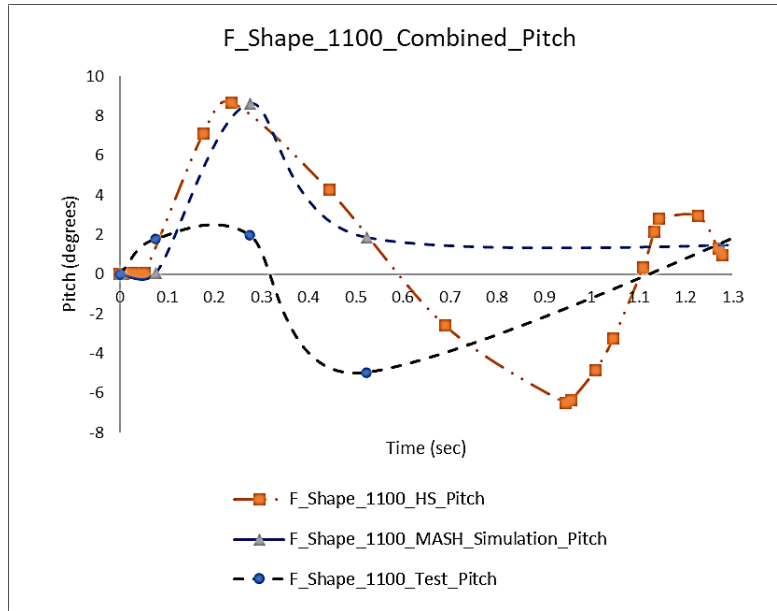
DESCRIPTION	F-Shape_2270_MASH_Simulation	F-Shape_2270_High_Speed_Simulation
The front tire of the vehicle contacted the barrier.		
Vehicle ramps up after impacting the system.		
Rear tire of the vehicle contacted the barrier.		
Rear tire lost contact with the system.		

A comparison of roll, pitch, and yaw angle time histories for the MASH and high-speed impact conditions for the passenger car with the F-Shape are shown in Figure 57 to Figure 59, respectively. A similar comparison for the pickup truck impacts with the F-Shape are shown in Figure 60 to Figure 62, respectively.

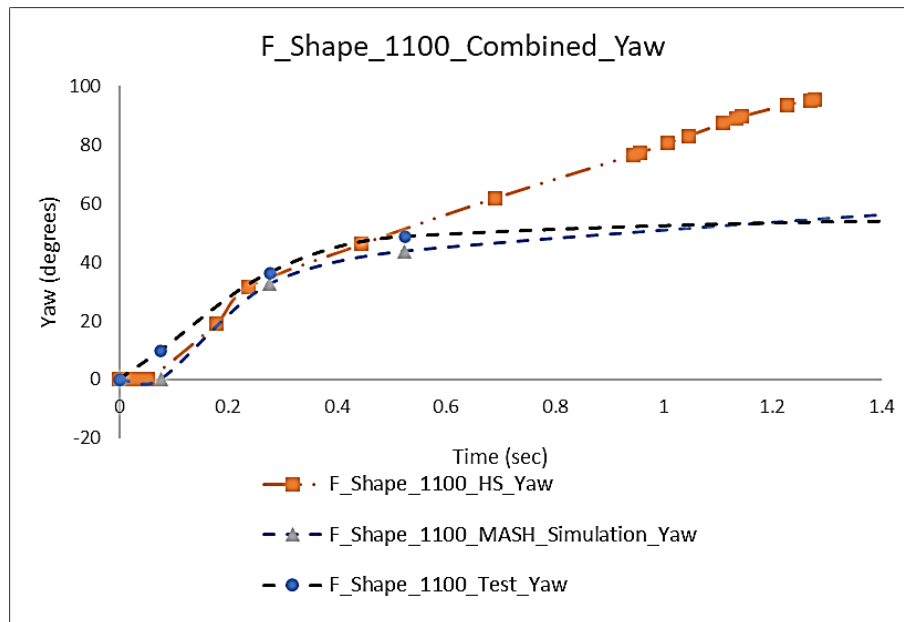
The TRAP was used to calculate the OIV, RA, and maximum roll, pitch, and yaw angles. A comparison of OIV, RA, and maximum roll, pitch, and yaw angles for the passenger car are shown in Figure 63 to Figure 65, respectively. These values are summarized and compared against MASH criteria in Table 61. A similar comparison for the pickup truck impacts with the SSCB are shown in Figure 66 to Figure 68, respectively. A summary against MASH criteria is provided in Table 62.



**Figure 57. Roll-Time History F-Shape-Car.**

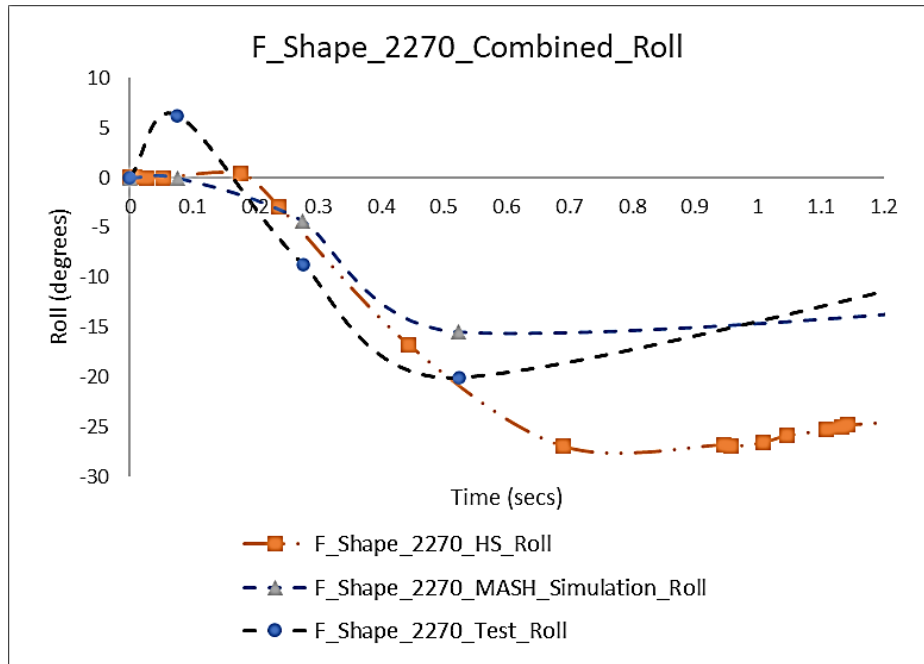


**Figure 58. Pitch-Time History for F-Shape-Car.**

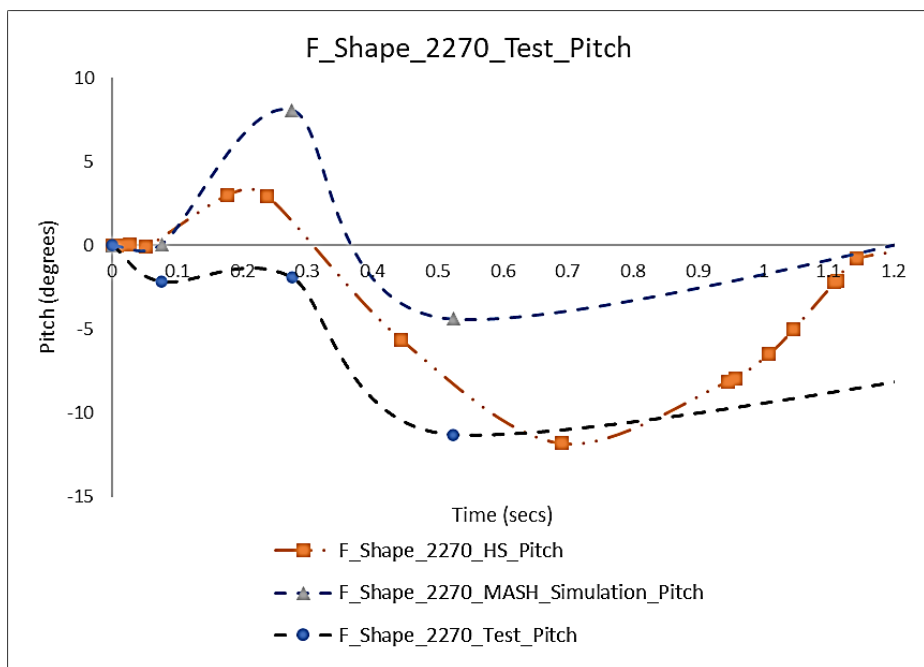


**Figure 59. Yaw-Time History for F-Shape-Car.**

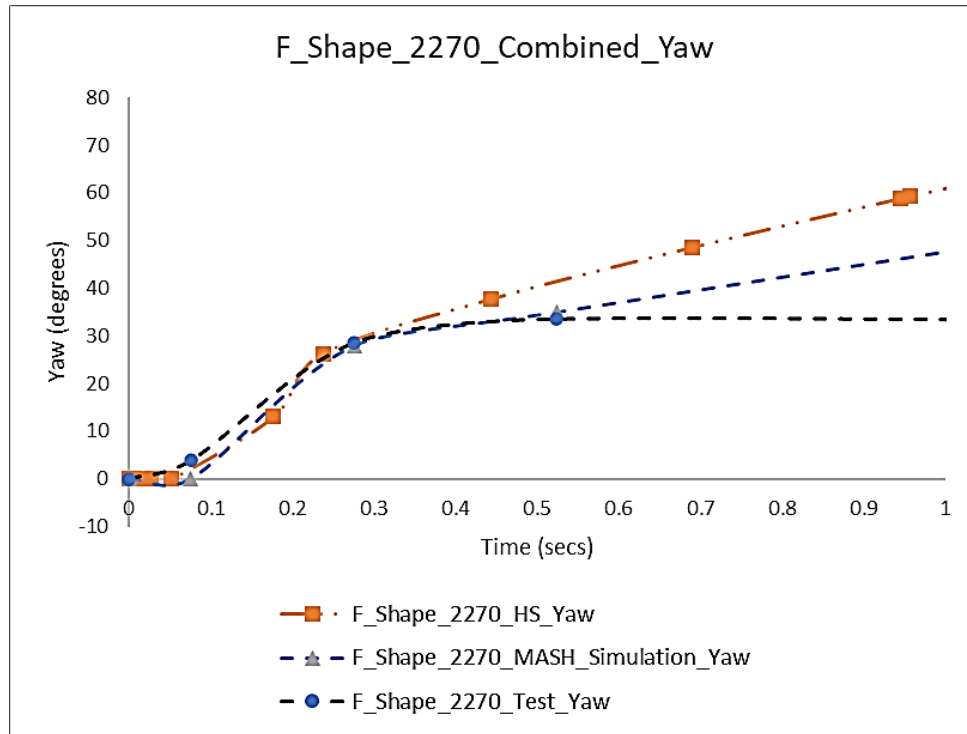




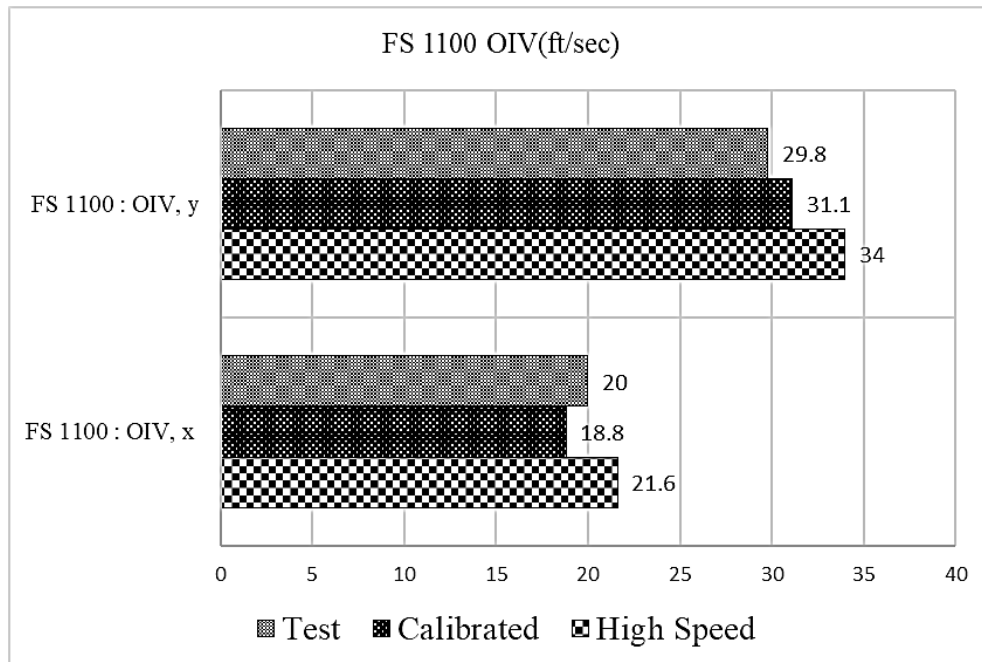
**Figure 60. Roll-Time History for F-Shape-Truck.**



**Figure 61. Pitch-Time History for F-Shape-Truck.**

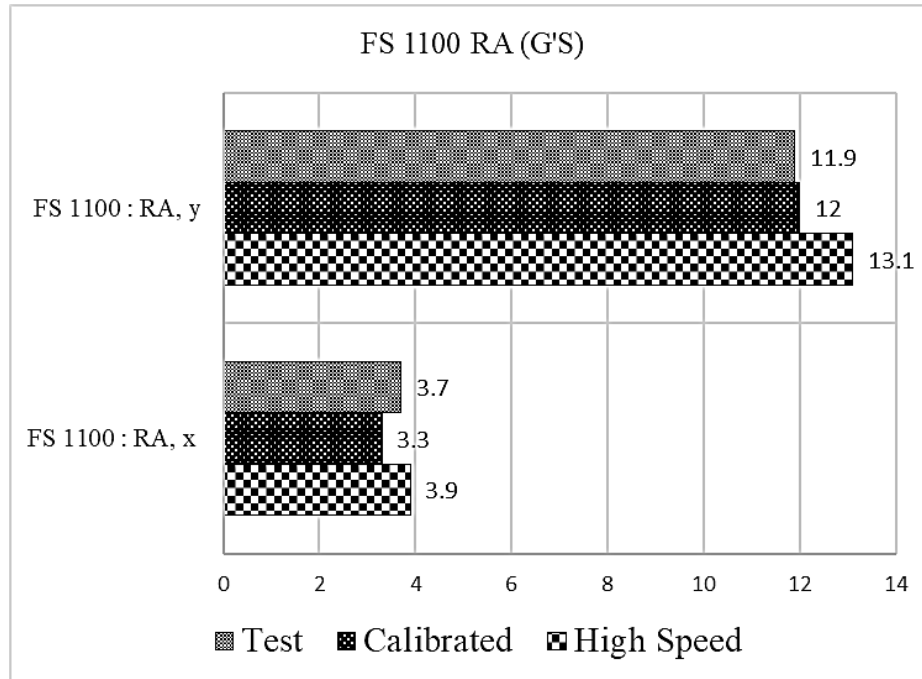


**Figure 62. Yaw-Time History for F-Shape-Truck.**

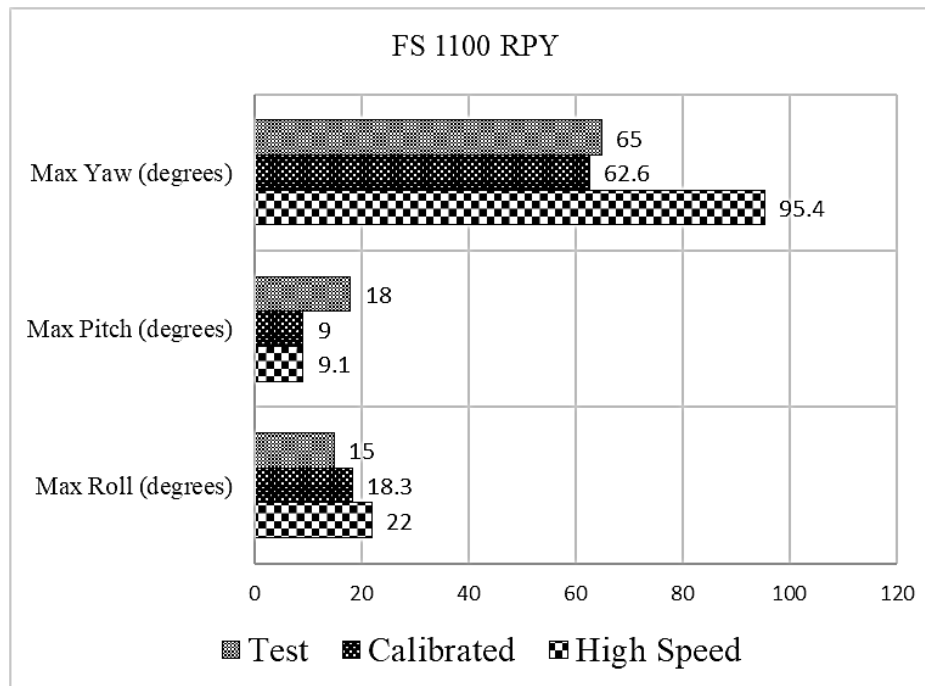


**Figure 63. Occupant Impact Velocity for F-Shape-Car.**





**Figure 64. Ridedown Acceleration for F-Shape-Car.**

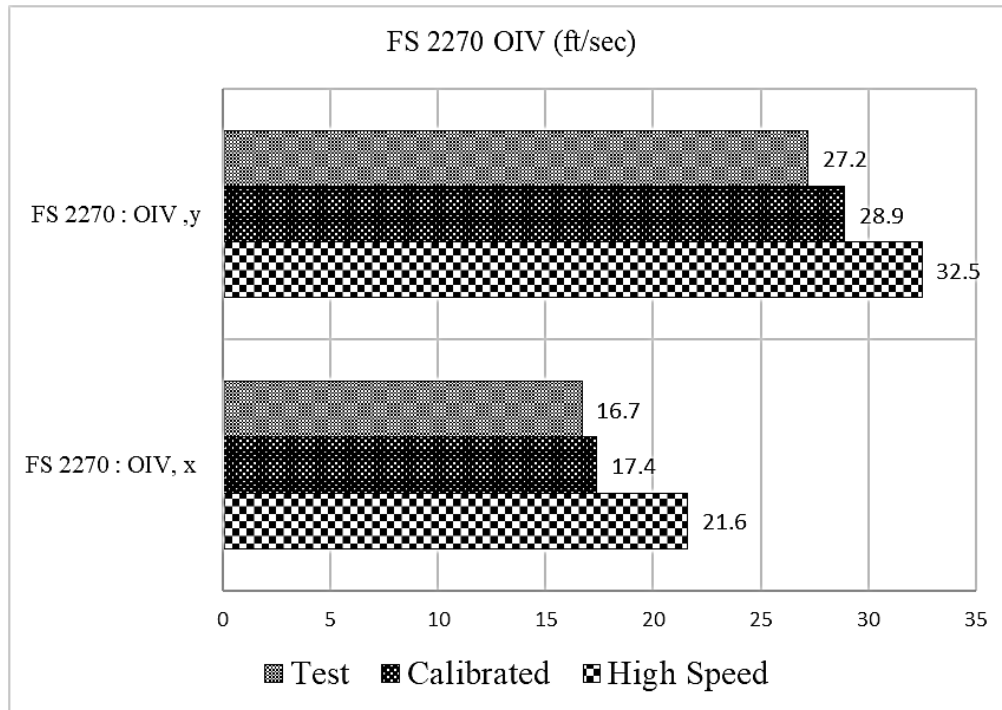


**Figure 65. Roll, Pitch, Yaw for F-Shape-Car.**

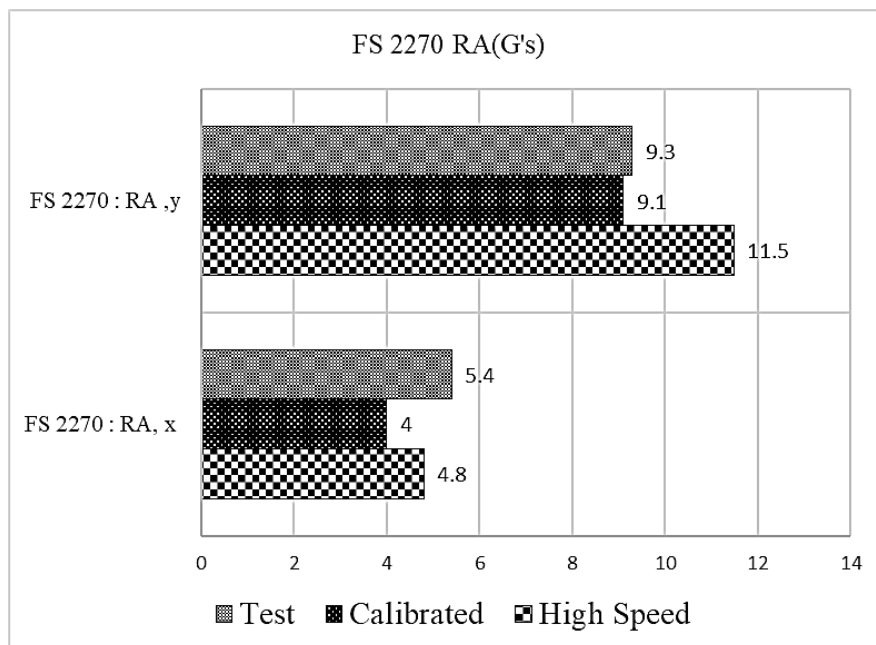
**Table 61. Occupant Risk Factors for F-Shape-Car.**

Test Parameter	MASH	Crash Test (19)	Baseline Simulation	High Speed Simulation
OIV, Longitudinal (ft/s)	≤ 40.0	20	18.8	21.6
OIV, Lateral (ft/s)	≤ 40.0	29.8	31.1	34.0

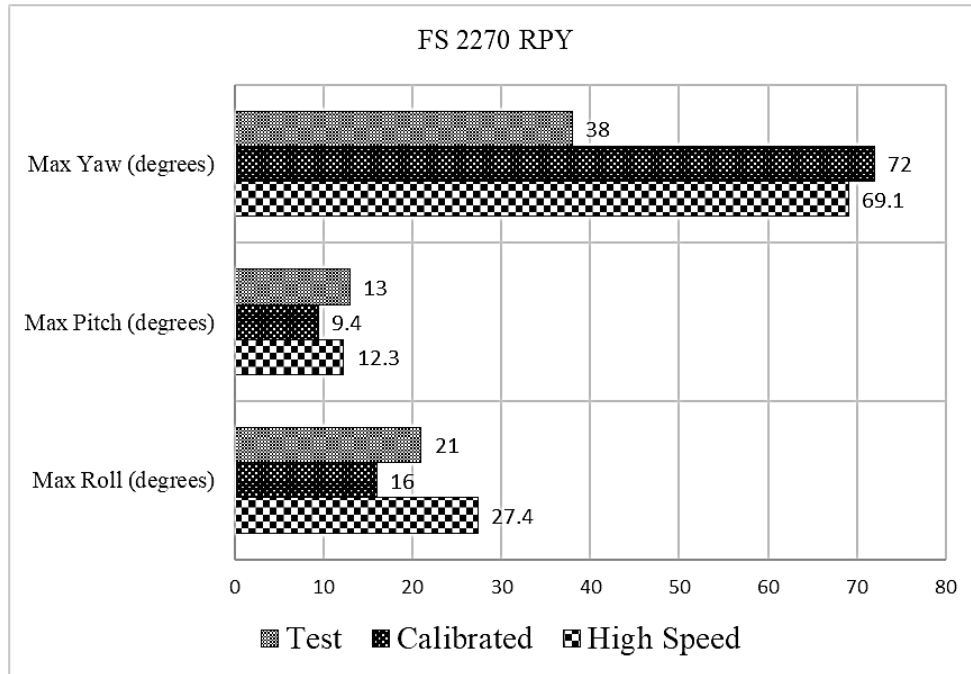
RA, Longitudinal (g)	$\leq 20.49$	3.7	3.3	3.9
RA, Lateral (g)	$\leq 20.49$	11.9	12.0	13.1
Roll (deg.)	$\leq 75$	15	18.3	22
Pitch (deg.)	$\leq 75$	18	9	9.1
Yaw (deg.)	N/A	65	62.6	95.4



**Figure 66. Occupant Impact Velocity for F-Shape-Truck.**



**Figure 67. Ridedown Acceleration for F-Shape-Truck.**



**Figure 68. Roll, Pitch, Yaw for F-Shape-Truck.**

**Table 62. Occupant Risk Factors for F-Shape-Truck.**

Test Parameter	MASH	Crash Test (19)	Baseline Simulation	High Speed Simulation
OIV, Longitudinal (ft/s)	$\leq 40.0$	16.7	17.4	21.6
OIV, Lateral (ft/s)	$\leq 40.0$	27.2	28.9	32.5
RA, Longitudinal (g)	$\leq 20.49$	5.4	4.0	4.8
RA, Lateral (g)	$\leq 20.49$	9.3	9.1	11.5
Roll (deg.)	$\leq 75$	21	16	27.4
Pitch (deg.)	$\leq 75$	13	9.4	12.3
Yaw (deg.)	N/A	38	72	69.1

Table 63 provides a comparison between the test and baseline validation simulation for the F-Shape concrete barrier for both passenger car and pickup truck. The comparison includes the maximum absolute values of OIV and RA, as well as the absolute percentage variation between the test and simulation. The comparison is good, with a maximum difference of approximately 6 percent for the OIV and 2 percent for RA.

**Table 63. MASH TL-3 FEA F-Shape System Validation.**

Vehicle	Parameter	Crash Test (19)	Baseline Simulation	$ \% \text{ Variation}  = 100 * (\text{MASH Simulation} - \text{Test}) / \text{Test}$
Passenger Car	OIV (ft/sec)	29.8	31.1	4.37
Passenger Car	RA (g)	11.9	12.0	0.84
Pickup Truck	OIV (ft/s)	27.2	28.9	6.25
Pickup Truck	RA (g)	9.3	9.1	2.15

The occupant risk metrics and angular displacements associated with the high-speed impact conditions increased for both vehicles for the F-Shape compared to the MASH impact conditions. However, the values were within MASH thresholds. Based on the simulation results, the F-Shape concrete barrier is likely to meet MASH evaluation criteria for the high-speed impact conditions associated with a posted speed limit of 85 mph.

#### 4.5. CONCLUSION

The researchers evaluated the impact performance of four concrete barrier systems under high-speed impact conditions associated with a posted speed limit of 85 mph through finite element simulation. The impact simulations were performed using models of a MASH 1100C passenger car (Toyota Yaris) and 2270P pickup truck (RAM pickup truck). In each case, the results of a baseline validation simulation under MASH impact conditions were compared with the results from the simulations using the determined high-speed impact conditions.

##### 4.5.1. Occupant Risk Comparison

Table 64 provides a comparison of OIV and RA values between the baseline MASH impact conditions and high-speed impact conditions for the passenger vehicle for all four concrete barrier types investigated. A similar comparison for the pickup truck simulations is shown in Table 65.

**Table 64. Comparison of Occupant Risk Metrics for Passenger Car Impacting Rigid Concrete Systems.**

System	Parameter	Baseline Simulation	High Speed Simulation	$ \% \text{ Variation}  = 100 * (\text{MASH Simulation} - \text{High Speed/MASH Simulation})$
SSTB	OIV, y (ft/s)	30.9	32.3	4.53
SSTB	RA, y (g)	14.3	13.4	6.30
SSTR	OIV, y (ft/s)	29.4	31.8	8.16
SSTR	RA, y (g)	11.9	12.9	8.40
T222	OIV, y (ft/s)	30.3	34.3	13.2
T222	RA, y (g)	14.3	14.7	2.80
F-Shape	OIV, y (ft/s)	31.1	34.0	8.68
F-Shape	RA, y (g)	12.0	13.1	9.17

**Table 65. Comparison of Occupant Risk Metrics for Pickup Truck Impacting Rigid Concrete Systems.**

System	Parameter	Baseline Simulation	High Speed Simulation	$ \% \text{ Variation}  = 100 * (\text{MASH Simulation} - \text{High Speed/MASH Simulation})$
SSTB	OIV, y (ft/s)	27.7	30.9	11.55
SSTB	RA, y (g)	14.6	12.6	13.70
SSTR	OIV, y (ft/s)	27.5	30.1	9.45
SSTR	RA, y (g)	13.0	12.4	4.61
T222	OIV, y (ft/s)	29.9	33.4	11.70
T222	RA, y (g)	9.4	10.2	8.51
F-Shape	OIV, y (ft/s)	28.9	32.5	12.45
F-Shape	RA, y (g)	9.1	11.5	26.37

The percent variation in occupant risk values for the passenger car between MASH and high-speed impact conditions is less than 10 percent for all barrier types, with the exception of the OIV for the T222 vertical concrete bridge rail, which is approximately 13 percent. The vertical profile of the T222 is expected to generate higher risk values compared to the single slope and F-Shape profiles that impart some vehicle climb.

The percent variation in occupant risk values for the pickup truck between MASH and high-speed impact conditions is less than 14 percent for all barrier types, with the exception of RA for the F-Shape concrete barrier, which is approximately 26 percent. Although, the percentage difference in RA for the F-Shape is higher than the metrics for the other concrete barriers, the RA value of 11.5 g is well below the MASH threshold of 20 g and is significantly below the preferred MASH value of 15 g.

#### 4.5.2. Angular Displacement Comparison

Table 66 provides a comparison of maximum roll, pitch, and yaw angles between the baseline MASH impact conditions and high-speed impact conditions for the passenger vehicle for all four concrete barrier types investigated. A similar comparison for the pickup truck simulations is shown in Table 67.

As shown in Table 66 and Table 67, the percentage difference in angular displacements is much more variable than the occupant risk metrics, ranging from approximately 1 percent to 76 percent for the passenger car and 2 percent to 71 percent for the pickup truck. The MASH threshold for roll and pitch angles is 75 degrees. The maximum roll and pitch angles for the passenger car across the different concrete barrier types for the high-speed impact conditions were 23 degrees and 14 degrees, respectively. Similarly, the maximum roll and pitch angles for the truck across the different concrete barrier types for the high-speed impact conditions were 29 degrees and 12 degrees, respectively. These values are indicative of stable vehicle redirection.

**Table 66. Comparison of Angular Displacements for Passenger Car Impacting Rigid Concrete Systems.**

<b>System</b>	<b>Parameter (degrees)</b>	<b>Baseline Simulation</b>	<b>High Speed Simulation</b>	<b> % Variation  = 100*(Baseline Model– High Speed)/Baseline Model)</b>
SSTB	Roll	18.6	23.1	24.20
SSTB	Pitch	12	12.3	2.5
SSTB	Yaw	54	73.5	36.12
SSTR	Roll	20.0	21.7	8.5
SSTR	Pitch	11.7	14.3	22.22
SSTR	Yaw	51.0	77.2	51.37
T222	Roll	10.6	18.7	76.41
T222	Pitch	7.6	8.2	7.90
T222	Yaw	37.2	48.3	29.84
F-Shape	Roll	18.3	22	20.20
F-Shape	Pitch	9	9.1	1.11
F-Shape	Yaw	62.6	95.4	52.40

**Table 67. Comparison of Angular Displacements for Pickup Truck Impacting Rigid Concrete Systems.**

<b>System</b>	<b>Parameter (degrees)</b>	<b>Baseline Simulation</b>	<b>High Speed Simulation</b>	<b> % Variation  = 100*(MASH Simulation– High Speed)/MASH Simulation)</b>
SSTB	Roll	12	14.2	18.34
SSTB	Pitch	7	8.1	15.71
SSTB	Yaw	37.2	45.2	21.50
SSTR	Roll	21.3	29.4	38.03
SSTR	Pitch	9.9	11.1	12.12
SSTR	Yaw	32.6	48.5	48.78
T222	Roll	11.7	17.8	52.14
T222	Pitch	6.2	6.3	1.61
T222	Yaw	43.2	58.6	35.65
F-Shape	Roll	16	27.4	71.25
F-Shape	Pitch	9.4	12.3	30.85
F-Shape	Yaw	72	69.1	4.03

Although the occupant risk metrics and angular displacements increased for the high-speed impact conditions compared to the MASH impact conditions, the values were all within MASH thresholds. Based on the simulation results, the SSCB, SSTR, T222, and F-Shape concrete barriers are likely to meet MASH evaluation criteria for the 1100C passenger car and 2270P pickup truck for the high-speed impact conditions associated with a posted speed limit of 85 mph.

## CHAPTER 5. STRUCTURAL ADEQUACY

Barriers must provide adequate structural capacity to contain and redirect vehicles impacting under the selected design conditions. Higher impact speeds increase the overall impact severity and result in increased impact loads that must be resisted by the barrier. In this chapter, the design impact loads associated with the impact conditions for roadways with higher posted speed limits are estimated and compared to the capacity of the various concrete barrier systems simulated in Chapter 4. The structural analysis procedures used to determine capacity of the solid concrete barrier systems follow the yield line analyses developed in Section 13 of the *AASHTO LRFD Bridge Design Specifications* (20).

### 5.1. DESIGN IMPACT LOADS

The design loads in the *AASHTO LRFD Bridge Design Specifications* are based on NCHRP Report 350 impact conditions. Updated design loads for MASH impact conditions were developed under NCHRP Project 22-20(2) (21). For MASH TL-3, the design impact load is 71 kips at a resultant height of 19 inches.

To estimate the design force for the high-speed impact conditions, TTI researchers scaled the MASH TL-3 design force of 71 kips based on the increase of IS between the two test conditions. The IS is defined as:

$$IS = \frac{1}{2} M(V \sin \theta)^2 \quad \text{Eqn. 1}$$

Where:

IS = Impact Severity, kip-ft

M = Vehicle mass, lb

V = Impact Speed, ft/s

$\theta$  = Impact Angle, degrees

For MASH Test 3-11, which is the structural adequacy test for TL-3, the nominal impact speed is 62 mph, the nominal impact angle is 25 degrees, and the weight of the 2270P pickup truck is 5,000 lb. This impact condition results in an IS of 114.7 kip-ft.

For a roadway with a posted speed limit of 80 mph, the associated 85th percentile impact speed is 66.4 mph, and the 85th percentile impact angle is 25.6 degrees. Considering the MASH 2270P pickup truck, which has a weight of 5,000 lb, the resulting IS is 137.5 kip-ft. This IS is 19.9 percent greater than the IS for MASH Test 3-11, resulting in a scaled design impact force of 85.1 kips.

For a roadway with a posted speed limit of 85 mph, the associated 85th percentile impact speed is 68.9 mph, and the 85th percentile impact angle is 27.3 degrees. Considering the MASH 2270P pickup truck, which has a weight of 5,000 lb, the resulting IS is 166.8 kip-ft. This IS is 45.4 percent greater than the IS for MASH Test 3-11, resulting in a scaled design impact force of 103.3 kips.

## 5.2. YIELD LINE ANALYSIS PROCEDURE

A strength analysis following the methodology of Section 13 of the *AASHTO LRFD Bridge Design Specifications* (20) was used to analyze the structural capacity of T222, F-Shape, and SSTR concrete barriers.

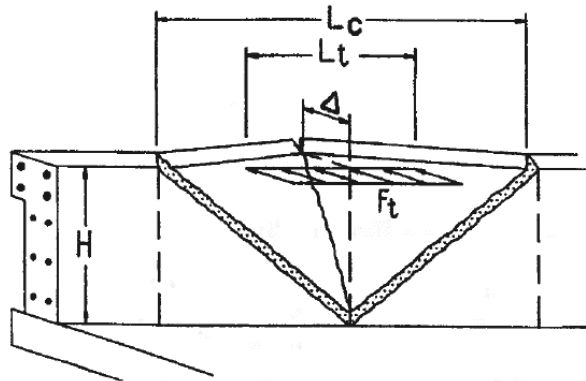
The total transverse resistance of a solid concrete parapet on an interior segment of the barrier away from a joint, as represented in Figure 69, is calculated using Equations A13.3.1-1 and A13.3.1-2 from AASHTO LRFD Section 13 (Equations 2 and 3 below):

$$R_W = \left( \frac{2}{2L_c - L_t} \right) \left( 8M_b + 8M_w + \frac{M_c L_c^2}{H} \right) \quad \text{Eqn. 2}$$

$$L_c = \frac{L_t}{2} + \sqrt{\left( \frac{L_t}{2} \right)^2 + \frac{8H(M_b + M_w)}{M_c}} \quad \text{Eqn. 3}$$

Where:

- $R_w$  = Total transverse resistance of the railing (kips)
- $L_c$  = Critical length of yield line failure pattern (ft)
- $L_t$  = Longitudinal length of distribution of impact force (ft)
- $M_w$  = Flexural resistance of the wall about its vertical axis (kip-ft)
- $M_b$  = Additional flexural resistance of beam in addition to  $M_w$ , if any, at top of the wall (kip-ft)
- $M_c$  = Flexural resistance of cantilevered walls about an axis parallel to the longitudinal axis of the bridge rail (kip-ft/ft)
- $H$  = Height of wall (ft)



**Figure 69. Yield Line Analysis of Concrete Parapet for Impact within Wall Segment (20).**

The total transverse resistance of a solid concrete parapet at the end of a segment or at a joint, as illustrated in Figure 70, can be calculated using Equations A13.3.1-3 and A13.3.1-4 from AASHTO Section 13 (Equations 4 and 5 below):

$$R_W = \left( \frac{2}{2L_c - L_t} \right) \left( M_b + M_w + \frac{M_c L_c^2}{H} \right) \quad \text{Eqn. 4}$$



$$L_c = \frac{L_t}{2} + \sqrt{\left(\frac{L_t}{2}\right)^2 + H \left(\frac{M_b + M_w}{M_c}\right)} \quad \text{Eqn. 5}$$

Where:

$R_w$  = Total transverse resistance of the railing (kips)

$L_c$  = Critical length of yield line failure pattern (ft)

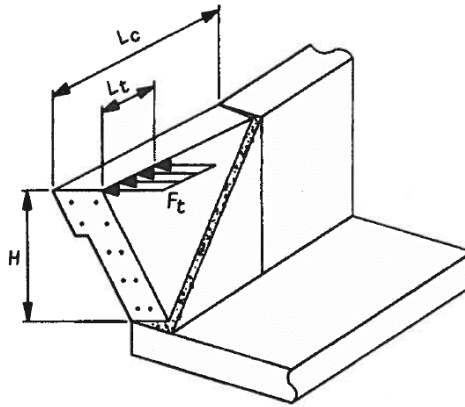
$L_t$  = Longitudinal length of distribution of impact force (ft)

$M_w$  = Flexural resistance of the wall about its vertical axis (kip-ft)

$M_b$  = Additional flexural resistance of beam in addition to  $M_w$ , if any, at top of the wall (kip-ft)

$M_c$  = Flexural resistance of cantilevered walls about an axis parallel to the longitudinal axis of the bridge rail (kip-ft/ft)

$H$  = Height of wall (ft)



**Figure 70. Yield Line Analysis of Concrete Parapet for Impact Near End of Segment (20).**

### 5.3. BARRIER CAPACITY

The transverse resistance of the SSTR, T222 vertical parapet, and F-Shaped concrete bridge rail (T551) computed using the yield line analysis approach of AASTHO LRFD Section 13 is shown in Table 68. The simulations of the F-Shape concrete barrier in Chapter 4 geometrically represented a symmetric median barrier profile. Since the barrier was rigidly modeled, the results equally applicable to a single-sided, F-Shape bridge rail such as the T551. The strength analysis was performed on the single-sided T551 F-Shape bridge rail because it represents a more critical section from a capacity standpoint.

**Table 68. Total Transverse Barrier Resistance.**

Barrier	T551	T222	SSTR
Within wall segment (kips)	159.0	184.6	162.0
Near the end of wall segment (kips)	90.0	97.6	90.9

Recall from Section 5.1 that the design impact load associated with an 80-mph posted speed limit is 85.1 kips. Therefore, according to the strength analysis, all barrier types analyzed have adequate capacity to resist impact loads associated with the design impact conditions for a roadway with a posted speed of 80 mph both within the barrier interior as well as at the end of a barrier segment or joint.

The design impact load associated with an 85-mph posted speed limit is 103.3 kips. The capacity of each barrier type within the barrier interior is sufficient for resisting this design impact load. However, at the end of a barrier segment, the calculated capacity is less than the design impact load. Thus, the reinforcement may need to be increased at the end of segments to accommodate the design impact load associated with an 85-mph posted speed limit.

The researchers performed additional strength analyses with the barrier vertical reinforcement and deck anchorage vertical reinforcement reduced from the original 6 inches. As shown in Table 69, a small decrease in spacing to 5.5 inches for the T222 and 5.0 inches for the F-Shape (T551) and SSTR provides sufficient capacity to accommodate the 103.3-kip design impact load associated with a posted speed limit of 85 mph. The length of the reduced barrier vertical reinforcement and deck anchorage reinforcement is 5 ft from the end for the F-Shape (T551) and 5.5 ft for the T222 and SSTR.

**Table 69. Transverse Strength for Recommended End Reinforcement Spacing and Length for 85 mph Posted Speed Limit.**

Parameter	T551	T222	SSTR
Barrier vertical reinforcement spacing at end/joint	5.0 in	5.5 in	5.0 in.
Deck anchorage reinforcement spacing at end/joint	5.0 in	5.5 in	5.0 in.
Barrier End Capacity, $R_{w\_end}$	103.5 kips	103.7 kips	104.4 kips
$L_{c\_end}$ (length needed for end reinforcement)	5.0 ft	5.5 ft	5.5 ft

## 5.4. CONCLUSION

The structural adequacy assessment of selected concrete barriers was investigated by comparing the structural capacity of the barrier systems with the design impact loads associated with posted speed limits of 80 mph and 85 mph. The F-Shape (T551), T222 vertical parapet, and SSTR were determined to be structurally adequate for an 80-mph posted speed limit both within the barrier interior and at the end of a segment.

While the transverse capacity of the barrier interior was also satisfactory for design impact loads for an 85-mph posted speed limit, the resistance at a segment end or joint was slightly below the design impact load. The end capacity was increased to resist the design impact load for an 85-mph posted speed limit by slightly reducing the spacing of the barrier vertical reinforcement and deck anchorage reinforcement for a short distance, as recommended in Table 69.

## CHAPTER 6. GUARDRAIL

A guardrail is a barrier used to help shield motorists from obstacles or non-traversable terrain features on the roadside. The TxDOT Metal Beam Guard Fence (MBGF) is a type of strong post, semi-rigid guardrail that incorporates a W-beam rail element mounted on  $W6 \times 8.5$  steel posts with wood or composite offset blocks inserted between the rail and posts. The 31-inch rail mounting height and placement of rail splices midspan between posts make the MBGF a variation of the MGS. Details of the MBGF can be found in TxDOT standard GF(31)-19. Consideration was given to the impact performance of this guardrail and other guardrail systems under high-speed impact conditions.

### 6.1. PREVIOUS GUARDRAIL TESTING AND PERFORMANCE LIMITS

The MGS guardrail and many associated design configurations, including the TxDOT MBGF, have satisfied MASH TL-3 impact conditions. However, recent testing of different guardrail applications under MASH TL-3 impact conditions have resulted in rail rupture or tearing, indicating that guardrail design may not have significant reserve capacity to accommodate high-speed impacts.

MASH Test 3-10 with the 1100C passenger car was performed on an MGS guardrail with 32-inch rail mounting height placed with the front face of the guardrail located 6 inches behind a 6-inch-tall AASHTO Type B curb and one post omitted near the middle of the system, resulting in a 12.5-ft span between two posts (22). The W-beam rail ruptured at the splice located within the unsupported span. The system was strengthened using 37.5 ft of nested W-beam rail around the location of the omitted post. In a test of the modified system, the vehicle was successfully contained and redirected without any evidence of rail tearing (22).

In another project, MASH Test 3-11 was performed on an MGS W-beam guardrail with the post spacing reduced from the standard spacing of 75 inches to a half post spacing of 37.5 inches (23). The objective of the project was to evaluate the dynamic deflection of stiffened guardrail systems. During the impact, the rail ruptured due to localized interaction between the W-beam rail and offset block (23). The system was modified by using a shortened offset block. The modified system successfully met MASH Test 3-11 criteria, and the pickup truck was contained and redirected without any evidence of rail tearing.

Under a project sponsored by the Roadside Safety Pooled Fund, a stiffened thrie-beam guardrail system was designed to reduce dynamic deflection for placement in close proximity to fixed objects on the roadside (24). A thrie-beam rail has a greater cross-sectional area and is generally considered to have more capacity than a W-beam rail. When MASH Test 3-11 was performed on the stiffened thrie-beam guardrail, the pickup truck was successfully contained and redirected, but the thrie-beam rail was partially torn.

Recall from Chapter 1 that the impact severity associated with MASH TL-3 impact conditions of 62 mph and 25 degrees is 114.7 kip-ft. For impact conditions associated with an 80-mph posted speed limit (66.4 mph and 25.6 degrees), the impact severity increases to 137.5 kip-ft., which is a 19.9 percent increase.

Although the MGS W-beam guardrail system has not been directly tested at higher impact speeds, it has been tested in various flared configurations that resulted in a higher impact

severity. The guardrail flare increases the effective impact angle, which increases the overall impact severity.

MASH Test 3-10 with the 1100C passenger car was performed on an MGS steel post, W-beam guardrail system installed on a 7:1 flare (25). The flare effectively increased the nominal impact angle by 8 degrees, with the actual IS being 91.4 kip-ft. During the test, the W-beam guardrail ruptured at a post location, permitting penetration of the test vehicle behind the system (25).

MASH Test 3-11 with the 2270P pickup truck was subsequently performed on an MGS steel post, W-beam guardrail system installed on a reduced 11:1 flare (25). The flare effectively increased the nominal impact angle by 5 degrees, with the actual IS being 149.8 kip-ft. During the test, the W-beam guardrail ruptured between post locations, permitting penetration of the test vehicle behind the system (25).

These tests raised concerns regarding the ability of standard MBGF to accommodate the increased impact severity associated with higher speed impacts estimated for roadways with higher posted speed limits. These failure modes often result from very localized interactions between the vehicle and rail element that can be difficult to capture through finite element modeling and simulation. Accurately modeling and predicting rail rupture is particularly challenging given current material models and modeling techniques. More commonly, predicted rail stresses and/or strains, rail deformation, and rail deflected shape are analyzed to evaluate propensity for rail failure.

After discussion with the project panel, it was decided to focus on the evaluation of two guardrail configurations considered to offer potential for enhanced capacity for higher severity impact conditions. These include an MGS W-beam guardrail system with shortened blockouts and a roadside thrie-beam guardrail system (RTGS) that was successfully tested to MASH TL-3 criteria (26).

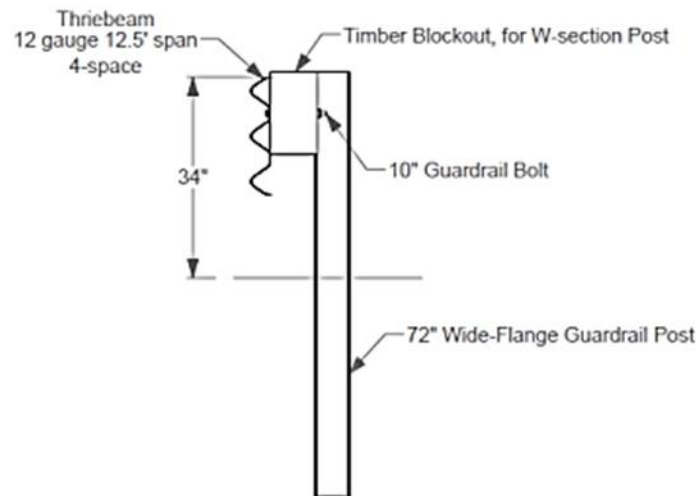
As referenced above, an MGS guardrail system with reduced (half) post spacing was successfully tested in accordance with MASH Test 3-11 criteria using shortened offset blocks after an unsuccessful test with conventional length offset blocks (23). Researchers theorized that the shortened offset blocks reduce stress concentrations on the bottom edge of the rail where rail tears often initiate.

The RTGS uses a stronger thrie-beam rail element with a taller mounting height of 34 inches in conjunction with shortened offset blocks (26). Researchers believe the attributes of this rail system may provide additional capacity to accommodate higher speed impacts.

The impact performance of these two guardrail systems was evaluated using finite element modeling and simulation. While the previously mentioned limitations are acknowledged, TTI researchers believed these simulations would add knowledge and increase understanding of guardrail behavior under high-speed impact conditions and avoid obvious failure modes. The simulation effort undertaken to investigate the performance of these systems following the impact conditions estimated for 80-mph posted speed limits is described in the following sections.

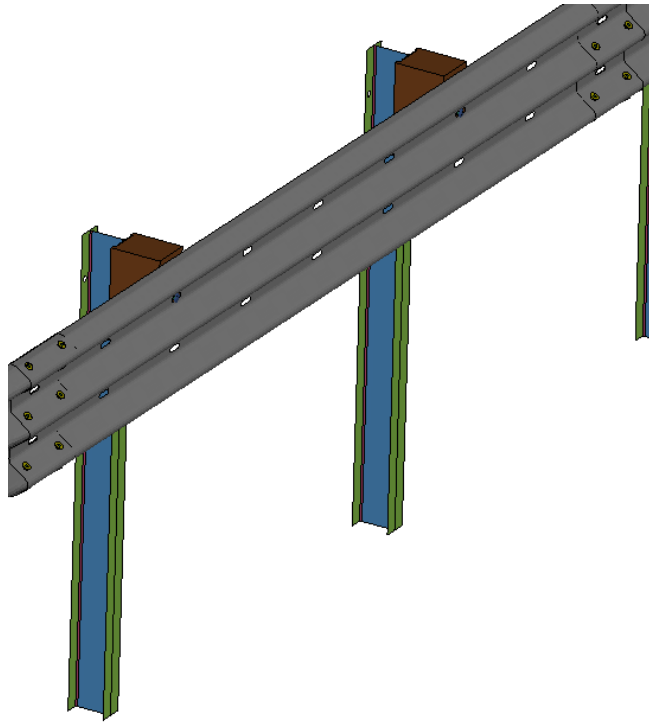
## 6.2. ROADSIDE THRIE-BEAM GUARDRAIL SYSTEM

The RTGS consists of a 12-gauge thrie-beam rail element mounted on standard 6-ft-long, W6×8.5 steel posts at a height of 34 inches (26). The support posts have a 75-inch spacing. A 14-inch-long wooden offset block, typical of W-beam guardrail systems, is incorporated between the rail and posts and secured with a single guardrail bolt. Figure 71 shows a cross section of the RTGS.

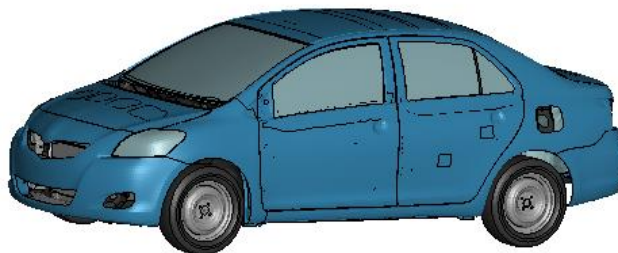


**Figure 71. Roadside Thrie-Beam Guardrail System (26).**

An existing finite element model of the RTGS system, shown in Figure 72, was used in the simulation effort. The model was previously validated and used in the development and evaluation of the RTGS for MASH TL-3 impact conditions (26). Figure 73 shows images of the MASH 1100C passenger car and 2270P pickup truck vehicle models used in the high-speed simulation analyses. These models were developed by researchers at George Mason University under sponsorship of FHWA and have been modified by TTI researchers to improve robustness and fidelity over the course of various simulation projects.



**Figure 72. Finite Element Model of Roadside Thrie-Beam Guardrail System.**



(a)



(b)

**Figure 73. MASH Test Vehicles: (a) 1100C and (b) 2270P.**

The predictive impact simulations on the RTGS were performed using impact conditions for a posted speed limit of 80 mph, which involved an impact speed of 66.4 mph and impact angle of 25.6 degrees. The researchers conducted the simulations at three different impact points to determine the critical impact point (CIP) for each design vehicle. Traditional impact locations

indicated by MASH are not necessarily applicable for higher speed impacts. The simulations were performed with the impact point occurring at a post as well as 2 ft upstream and downstream of a post.

The RTGS system was evaluated for vehicle stability and occupant risk factors. Results from the three high-speed simulations with the 1100C passenger car are shown in Table 70 to Table 72 for impact at a post, 2 ft downstream of a post, and 2 ft upstream of a post, respectively. In all cases, the occupant risk criteria and angular displacements satisfied MASH criteria.

Based on a review of the results, the researchers recommend impacting at a post as the CIP for the 1100C passenger car impacting the RTGS at high speed. It has marginally higher occupant risk metrics and roll angle compared to the simulations at the other impact points.

**Table 70. RTGS 1100C Simulation Results with Impact Point at Post.**

Test Parameter	MASH Criteria	High Speed Impact at Post
OIV, Longitudinal (ft/s)	$\leq 40.0$	20.8
OIV, Lateral (ft/s)	$\leq 40.0$	22.3
RA, Longitudinal (g)	$\leq 20.49$	-19.1
RA, Lateral (g)	$\leq 20.49$	-13.5
Max. Roll (deg.)	$\leq 75$	-13.0
Max. Pitch (deg.)	$\leq 75$	3.6
Max. Yaw (deg.)	N/A	-42.9
Max. Rail Deflection (inches)	N/A	33.1

**Table 71. RTGS 1100C Simulation Results with Impact Point 2 ft Downstream of Post.**

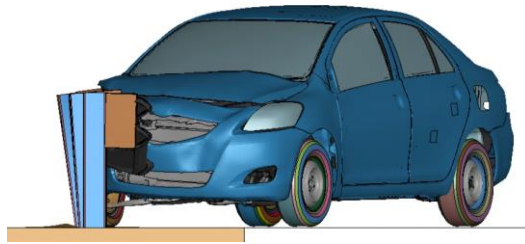
Test Parameter	MASH Criteria	High Speed Impact 2 ft Downstream of Post
OIV, Longitudinal (ft/s)	$\leq 40.0$	21.8
OIV, Lateral (ft/s)	$\leq 40.0$	19.1
RA, Longitudinal (g)	$\leq 20.49$	-18.1
RA, Lateral (g)	$\leq 20.49$	-11.9
Max. Roll (deg.)	$\leq 75$	11.8
Max. Pitch (deg.)	$\leq 75$	-5.0
Max. Yaw (deg.)	N/A	-64.1
Max. Rail Deflection (inches)	N/A	38.1

**Table 72. RTGS 1100C Simulation Results with Impact Point 2 ft Upstream of Post.**

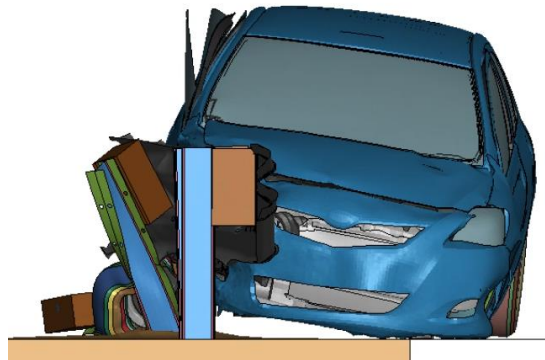
Test Parameter	MASH Criteria	High Speed Impact 2 ft Upstream of Post
OIV, Longitudinal (ft/s)	$\leq 40.0$	26.4
OIV, Lateral (ft/s)	$\leq 40.0$	19.7
RA, Longitudinal (g)	$\leq 20.49$	-14.8
RA, Lateral (g)	$\leq 20.49$	-12.5
Max. Roll (deg.)	$\leq 75$	-5.9

Max. Pitch (deg.)	$\leq 75$	-4.0
Max. Yaw (deg.)	N/A	-48.1
Max. Rail Deflection (inches)	N/A	41

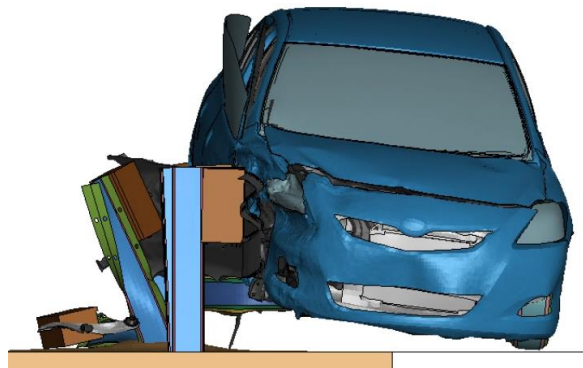
Figure 74 to Figure 77 present images from the high-speed passenger car simulation with the RTGS system at the CIP (i.e., impact at a post). The 1100C vehicle is successfully contained and redirected. Significant wheel interaction with the posts is evident. The vehicle model used in the simulations incorporated suspension failure, and the front impact side wheel separated from the vehicle.



**Figure 74. Front Tire of Car Contacts Post in RTGS (T = 0.08 sec).**

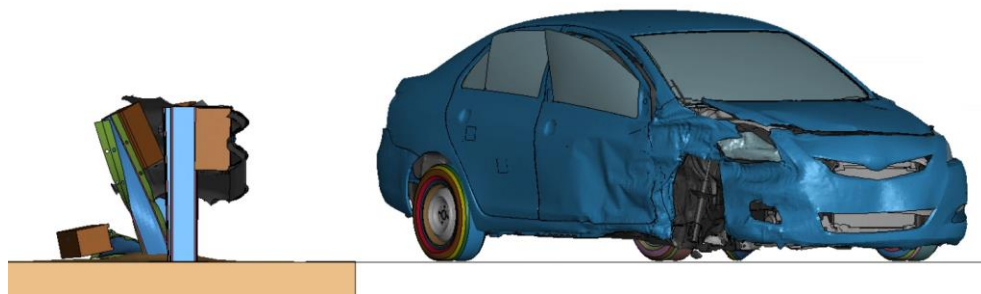


**Figure 75. Wheel Snagging on Post during Car Interaction with RTGS (T = 0.24 sec).**



**Figure 76. Rear of Car Interacts with RTGS (T = 0.335 sec).**

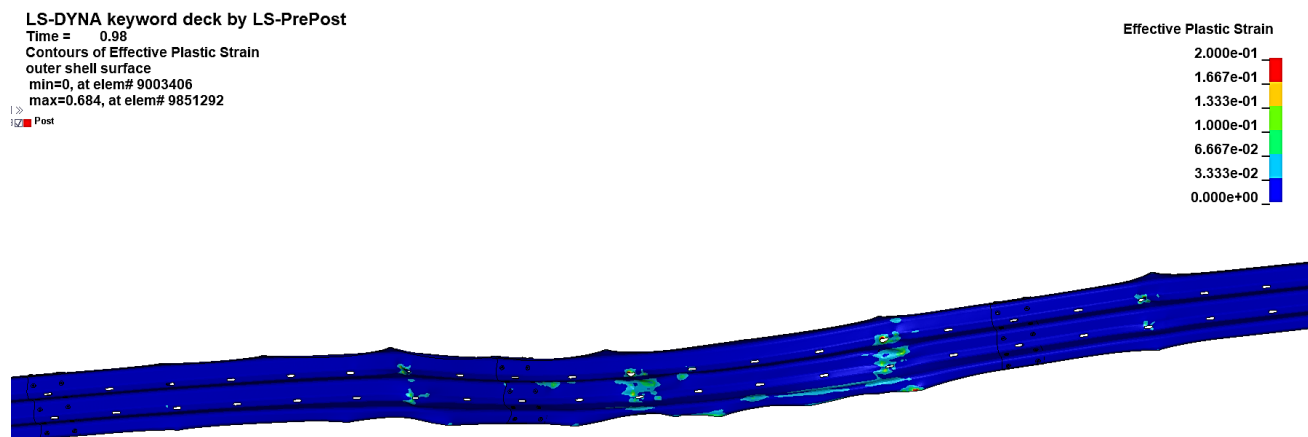




**Figure 77. Car Exits RTGS in Stable Manner (T = 0.865 sec).**

The occupant risk factors for the RTGS impacted by the passenger car at the CIP were within MASH limits. The maximum dynamic rail deflection was 38.1 inches. The maximum effective plastic strain of the rail segment above a selected 20 percent threshold and is shown in Figure 78. Yielding of the rail is isolated and indicates that rail rupture is not likely.

A similar set of simulations with the 2270P pickup truck were performed on the RTGS at the impact conditions associated with an 80-mph speed limit. The researchers performed simulations at three different impact locations to determine the CIP. The results were used to assess vehicle stability, occupant risk factors, and structural adequacy. Table 73 to Table 75 show the occupant risk metrics, angular displacements, and maximum dynamic deflection for impact at a post, 2 ft downstream of a post, and 2 ft upstream of a post, respectively.



**Figure 78. Effective Plastic Strain in RTGS Rail Segment during Passenger Car Impact at CIP.**

In all cases, the occupant risk criteria and angular displacements satisfied MASH criteria. The researchers recommend 2 ft downstream from the post as the CIP for the 2270P pickup truck due to the high roll angle that occurs after the vehicle exits the system.

Figure 80 to Figure 83 present images from the high-speed pickup truck simulation with the RTGS system at the CIP (i.e., 2 ft downstream of a post). The 2270P vehicle was successfully contained and redirected. After exiting the system, the pickup truck experiences a high roll angle (52 degrees) but remains upright and returns to the ground thereafter.

**Table 73. RTGS 2270P Simulation Results with Impact Point at Post.**

Test Parameter	MASH	High Speed Analysis Impacting at Post
OIV, Longitudinal (ft/s)	$\leq 40.0$	17.5
OIV, Lateral (ft/s)	$\leq 40.0$	17.5
RA, Longitudinal (g)	$\leq 20.49$	-12.7
RA, Lateral (g)	$\leq 20.49$	-9.9
Max. Roll (deg.)	$\leq 75$	16.5
Max. Pitch (deg.)	$\leq 75$	-8.0
Max. Yaw (deg.)	N/A	-45.8
Max. Rail Deflection (inches)	N/A	44.6

**Table 74. RTGS 2270P Simulation Results with Impact Point 2 ft Downstream of Post.**

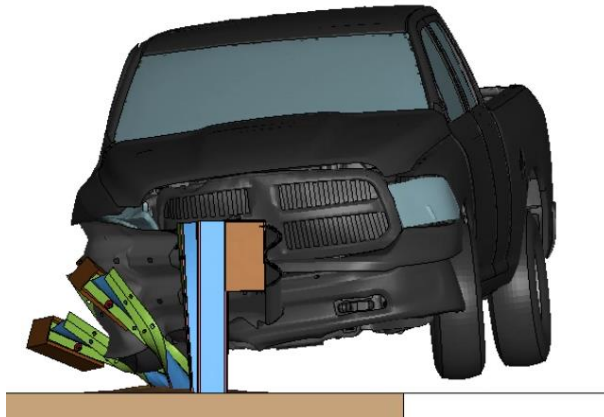
Test Parameter	MASH	High Speed Analysis Impacting 2 ft Downstream from Post
OIV, Longitudinal (ft/s)	$\leq 40.0$	15.8
OIV, Lateral (ft/s)	$\leq 40.0$	17.7
RA, Longitudinal (g)	$\leq 20.49$	-8.0
RA, Lateral (g)	$\leq 20.49$	-9.5
Max. Roll (deg.)	$\leq 75$	52.2
Max. Pitch (deg.)	$\leq 75$	-13.5
Max. Yaw (deg.)	N/A	-47.3
Max. Rail Deflection (inches)	N/A	45

**Table 75. RTGS 2270P Simulation Results with Impact Point 2 ft Upstream of Post.**

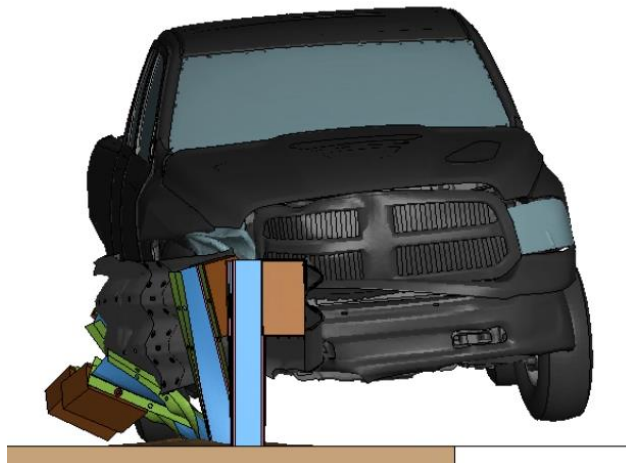
Test Parameter	MASH	High Speed Analysis Impacting 2 ft Upstream from Post
OIV, Longitudinal (ft/s)	$\leq 40.0$	16.6
OIV, Lateral (ft/s)	$\leq 40.0$	15.4
RA, Longitudinal (g)	$\leq 20.49$	-6.9
RA, Lateral (g)	$\leq 20.49$	-9.2
Max. Roll (deg.)	$\leq 75$	25.3
Max. Pitch (deg.)	$\leq 75$	-11.9
Max. Yaw (deg.)	N/A	-47.7
Max. Rail Deflection (inches)	N/A	44.5



**Figure 79. Front Tire of Pickup Truck Contacts Post in RTGS (T = 0.08 sec).**



**Figure 80. Pickup Truck Interaction with RTGS (T = 0.22 sec).**

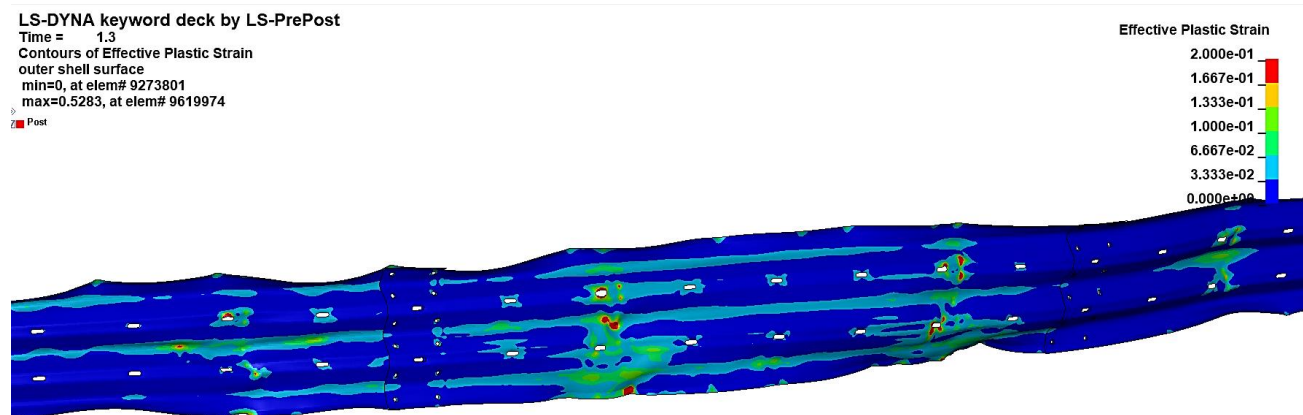


**Figure 81. Rear of Pickup Truck Interacts with RTGS (T = 0.29 sec).**



**Figure 82. Maximum Roll of Pickup Truck after Exiting System (T = 0.93 sec).**

The occupant risk factors for RTGS impacted by the pickup truck at the CIP were well within MASH limits. The maximum dynamic rail deflection was 45 inches. The maximum effective plastic strain of the rail segment above a selected 20 percent threshold is shown in Figure 83. Yielding of the rail is localized and indicates that rail rupture is not likely.



**Figure 83. Effective Plastic Strain in RTGS Rail Segment during Pickup Truck Impact at CIP.**

### 6.3. MIDWEST GUARDRAIL SYSTEM WITH SHORTENED BLOCKOUTS

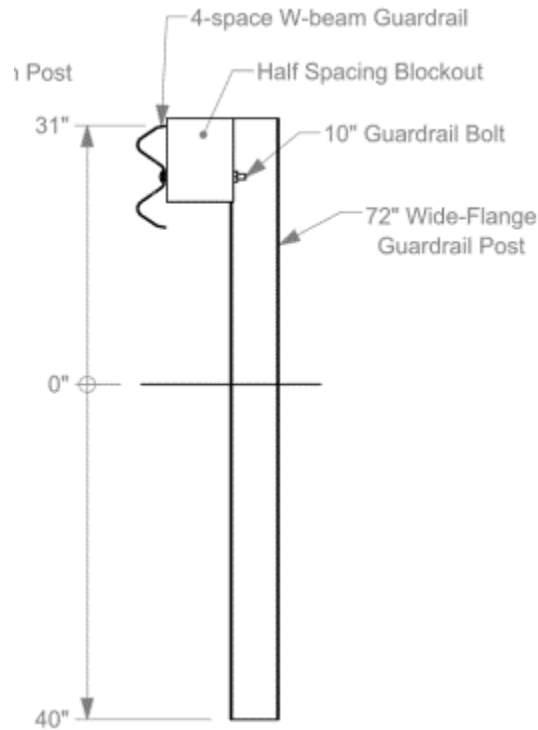
The MGS consists of a 12-gauge W-Beam rail element mounted on standard 6-ft-long, W6×8.5 steel posts at a height of 31 inches. The support posts have a 75-inch spacing. A shortened, 10-inch-long wooden offset block is incorporated between the rail and posts and secured with a single guardrail bolt. Figure 71 shows a cross section of the MGS with shortened blockouts.

An existing finite element model of the MGS with shortened blockouts, shown in Figure 85, was used in the simulation effort. The model was previously validated and used in the development and evaluation of a W-beam guardrail with reduced post spacing (23).

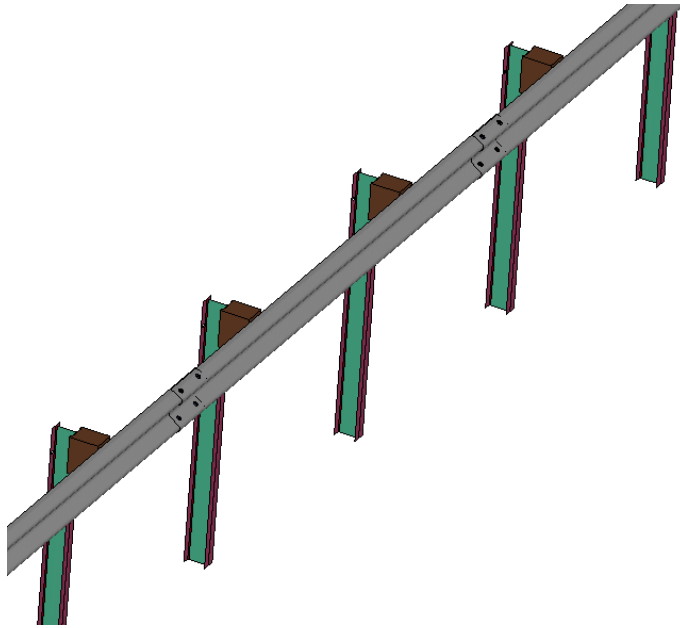
The predictive impact simulations on the MGS with shortened blockouts were performed using impact conditions for a posted speed limit of 80 mph, which involved an impact speed of 66.4 mph and impact angle of 25.6 degrees. The researchers conducted the simulations at three different impact points to determine the CIP for each design vehicle. The simulations were

performed with the impact point occurring at a post as well as 2 ft upstream and downstream of a post.

The MGS with shortened blockouts was evaluated for vehicle stability and occupant risk factors. Results from the three high-speed simulations with the 1100C passenger car are shown in Table 76 to Table 78 for impact at a post, 2 ft downstream of a post, and 2 ft upstream of a post, respectively. In all cases, the occupant risk criteria and angular displacements satisfied MASH criteria.



**Figure 84. MGS with Shortened Blockout (23).**



**Figure 85. Finite Element Model of MGS with Shortened Blockout.**

**Table 76. MGS with Shortened Blockout 1100C Simulation Results with Impact at Post.**

Test Parameter	MASH	High Speed Analysis Impacting at Post
OIV, Longitudinal (ft/s)	$\leq 40.0$	21.9
OIV, Lateral (ft/s)	$\leq 40.0$	16.4
RA, Longitudinal (g)	$\leq 20.49$	-16.2
RA, Lateral (g)	$\leq 20.49$	-12.1
Max. Roll (deg.)	$\leq 75$	-9.6
Max. Pitch (deg.)	$\leq 75$	-3.4
Max. Yaw (deg.)	N/A	68.3
Max. Rail Deflection (inches)	N/A	35.6

**Table 77. MGS with Shortened Blockout 1100C Simulation Results with Impact 2 ft Downstream of Post.**

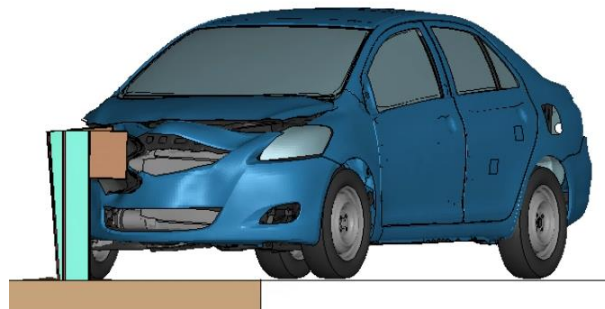
Test Parameter	MASH	High Speed Analysis Impacting 2 ft Downstream from Post
OIV, Longitudinal (ft/s)	$\leq 40.0$	29.4
OIV, Lateral (ft/s)	$\leq 40.0$	17.7
RA, Longitudinal (g)	$\leq 20.49$	-13.7
RA, Lateral (g)	$\leq 20.49$	-9.8
Max. Roll (deg.)	$\leq 75$	-9.0
Max. Pitch (deg.)	$\leq 75$	-8.6
Max. Yaw (deg.)	N/A	-25.8
Max. Rail Deflection (inches)	N/A	34.3

**Table 78. MGS with Shortened Blockout 1100C Simulation Results with Impact 2 ft Upstream of Post.**

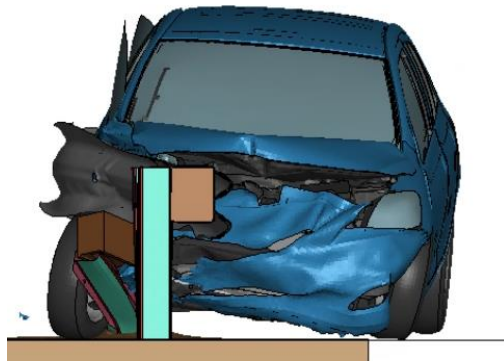
Test Parameter	MASH	High Speed Analysis impacting 2 ft upstream from the post
OIV, Longitudinal (ft/s)	$\leq 40.0$	26.6
OIV, Lateral (ft/s)	$\leq 40.0$	16.6
RA, Longitudinal (g)	$\leq 20.49$	-19.2
RA, Lateral (g)	$\leq 20.49$	-13.3
Max. Roll (deg.)	$\leq 75$	-11.4
Max. Pitch (deg.)	$\leq 75$	-16.9
Max. Yaw (deg.)	N/A	46.1
Max. Rail Deflection (inches)	N/A	34.8

Based on a review of the results, the researchers recommend impacting 2ft upstream from a post as the CIP for the 1100C passenger car impacting the MGS with shortened blockouts at high speed. It has the highest ridedown acceleration and roll angle compared to the simulations at the other impact points.

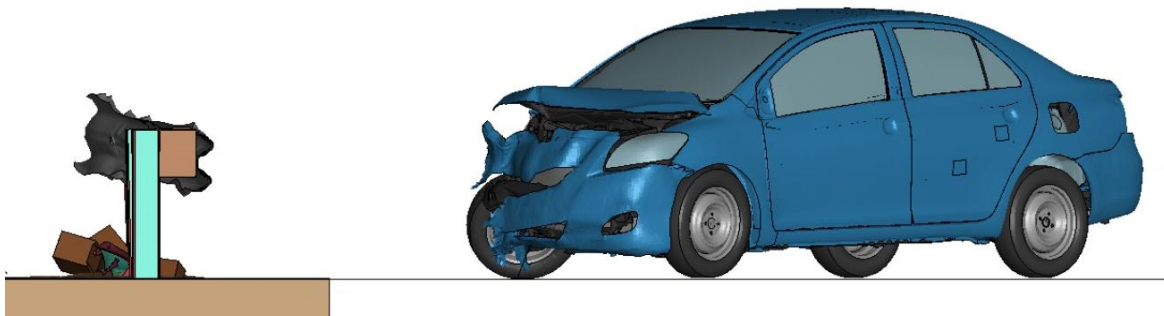
Figure 86 to Figure 88 present images from the high-speed passenger car simulation with the MGS with shortened blockouts at the CIP (i.e., 2ft upstream from a post). Significant wheel interaction with the posts is evident, but the 1100C vehicle is successfully contained and redirected. The wheel snagging did result in the vehicle yawing in a clockwise direction after exiting the system, but all MASH criteria were satisfied.



**Figure 86. Front Tire of Car Contacts Post in MGS with Shortened Blockout (T = 0.08 sec).**

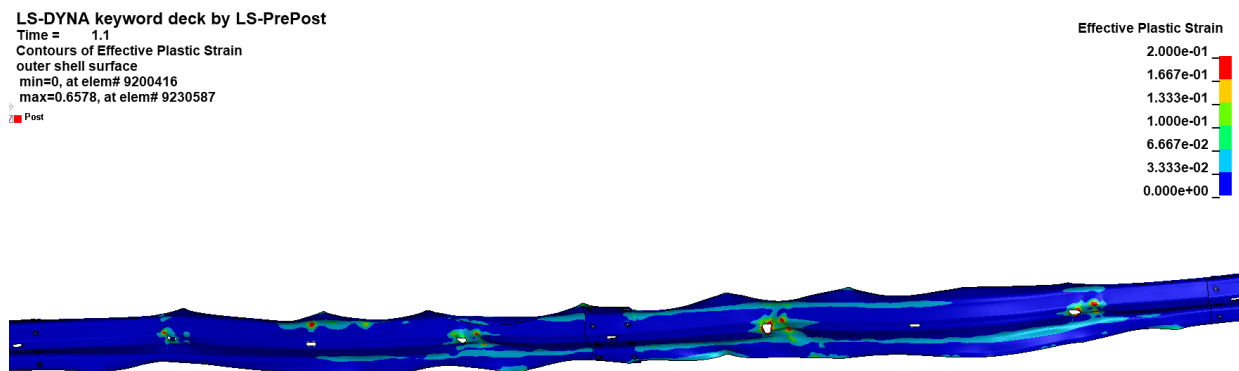


**Figure 87. Car Interaction with MGS with Shortened Blockout (T = 0.31 sec).**



**Figure 88. Post Impact Trajectory of Car for MGS with Shortened Blockout (T = 1.1 sec).**

The occupant risk factors for the MGS with shortened blockouts impacted by the passenger car at the CIP were within MASH limits. The maximum dynamic rail deflection was 35 inches. The maximum effective plastic strain of the rail segment above a selected 20 percent threshold is shown in Figure 89. Yielding of the rail is isolated and indicates that rail rupture is not likely.



**Figure 89. Effective Plastic Strain of MGS Rail Segment Impacted by Passenger Car at CIP.**

A similar set of simulations with the 2270P pickup truck were performed on the MGS with shortened blockouts at the impact conditions associated with an 80-mph speed limit. The researchers performed simulations at three different impact locations to determine the CIP. The



results were used to assess vehicle stability, occupant risk factors, and structural adequacy. Table 79 to Table 81 show the occupant risk metrics, angular displacements, and maximum dynamic deflection for impact at a post, 2 ft downstream of a post, and 2 ft upstream of a post, respectively.

**Table 79. MGS with Shortened Blockouts 2270P Simulation Results with Impact at Post.**

Test Parameter	MASH	High Speed Analysis impacting at post
OIV, Longitudinal (ft/s)	$\leq 40.0$	19.4
OIV, Lateral (ft/s)	$\leq 40.0$	14.6
RA, Longitudinal (g)	$\leq 20.49$	-9.7
RA, Lateral (g)	$\leq 20.49$	-9.4
Max. Roll (deg.)	$\leq 75$	-7.8
Max. Pitch (deg.)	$\leq 75$	-3.0
Max. Yaw (deg.)	N/A	-32.3
Max. Rail Deflection (inches)	N/A	47.25

**Table 80. MGS 2270P Simulation Results with Impact Point 2ft Downstream of Post.**

Test Parameter	MASH	High Speed Analysis Impacting 2 ft Downstream from Post
OIV, Longitudinal (ft/s)	$\leq 40.0$	26.6
OIV, Lateral (ft/s)	$\leq 40.0$	16.6
RA, Longitudinal (g)	$\leq 20.49$	-19.2
RA, Lateral (g)	$\leq 20.49$	-13.3
Max. Roll (deg.)	$\leq 75$	11.4
Max. Pitch (deg.)	$\leq 75$	-16.9
Max. Yaw (deg.)	N/A	46.1
Max. Rail Deflection (inches)	N/A	49.9

**Table 81. MGS 2270P Simulation Results with Impact Point 2ft Upstream of Post.**

Test Parameter	MASH	High Speed Analysis impacting 2 ft upstream from post
OIV, Longitudinal (ft/s)	$\leq 40.0$	20.8
OIV, Lateral (ft/s)	$\leq 40.0$	15.7
RA, Longitudinal (g)	$\leq 20.49$	-7.9
RA, Lateral (g)	$\leq 20.49$	-9.0
Max. Roll (deg.)	$\leq 75$	3.8
Max. Pitch (deg.)	$\leq 75$	-2.7
Max. Yaw (deg.)	N/A	-41.4
Max. Rail Deflection (inches)	N/A	47.7

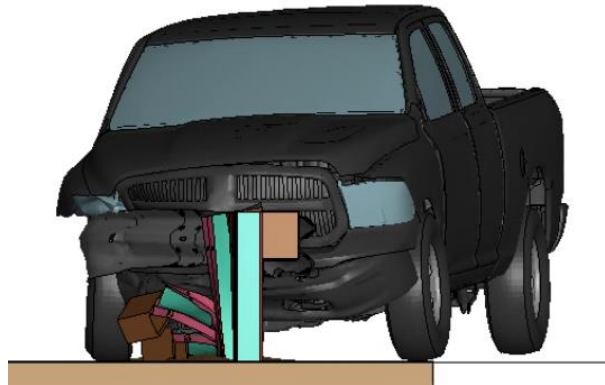
In all cases, the occupant risk criteria and angular displacements satisfied MASH criteria. The researchers recommend 2 ft downstream from the post as the CIP for the 2270P pickup

truck. This impact location generated the highest occupant risk metrics and angular displacements.

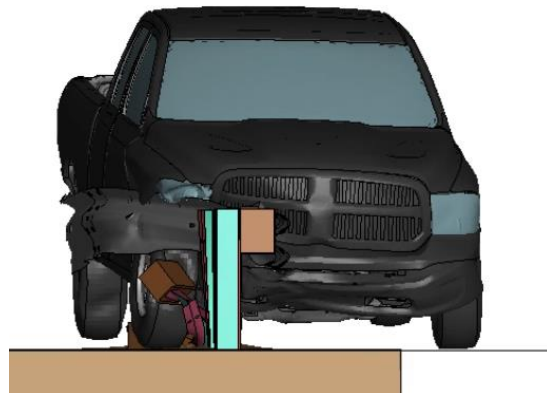
Figure 90 to Figure 93 present images from the high-speed pickup truck simulation with the RTGS system at the CIP (i.e., 2 ft downstream of a post). The 2270P vehicle was successfully contained and redirected in a stable manner.



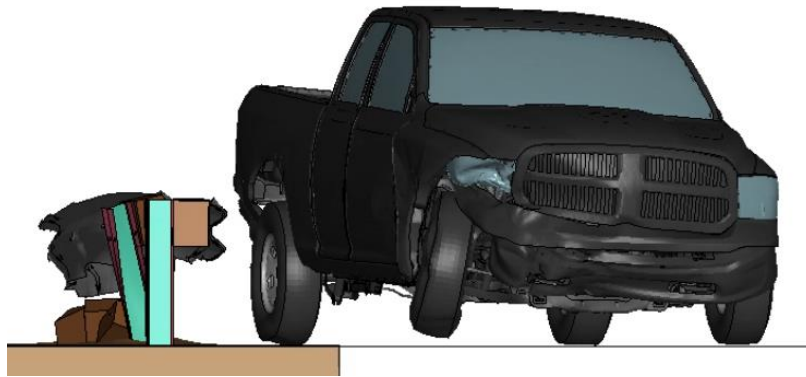
**Figure 90. Front Tire of Pickup Truck Interacts with Post (T = 0.1 sec).**



**Figure 91. Truck Interaction with MGS with Shortened Blockout System (T = 0.25 sec).**

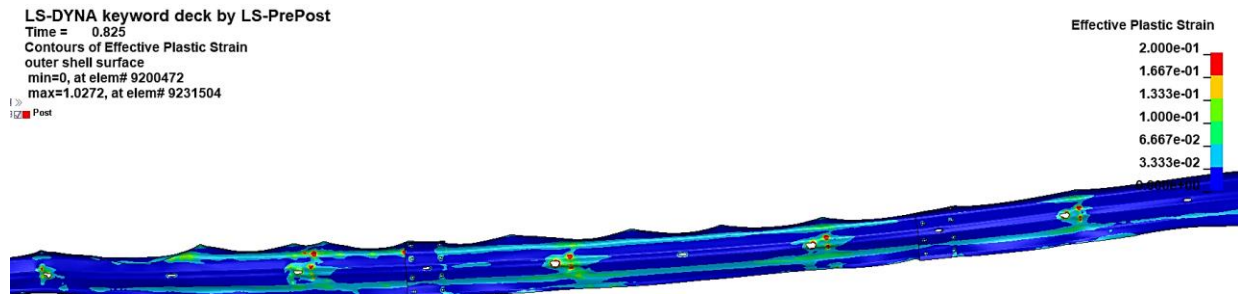


**Figure 92. Rear of Pickup Truck Interacts with MGS with Shortened Blockout System (T = 0.38 sec).**



**Figure 93. Pickup Truck Exits MGS with Shortened Blockout System in Stable Manner (T = 0.79 sec).**

The occupant risk factors for the MGS with shortened blockouts impacted by the pickup truck at the CIP were within MASH limits. The maximum dynamic rail deflection was 50 inches. The maximum effective plastic strain of the rail segment above a selected 20 percent threshold is shown in Figure 94. Yielding of the rail is localized and indicates that rail rupture is not likely.



**Figure 94. Effective Plastic Strain of RTGS Rail Segment Impacted by Pickup Truck at CIP.**

## 6.4. CONCLUSIONS AND RECOMMENDATIONS

Finite element simulations were performed to evaluate the high-speed impact performance of an MGS guardrail system with shortened blockouts and a RTGS. The impact conditions used in the simulations included an impact speed of 66.4 mph and impact angle of 25.6 degrees, which correspond to the impact conditions associated with a posted speed limit of 80 mph, as determined in this project.

Both these systems satisfied MASH evaluation criteria for both the 1100C passenger car and 2270P pickup truck design vehicles. Researchers consider both of these systems to have a reasonable probability of complying with MASH for the high-speed impact conditions. However, due to a lack of validation of the barrier models for high-speed impact conditions and various limitations associated with predicting some failure modes such as rail rupture, researchers recommend performing crash tests of these systems to verify impact performance.



## CHAPTER 7. CONCLUSIONS AND IMPLEMENTATION RECOMMENDATIONS

This research evaluates the impact performance of selected barrier systems for high-speed impact conditions estimated for roadways having posted speed limits of 75 mph, 80 mph, and 85 mph. TTI researchers predicted 85th percentile impact conditions for these high-speed roadways by using linear regressions to extrapolate available reconstructed crash data for freeways and interstate facilities. It was found that the impact conditions associated with a 75-mph posted speed limit were within current tolerance for the MASH TL-3 impact speed and angle. Therefore, it was concluded that MASH compliant barriers should be suitable for use on roadways with a posted speed limit of 75 mph. Impact conditions estimated for roadways with an 80-mph posted speed limit included an impact speed of 66.4 mph and an impact angle of 25.6 degrees. The impact conditions associated with an 85-mph posted speed limit involved an impact speed of 68.9 mph and an impact angle of 27.3 degrees.

TTI researchers evaluated four concrete barrier systems for high-speed impact conditions. These included a 42-inch-tall SSCB, 36-inch-tall SSTR, 32-inch-tall F-Shape barrier, and 36-inch-tall T222. Finite element impact simulations were performed on each of these systems using impact conditions associated with an 85-mph posted speed limit for both the MASH 1100C passenger car and 2270P pickup truck. Barrier performance was evaluated using MASH criteria. Although the occupant risk metrics and angular displacements increased for the high-speed impact conditions compared to MASH TL-3 impact conditions, the values were all within MASH thresholds. Based on the simulation results, the SSCB, SSTR, T222, and F-Shape concrete barriers are likely to meet MASH evaluation criteria for the 1100C passenger car and 2270P pickup truck for the high-speed impact conditions associated with a posted speed limit of 85 mph.

The concrete barriers evaluated through finite element simulation were modeled as rigid without any deflection or deformation. Consequently, the simulation results are applicable to both symmetric median profiles and single-side bridge rails provided sufficient structural capacity is provided. The results are only applicable to cast-in-place barrier. Further research is needed to evaluate precast concrete barrier to consider the connections between segments and the associated barrier deflection.

The structural adequacy of the concrete barrier systems was investigated at both the barrier interior and ends using the yield line methodology recommended in Section 13 of the *AASHTO LRFD Bridge Design Specification* (20). Design impact loads for the high-speed impact conditions were estimated based on impact severity and compared to the calculated barrier capacity. Researchers found that the existing concrete barrier designs have sufficient strength both on the interior and at the ends to resist impact forces associated with an 80-mph posted speed limit. When the designs were assessed for a posted speed limit of 85 mph, it was found that the barrier interiors had sufficient capacity, but the strength of the barrier ends was slightly below the estimated design impact loads. Researchers recommended a reduced spacing of the vertical barrier reinforcement and anchorage bars at the ends of the barriers to increase the resistance to meet the 85-mph impact loads.

Previous crash testing indicates that current guardrail systems may be near their performance limits under MASH TL-3 impact conditions. Testing of various guardrail

configurations has resulted in rail tearing or rupture at impact severities at or below those associated with the high-speed impact conditions.

The project panel selected two guardrail systems to investigate for high-speed impact conditions associated with a posted speed limit of 80 mph. These included a MGS with shortened 10-inch-long offset blocks and a RTGS that incorporates a stronger three-beam rail element with a taller mounting height of 34 inches in conjunction with shortened offset blocks.

The impact performance of these two guardrail systems was evaluated using finite element modeling and simulation. Both of these guardrail systems satisfied MASH evaluation criteria for the high-speed impact conditions for both the 1100C passenger car and 2270P pickup truck design vehicles. Researchers consider both of these systems to have a reasonable probability of complying with MASH for the high-speed impact conditions. However, due to a lack of validation of the barrier models for high-speed impact conditions and various limitations associated with predicting some failure modes such as rail rupture, researchers recommend performing crash tests of these systems to verify impact performance.

A discussion on the value of this research is presented in Appendix E.

## REFERENCES

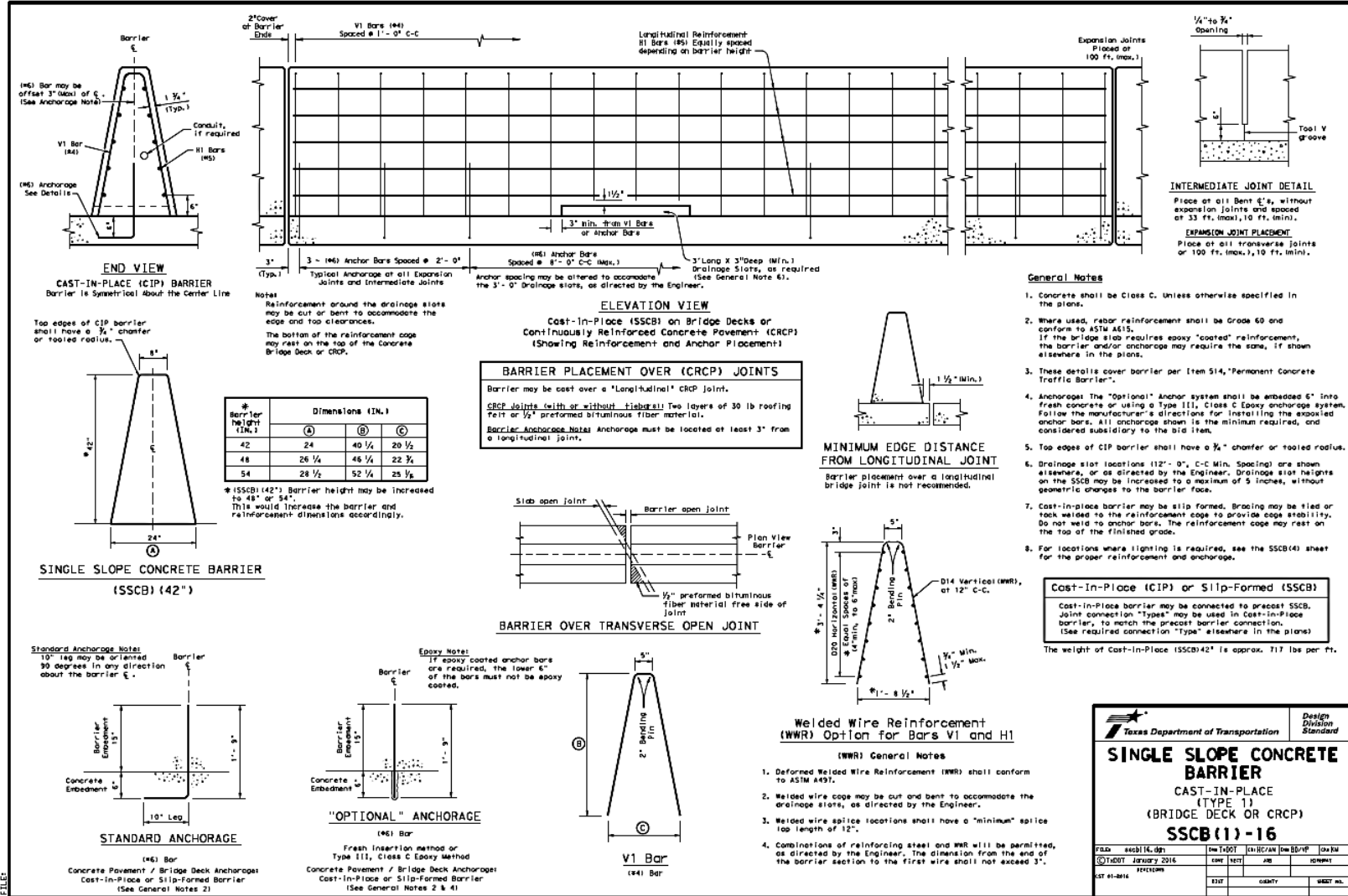
1. American Association of State Highway and Transportation Officials, 2009, *Manual for Assessing Safety Hardware*.
2. Ross, Jr., H.E., Sicking, D.L., Zimmer, R.A. and Michie, J.D., "Recommended Procedures for the Safety Performance Evaluation of Highway Features," *NCHRP Report 350*, TRB, Washington, DC, 1993.
3. American Association of State Highway and Transportation Officials, 2016, *Manual for Assessing Safety Hardware*.
4. Sheikh, N.M., R. Ferdous, R. P. Bligh, and A. Y. Abu-Odeh. "Criteria for High Design Speed Facilities," Report No. 0-6071-1. Texas Transportation Institute, College Station, Texas, 2009.
5. Bligh, R. P., N. M. Sheikh, A. Y. Abu-Odeh, and W. L. Menges. "Evaluation of Barriers for Very High-Speed Roadways," Test Report No. 0-6071-2. Texas Transportation Institute, College Station, Texas, 2010.
6. Xavier, C., Lord, D., Dobrovolny, C., and R. Bligh "Evaluating the Relevancy of Current Crash Test Guidelines for Roadside Safety Barriers on High-Speed Roads" TRC, 1<sup>st</sup> International Roadside Safety Conference, 2017: p. 452–465.
7. Xavier, C., "Evaluating the Relevancy of Crash Test Guidelines for Roadside Safety Barriers Placed on High-Speed Roads," Undergraduate Research Scholars Thesis, Texas A&M University, College Station, Texas, 2015.
8. Mak, K.K., D. L. Sicking, F. D. B. de Albuquerque, and B. A. Coon. "Identification of Vehicular Impact Conditions Associated with Serious Run-off-road-Crashes." Final Report on NCHRP Project 17-22. MwRSF, UNL, 2009.
9. de Albuquerque, D.B., D. L. Sicking, and C. S. Stolle. "Roadway Departure and Impact Conditions," Transportation Research Record: Journal of the Transportation Research Board, No. 2195, Transportation Research Board of the National Academies, Washington, DC, 2010, pp. 106–114.
10. Riexinger, L.E and H.C Gabler, Expansion of NASS/CDS for characterizing run-off-road crashes. Traffic Injury Prevention 2020: p.1–5, DOI: 10.10.
11. "Safety Effects of Raising Speed Limits to 75 mph and Higher," NCHRP Project 17-79, TRB (Active).
12. Roadside Design Guide. American Association of State Highway and Transportation Officials, Washington, DC, 2002.
13. Dobrovolny, C.S., "Testing and Evaluation of the MGS System with Critical Flare at MASH test Level 3 Conditions". Project No. 609971. Texas A&M Transportation Institute, College Station, Texas. (Ongoing Project).
14. N. M. Sheikh, R. P. Bligh, W. L. Menges. *Determination of Minimum Height and Lateral Design Load for MASH Test Level 4 Bridge Rails*. Report No. 9-1002-5. Texas Transportation Institute, College Station, Texas. December 2011.
15. C. Dobrovolny, M. Kiani, W. Menges, W. Schroeder, B. Griffith, D. Kuhn. *MASH TL-4 Evaluation of Flared Cast-In-Place Concrete Barrier*. Report No. 611901-06. Texas A&M Transportation Institute, College Station, Texas. August 2021.
16. David W., John J., Robert M. *Compliance Crash Testing of the Type 60 Median Barrier*. Report No. CA17-2654. Texas A&M Transportation Institute, College Station, Texas. May 2018.

17. W. Williams, R. Bligh, W. Menges. *MASH Test 3-11 of the TxDOT Single Slope Bridge Rail (Type SSTR) on Pan-formed Bridge Deck*. Report No. 9-1002-3. Texas A&M Transportation Institute, College Station, Texas. November 2010.
18. W. Williams, R. Bligh, W. Menges. *MASH Test 3-11 of the TxDOT T222 Bridge Rail*. Report No. 9-1002-12-13. Texas A&M Transportation Institute, College Station, Texas. August 2014.
19. C. Dobrovolny, R. Bligh, W. Menges. *Crash Testing of Pedestrian Railing on Top of Barriers in Big Dig Tunnels*. Report No. 603111-1-12. Texas A&M Transportation Institute, College Station, Texas. November 2014.
20. AASHTO LRFD Bridge Design Specifications, Section 13: Railings, 8th Edition, 2017.
21. R. P. Bligh, J. Briaud, A. Abu-Odeh, D. Saez, L. Maddah, K. Kim. *Design Guidelines for Test Level 3 through Test Level 5 Roadside Barrier Systems Placed on Mechanically Stabilized Earth Retaining Walls*. National Cooperative Highway Research Program Web Only Document 326; Transportation Research Board; National Academies of Sciences, Engineering, and Medicine, Washington, DC, 2022.
22. S. Rosenbaugh., C. Stolle, K. Ronspies. *MGS with Curb and Omitted Post: Evaluation to MASH 2016 Test Designation No. 3-10*. Report No. TRP-03-393-19. Texas A&M Transportation Institute, College Station, Texas. April 2019.
23. J. Kovar, W. Menges, W. Schroeder, and B. Griffith. *MASH Crash Testing and Evaluation of the MGS with Reduced Post Spacing*. Report No. 610211-01. Texas A&M Transportation Institute, College Station, Texas, 2021.
24. J. Kovar, M. Kiani, S. Wegenest, and D. Kuhn. *MASH TL-3 Testing of a Thrie-Beam Guardrail System at a Fixed Object*, Report No. 614031-01-1&2. Texas A&M Transportation Institute, College Station, Texas, in publication.
25. C. Dobrovolny, S. Park, B. Griffith, and D. Kuhn. *Testing and Evaluation of Flared MGS System at MASH Test Level 3 Conditions*. Report No. 609971-01. Texas A&M Transportation Institute, College Station, Texas. January 2023.
26. M. Kiani, J. Kovar, W. Menges, W. Schroeder, B. Griffith, and D. Kuhn, *Design and Testing of MASH TL-3 Thrie-Beam Guardrail System (TGS) for Roadside and Median Applications, Roadside Safety Pooled Fund* Report No.614341-01. Texas A&M Transportation Institute, College Station, Texas, 2021.



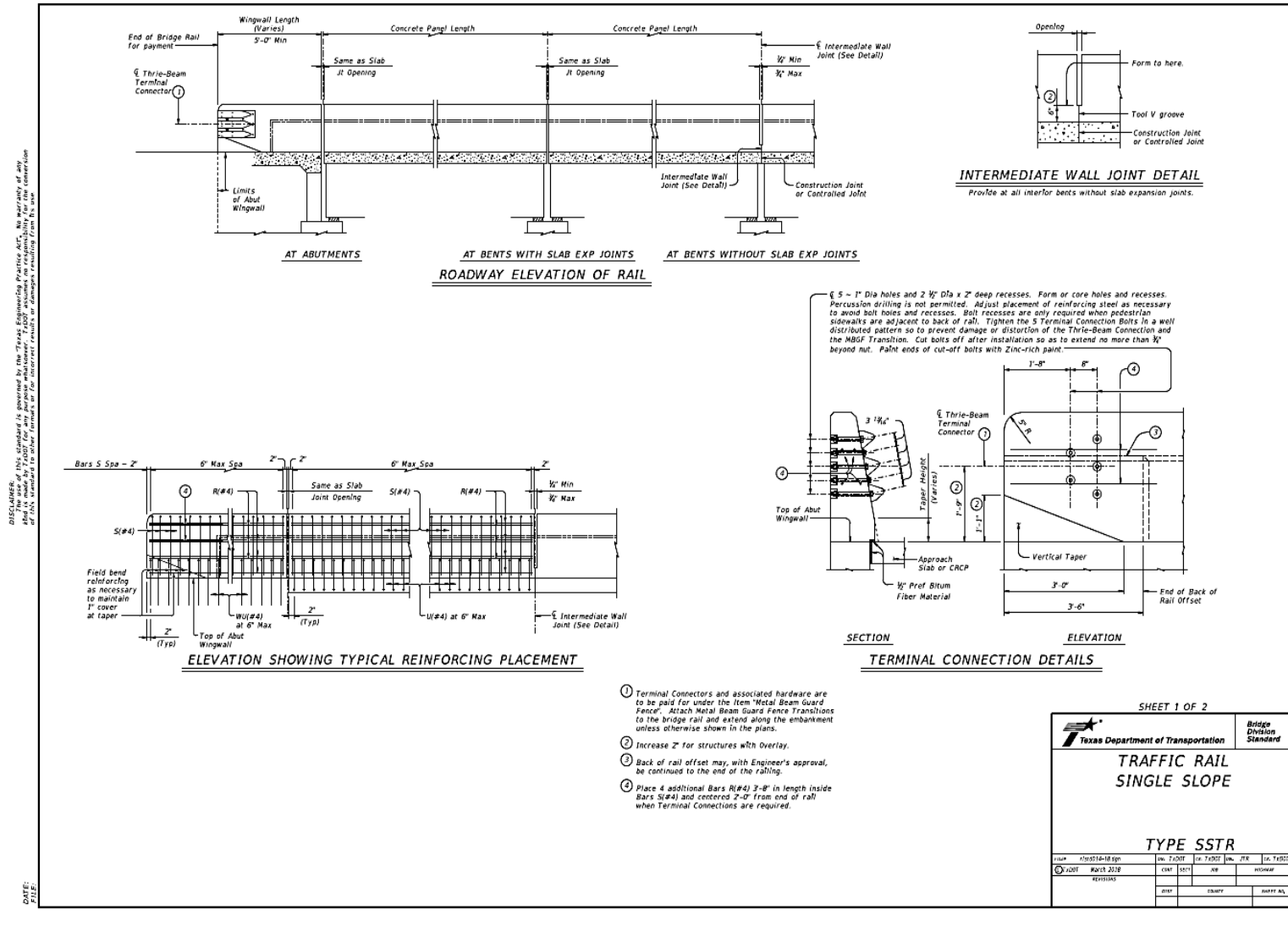
# APPENDIX A. SSCB DETAILS

DISCUSSION: This standard is approved by the Texas Department of Transportation. No warranty is made by TxDOT for any purpose whatsoever. TxDOT disclaims any responsibility for the use of this standard for any purpose other than that for which it was intended.



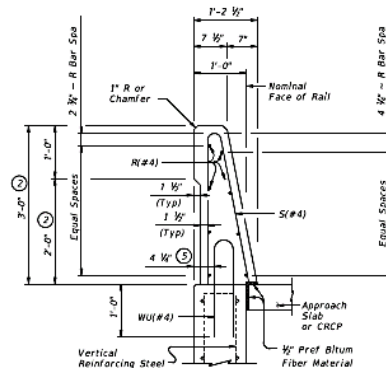


## APPENDIX B. SSTR DETAILS

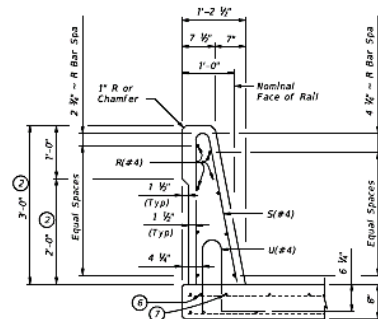


DISCLAIMER: This standard is provided by the Texas Engineering Practice Act. No warranty of any kind is made by TCEP for any purpose whatsoever. TCEP assumes no responsibility for the conversion of this standard to other formats or for incorrect results or damages resulting from its use.

DATE: FILE:

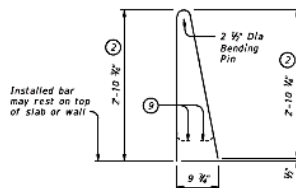


ON ABUTMENT WINGWALLS  
OR CIP RETAINING WALLS

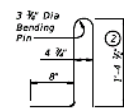


ON BRIDGE SLAB

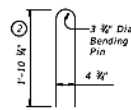
### SECTIONS THRU RAIL



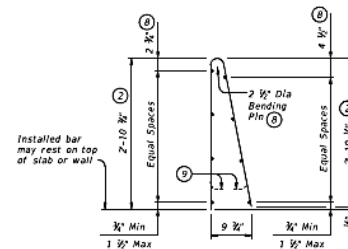
BARS S (#4)



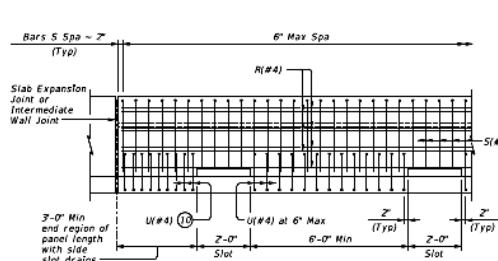
BARS U (#4)



BARS WU (#4)

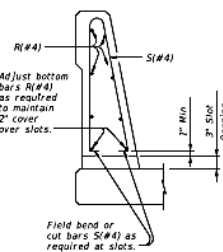


OPTIONAL WELDED WIRE  
REINFORCEMENT (WWR)



OPTIONAL SIDE SLOT DRAIN DETAIL

Note: Side Slot Drains may be used where shown elsewhere on the plans or as directed by the Engineer. Drains should not be placed over railroad tracks, lower roadways, or sidewalks. When this rail is used as a separator between a roadway surface and a sidewalk surface, side drain slots will not be permitted.



SECTION THRU  
OPTIONAL SIDE SLOT DRAIN

- ② Increase 2" for structures with overlay.
- ③ 5/8" when vertical reinforcing has closer clear cover over horizontal reinforcing in abutment wingwalls or retaining walls on traffic side of wall.
- ④ As an aid in supporting reinforcement, additional longitudinal bars may be used in the slab with the approval of the Engineer. Such bars must be furnished at the Contractor's expense.
- ⑤ Top longitudinal slab bar may be adjusted laterally 3" plus or minus to tie reinforcing.
- ⑥ No longitudinal wires may be within upper bend.
- ⑦ Bend or cut as required to clear drain slots.
- ⑧ Space U(#4) bars at 4" Max when end region of panel length is less than 6'-0" to side slot drain. Space U(#4) bars at 6" Max when end region of panel length is 6'-0" and greater to side slot drain.

### CONSTRUCTION NOTES:

This railing may be constructed with slip-forms when approved by the Engineer, with equipment approved by the Engineer. Provide sensor control for both line and grade. Tack welding to provide bracing for slip-form operations is acceptable. Welding can be performed at a minimum spacing of 3 ft between the cage and the anchorage. It is permissible to weld to U, WU and S bars at any location on the cage. If increased bracing is needed, provide additional anchorage devices and weld in the upper two thirds of the cage. The back of railing must be vertical unless otherwise shown in the plans or approved by the Engineer.

### MATERIAL NOTES:

Provide Class "C" concrete. Provide Class "C" (HPC) if required elsewhere.  
Provide Grade 60 reinforcing steel.  
Epoxy coat or galvanize all reinforcing steel if slab bars are epoxy coated or galvanized.  
Deformed Welded Wire Reinforcement (WWR) (ASTM A1064) of equal size and spacing may be substituted for Bars U and WU unless noted otherwise. Deformed WWR (ASTM A1064) may be substituted for Bars R and S, as shown. Combinations of reinforcing steel and WWR or configurations of WWR other than shown are permitted if conditions in the table are satisfied. Provide the same laps as required for reinforcing bars.  
Provide bar laps, where required, as follows:  
Uncoated or galvanized - #4 = 1'-7"  
Epoxy coated - #4 = 2'-5"

### GENERAL NOTES:

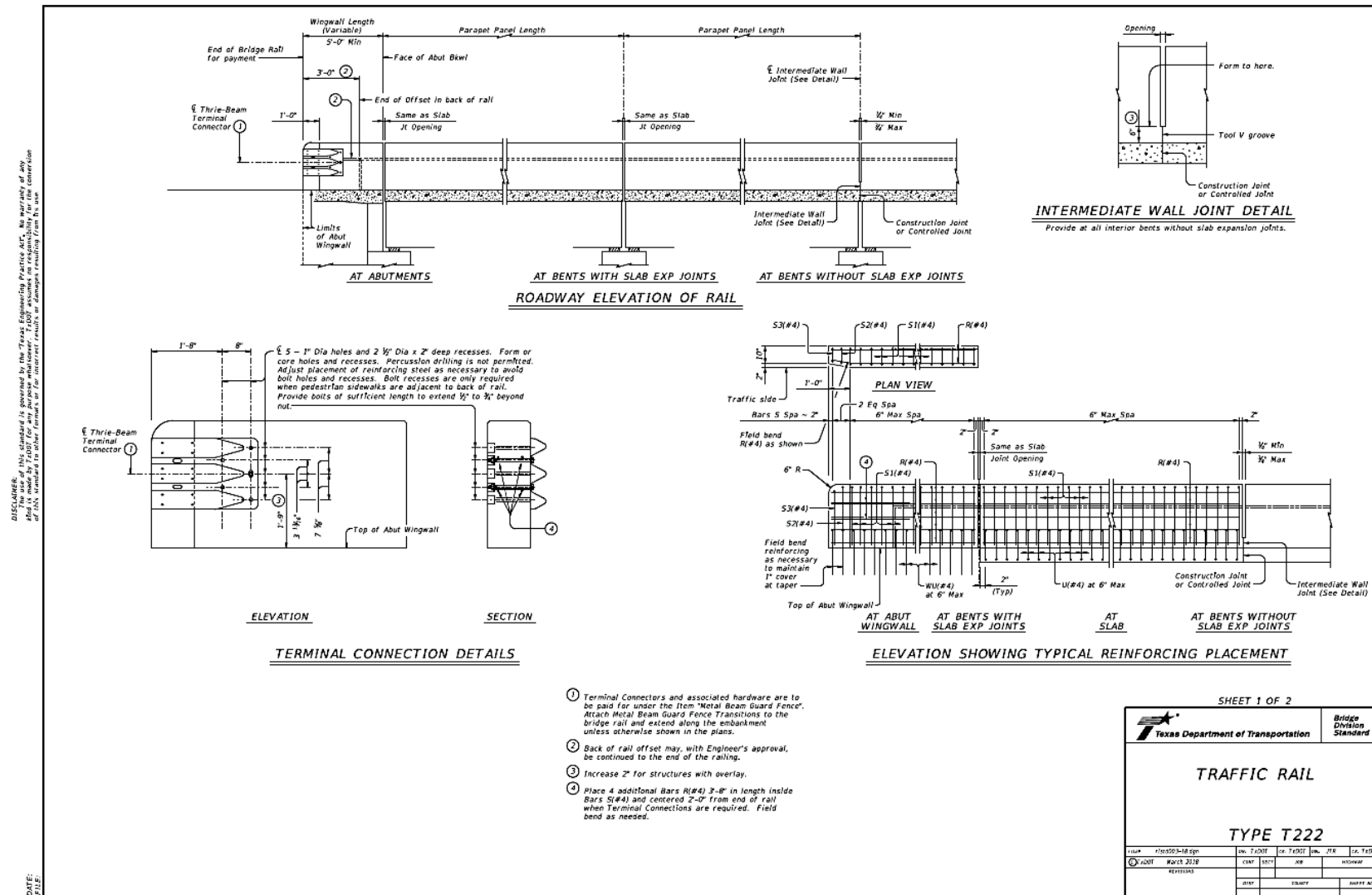
This rail has been successfully evaluated by full-scale crash test to meet MASH TL-4 criteria. This rail can be used for speeds of 50 mph and greater when a TL-3 rated guard fence transition is used. When a TL-2 rated guard fence transition is used, this rail can only be used for speeds of 45 mph and less.  
Do not use this railing on bridges with expansion joints providing more than 5" movement.  
Rail anchorage details shown on this standard may require modification for select structure types. See appropriate details elsewhere in plans for these modifications.  
Shop drawings will not be required for this rail.  
Average weight of railing with no overlay is 376 plf.

Cover dimensions are clear dimensions, unless noted otherwise.  
Reinforcing bar dimensions shown are out-to-out of bar.

SHEET 2 OF 2

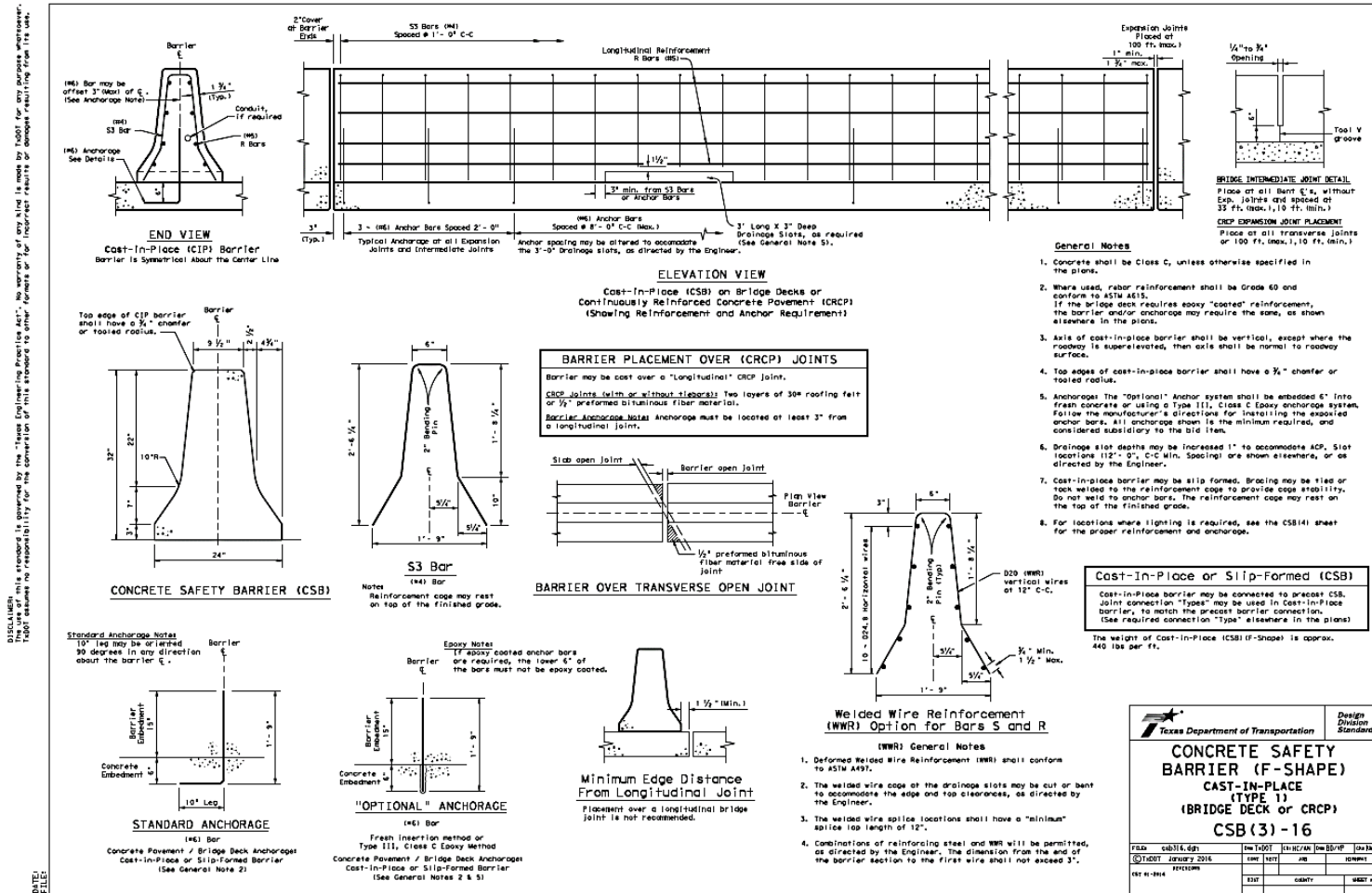
Texas Department of Transportation		Bridge Division Standard	
<b>TRAFFIC RAIL SINGLE SLOPE</b>			
<b>TYPE SSTR</b>			
FILE#	PROJECT	DATE	BY
2007	MAV 2018	08/18	08/18
REVISION	DATE	BY	REASON

## APPENDIX C. T222 DETAILS





## APPENDIX D. F-SHAPE DETAILS







## APPENDIX E. VALUE OF RESEARCH

The Centers for Disease Control and Prevention estimates that the total societal cost of highway crashes in Texas is over \$5.7 billion per year. The value of research (VOR) for this project is defined in terms of its economic benefits. The economic benefit is safety related and expressed in terms of potential lives saved and associated societal cost associated with implementation of the evaluated guardrail systems on high-speed roadways. Use of enhanced guardrail designs on high-speed facilities may offer an increase in effective barrier capacity, which can result in fewer barrier penetrations or vehicle rollovers compared to conventional guardrail systems. Finite element impact simulations of existing concrete barriers found that these barriers are likely to meet occupant risk and vehicle stability requirements for posted speeds up to 85 mph. Therefore, although this is a significant finding, the continued implementation of these concrete barriers on high-speed roadways will not result in additional safety benefits beyond those already being realized.

In support of the economic safety analysis of this research, four years of crash data from CRIS was analyzed from the years 2016 through September 2021. A total of 17 fatal crashes were coded as Hit Concrete Traffic Barrier and 88 fatal crashes were coded as Hit Guardrail System on high-speed roadways having posted speed limits of 75 mph or greater. Under this project, the impact conditions estimated for roadways with a speed limit of 75 mph were within MASH impact tolerances for TL-3. Therefore, MASH TL-3 compliant barriers are considered satisfactory for roadways with a posted speed limit of 75 mph. Additionally, Texas only has about 30 miles of roadway with a posted speed limit of 85 mph. Therefore, the VOR analysis focused on roadways with a posted speed limit of 80 mph.

Table 82 shows the number of fatal and serious injury guardrail crashes on roadways with a posted speed limit of 80 mph. There was a total of 14 fatal and 33 serious injury crashes coded as Hit Guardrail during the period 2016 through September 2021. This equates to 2.43 fatalities and 5.74 serious injury guardrail related crashes per year.

**Table 82 Guardrail Crashes for 80-mph Posted Speed Limit.**

Year	No. of Fatal Crashes	No. of Serious Injury Crashes
2016	3	3
2017	1	7
2018	1	3
2019	4	5
2020	1	8
Jan.–Sept. 2021	4	7
Total	14	33

While the performance limits of existing guardrails have not been well defined, previous crash testing has indicated that current guardrail designs may be near their capacity under MASH TL-3 impact conditions. The alternative guardrail systems evaluated through finite element

simulation under this research indicate they have a reasonable probability of satisfying MASH criteria for impact speeds up to 66.4 mph, which is the 85th percentile impact speed estimated for roadways with a posted speed limit of 80 mph. Thus, if these guardrail systems are implemented on roadways with a posted speed limit of 80 mph, they will theoretically accommodate a broader range of impact speeds than the conventional metal beam guard fence. Specifically, the safety benefit associated with these barriers will be realized for impact speeds ranging from 62 mph (the MASH TL-3 impact speed) to 66.4 mph (the impact speed estimated for roadways with a posted speed limit of 80 mph).

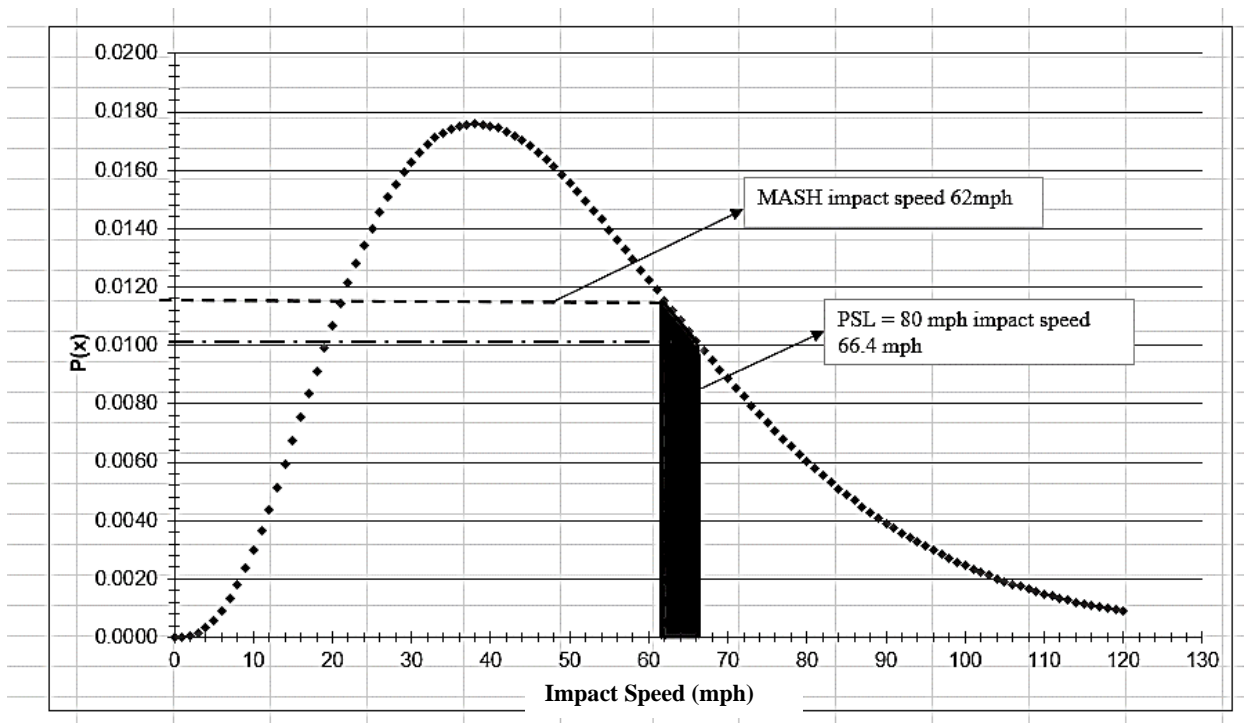
The NCHRP 17-43 database is comprised of clinically reconstructed run-off-road crashes. Both impact speed and posted speed are available in this database. The researchers assumed that the mean impact speed for a given facility type is proportional to the posted speed limit. For this analysis, which relates to high-speed facilities, data for interstate and freeway classes were used. Mean impact speeds for the higher posted speed limits for which crash data were unavailable were estimated using linear regression of mean impact speed for other posted speed limits for these facility types.

Previous research has found that a gamma function provides the best fit for both univariate impact speed distributions. The gamma function is uniquely defined by two coefficients that can be used to describe the mean and variance of the distribution. Therefore, by assuming a mean impact speed for a given posted speed, a gamma function can be defined.

Figure 95 shows the probability density function of the gamma distribution for impact speed associated with a posted speed limit of 80 mph. The percentage change between the MASH impact speed of 62 mph and the impact speed of 66.4 mph was calculated, as highlighted in Figure 95. This graph indicates an impact speed of 66.4 encompasses 4.84 percent more crashes beyond an impact speed of 62 mph.

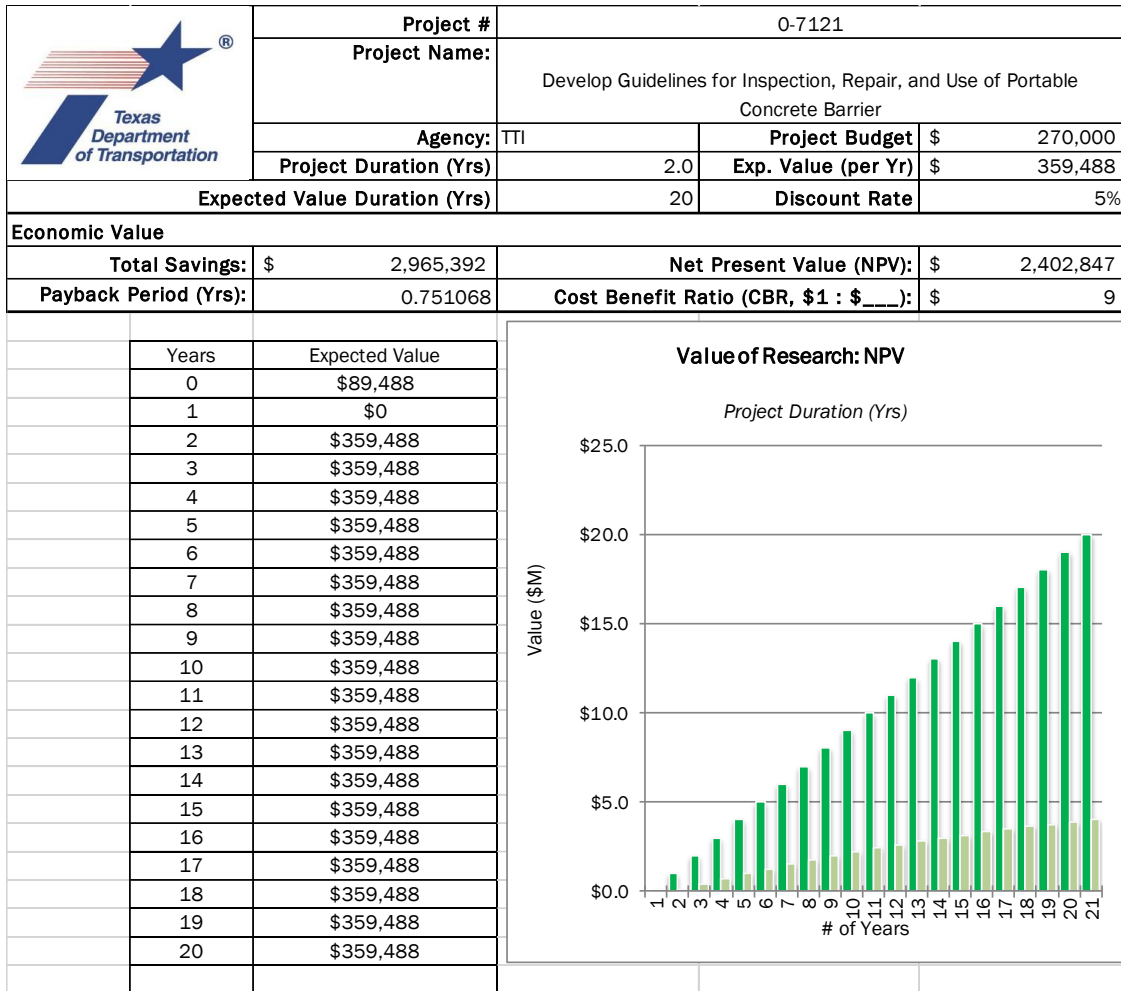
A recent published report by NHTSA entitled *The Economic and Societal Impact of Motor Vehicle Crashes* (2019) indicates that the economic cost to society of each fatality in a fatal crash is \$1,584,326. The economic cost of a serious injury crash (average cost of MAIS 3-5) is approximately \$623,262. Thus, the economic safety benefit associated with implementation of the high-speed guardrail systems on roadways with a posted speed limit of 80 mph posted speed limit can be estimated as follows:

$$(2.43 \text{ fatalities/year} \times \$1,584,326/\text{fatality} + 5.74 \text{ serious injuries/year} \times \$623,262/\text{serious injury}) \times 0.0484 = \$359,488/\text{year}.$$



**Figure 95. Probability Density Function for Impact Speed for Posted Speed Limit of 80 mph.**

The total economic value of the project over a 20-year period is summarized in Figure 96. Implementing the guardrail systems on roadways with a posted speed limit of 80 mph or greater will provide a safety benefit in terms of a reduction in fatal and serious injury guardrail crashes. Researchers suggest performing full-scale crash testing of the guardrail systems to confirm impact performance at the higher impact speed associated with a posted speed limit of 80 mph.



**Figure 96. Estimated Economic Value of Project.**